NUMERICAL INVESTIGATION OF NONLINEAR CONSOLIDATION

AND SECONDARY COMPRESSION

by

HYEON JUNG KIM

B.S., University of Colorado, 2017

A thesis submitted to the

Faculty of the Graduate School of the

University of Colorado in partial fulfillment

of the requirement for the degree of

Master of Science

Department of Civil, Environmental and Architectural Engineering

2017

ProQuest Number: 10680757

ProQuest 10680757

This thesis entitled:

Numerical Investigation of Nonlinear Consolidation and Secondary Compression

written by Hyeon Jung Kim

has been approved for the Department of Civil, Environmental and Architectural Engineering

Dobroslav Znidarcic

Gordan Gjerapic

Date

The final copy of this thesis has been examined by the signatories, and we

find that both the content and the form meet acceptable presentation standards

of scholarly work in the above mentioned discipline.

ABSTRACT

Kim, Hyeon Jung (M.S., Civil, Environmental and Architectural Engineering)

Numerical Investigation of Nonlinear Consolidation and Secondary Compression

Thesis directed by Professor Dobroslav Znidarcic

The purpose of this thesis is to investigate different numerical models evaluating large strain consolidation and creep and to provide assessment of potential impacts of these models to engineering designs. Several models were used to conduct calculations presented in this thesis: CONDES, iConsol.js, PLAXIS and a finite difference code developed in Mathematica. The model developed in Mathematica was used to investigate differences between the classical (linear) and the non-linear consolidation equations with the goal to identify limitations of the classical approach. In addition, a simplified creep model developed in Mathematica was used to evaluate differences between iConsol.js and PLAXIS, two selected models that are available to practicing engineers for the assessment of secondary compression. Results of this study indicate that a model selection should be tailored to specific design requirements after considering results of the available geotechnical investigations and monitoring because all computer codes considered in this study exhibit limitations in terms of the available constitutive models, the ability to account for secondary compression effects, and the flexibility to account for changes in the boundary condition, i.e. model results may not be able to represent actual soil behavior when considering general (pre-defined) material, boundary and loading conditions.

ACKNOWLEDGEMENTS

With endless respect and appreciation, the researcher would like to give thanks to the people who helped him bring this study into reality.

Foremost, I want to offer this endeavor to our God for the wisdom he bestowed upon me, the strength, peace of my mind and good health in order to finish this research.

I would like to express my sincere appreciation to my advisor Professor Dobroslav Znidarcic and the other committee members Doctor Gordan Gjerapic, and Professor Harihar Rajaram.

I owe my deepest gratitude to my advisor, Professor Dobroslav Znidarcic providing me the opportunity to develop my skills and experience about geotechnical engineering with imparting his knowledge and expertise in this study.

I am deeply grateful to Doctor Gordan Gjerapic for guiding and helping me in order to make the study a well done achievement by sharing his knowledge and technical know-how mainly on primary consolidation and secondary compression.

I am thankful to Professor Harihar Rajaram for giving me many good advices for how to make better numerical result of this study.

I further extend my personal gratitude to my colleagues and people who, directly or indirectly, have lent their helping hand in this research.

Lastly, I would like to thank my family, especially my mother, father, and sister for their moral and financial support in order to finish this study.

Table of Contents

vi

TABLES

ix

FIGURES

xi

1. INTRODUCTION

1.1 Background

Issues of settlement and consolidation are important when considering the safety of engineering structures. The related process of soil compaction, associated with the soil volume reduction by removal of air from the porous structure, typically due to mechanical means, is not a subject of this thesis. The process of consolidation involves a gradual decrease in the water content (compression) of saturated soils when subjected to external loads.

The consolidation process governs the long-term deformation of structures for which foundation materials consist of saturated fine-grained soils. This process, first studied by Karl Terzaghi (Terzaghi, 1942), is manifested by vertical movements (settlements) of surface structures as the water is being expelled from the pores of soil matrix due to the dissipation of excess pore pressures. The purpose of the consolidation theory is to determine both the rate and the magnitude of soil deformations to predict surface settlements, and to determine the rate and the magnitude of excess pore pressure generation to address potential seepage and stability concerns.

Three types of settlements are associated with the consolidation process: the immediate settlement, the primary consolidation settlement, and the secondary compression settlement. The immediate settlement is caused by elastic deformation of soil without change in the water content. The primary consolidation settlement is caused by the volume change in saturated cohesive soils due to expulsion of water from the void spaces. The secondary compression settlement occurs in saturated cohesive soils due to visco-plastic adjustments of soil fabric see e.g. Coduto, (2015).

1

Terzaghi's theory, also known as a classical theory of consolidation, assumes that the coefficient of consolidation is constant. Consequently, the classical theory of consolidation implies that the hydraulic conductivity and the coefficient of compressibility are also constant, the assumption that may not be representative of actual field conditions since both of these quantities change during the consolidation process. As a result, the classical consolidation theory is applicable to relatively dense soils, for which the total consolidation-induced volumetric strain remains relatively small. This is also the reason why Terzaghi's theory is often referred to as the small strain consolidation theory. As mentioned previously, the classical theory implies that the soil's compressibility and hydraulic conductivity are constant throughout the consolidation process. To relax this limitation, a finite strain consolidation approach may be used allowing for the analysis with the non-linear material properties.

Furthermore, Terzaghi's theory doesn't account for secondary compression effects, which may be of significance when considering settlements of clayey soils exhibiting creep. To account for the secondary compression, engineering calculations often assume that the creep mechanism is activated only after the primary consolidation is completed. For sands, the settlement caused by the secondary compression is typically considered negligible. The secondary compression has been a controversial topic in the geotechnical engineering literature for over 50 years with researchers arguing whether the effects of creep should be accounted for throughout the consolidation process, i.e. whether the creep mechanism is active during both the primary and the secondary consolidation process. There were numerous attempts to describe the secondary compression using both empirical and theoretical models (e.g., by using rheological models). A comparison between several numerical models accounting for the creep mechanism (most of them readily available to practicing geotechnical engineers) is provided in this thesis.

2

1.2 Arrangement of the Thesis

This thesis is organized with the goal to present results of several numerical models and the underlying theoretical background for: 1) large strain consolidation and 2) secondary compression. Introductory remarks are provided in Chapter 1, including the general background of consolidation theory and the organizational outline of this thesis. A literature review of consolidation theories, including the classical approach by Terzaghi, are provided in Chapter 2. Chapter 3 provides general description of different models (CONDES, PLAXIS, Mathematica, and iConsol.js) used for the numerical investigation of large strain consolidation and creep. Chapter 4 presents the benchmark large strain consolidation case from the literature (Benchmark No 1) and provides a comparison between numerical results from the simple model developed in Mathematica and results from other models available in today's engineering practice. Chapter 5 demonstrates potential shortcomings of the classical consolidation theory when solving large strain consolidation problems. Chapter 6 discusses the approach to solve the non-linear consolidation problem including creep for a pre-defined set of input parameters (Research Case). Chapter 7 contains summary remarks and conclusions. Chapter 8 includes the list of references. Details of the Cassagrande and Taylor's graphical methods are presented in Appendix A.

2. LITERATURE REVIEW

2.1 Small Strain Consolidation

2.1.1 Terzaghi's 1D Consolidation Theory

Terzaghi's theory is commonly used by geotechnical engineers to calculate consolidation settlements. The theory is based on the continuity equation (mass conservation law), the one-dimensional fluid flow relationship (Darcy's law) and the principle of effective stress. The governing differential equation can be expressed as

$$c_v \frac{\partial^2 u}{\partial z^2} = \frac{\partial u}{\partial t} , \qquad (2.1a)$$

where u is the excess pore pressure, t is time, c_v is the coefficient of consolidation and z is the vertical coordinate (i.e. the theory assumes that the vertical drainage is a dominant mechanism for the excess pore pressure dissipation after loading).

Terzaghi's theory is based on several assumptions, see e.g. Craig (1997). First, the soil is homogeneous. Second, the soil is fully saturated. Third, both water and the solid particles are incompressible. Fourth, the soil deformation and the flow of water are one-dimensional (vertical). Fifth, strains are small. Sixth, Darcy's law is valid at all hydraulic gradients. Seventh, the coefficient of permeability and the coefficient of volume compressibility remain constant throughout the consolidation process. Eighth, there is a unique relationship, independent of time, between void ratio and effective stress. The classical theory doesn't account for secondary compression. Consequently, Terzaghi's theory may not be applicable for general settlement predictions, e.g. the use of Terzaghi's theory to describe consolidation of very soft/compressible soils may result in significant errors in both the predicted consolidation time and the settlement magnitude. These errors can be traced to the inability of the classical theory to account for large strains, as well as its inability to account for the non-linearity of the governing equation caused

4

by changes in the compressibility and hydraulic conductivity with the progressive soil settlements.

2.1.2 Degree of Consolidation for Terzaghi's 1D Consolidation Theory

The average degree of consolidation, U_z, for the deforming soil layer can be defined in terms of the average excess pore pressure and in terms of the total settlement. The average degree of consolidation in terms of the consolidation settlement is defined by Equation (2.1b)

$$U_z = \frac{\delta_c(t)}{\delta_{c,ult}} = \frac{e_0 - e(t)}{e_0 - e_f} \ , \tag{2.1b}$$

where $\delta_c(t)$ is the consolidation settlement dependent on time, $\delta_{c,ult}$ is the ultimate consolidation settlement at the end of the primary consolidation, e_0 is the initial void ratio, $e(t)$ is the void ratio at time t after the start of consolidation, and e_f is the void ratio at the end of consolidation. The average degree of consolidation in terms of excess pore pressures is defined by Equation (2.1.c)

$$U_z = 1 - \frac{\frac{1}{2H_{dr}} \int_0^{2H_{dr}} u_e(z,t)dz}{u_i} \ , \tag{2.1c}$$

where u_i is the initial excess pore pressure (equal to $\Delta\sigma_z$, i.e. the change in the vertical total stress due to the applied load), $u_e(z,t)$ is the excess pore pressure at depth, z, and time, t, and H_{dr} is the longest drainage path required for the water particle to exit the soil during the consolidation process. Due to the assumed linear relationship between stresses and displacements, the calculated degrees of consolidation, U_z, defined either in terms of displacements (Equation 2.1b) or in terms of excess pore pressures (Equation 2.1.c) are equal. I.e., in the classical theory of consolidation, Equations (2.1b) and (2.1c) are interchangeable.

To calculate U_z for the time of interest, one needs to integrate the excess pore water pressure profile $u_e(z,t)$ with depth. The excess pore water pressure is defined by Equation (2.1d).

$$\frac{u_e(z,t)}{\Delta\sigma_z} = \sum_{N=0}^{\infty}\left(\frac{4}{(2N+1)\pi}sin\left[\frac{(2N+1)\pi}{2}\left(\frac{z}{H_{dr}}\right)\right]e^{-\left[\frac{(2N+1)^2\pi^2}{4}T_v\right]}\right) \qquad (2.1d)$$

where

$\frac{u_e(z,t)}{\Delta\sigma_z} =$ the excess pore pressure at a given depth, z, and a given time, t, normalized by the initial load (i.e. normalized by the initial total stress increment)

$\frac{z}{H_{dr}} =$ the depth of the consolidating layer (measured from the layer surface) normalized by the maximum drainage distance

N $=$ summation index

$T_v =$ dimensionless measure of time called the time factor

The time factor is defined as

$$T_v = \frac{c_v t}{(H_{dr})^2} \qquad (2.1e)$$

where t denotes the elapsed time measured from the moment of the load application and c_v is the coefficient of consolidation (discussed in more detail in Chapter 3). When using the Terzaghi's consolidation theory, the time factor, T_v, can be determined from the known degree of consolidation, U_z, utilizing Equations (2.1f) and (2.1g).

$$T_v = \frac{\pi}{4}\left(\frac{U_z(\%)}{100}\right)^2 \quad U_z \leq 0.6 \qquad (2.1f)$$

$$T_v = 1.781 - 0.933\,log\big(100 - U_z(\%)\big), \quad U_z > 0.6 \qquad (2.1g)$$

Based on the Terzaghi's 1D consolidation theory, the excess pore pressure generated by an increase in total stress on the soil mass becomes zero at the infinite time. For the finite

6

time values, the excess pore pressure never becomes zero but follows the exponential decay in time as defined by Equation (2.1d). Consequently, the degree of consolidation of 100% cannot be achieved during the finite time (measured from the moment of the load application). In practice, however, the calculated degree of consolidations of 95%, 99% or higher, is often rounded to 100% with the associated time of consolidation assumed to correspond to the end of primary consolidation.

2.1.3 Coefficient of Consolidation for Terzaghi's 1D Consolidation Theory

To solve the governing equation for the Terzaghi's 1D consolidation, Equation (2.1a), one needs to define the coefficient of consolidation c_v.

$$c_v = \frac{k}{m_v * \gamma_w} \qquad (2.1h)$$

where γ_w stands for the unit weight of water, k is the hydraulic conductivity, and m_v is the coefficient of volume compressibility. The m_v parameter can be expressed as

$$m_v = \frac{a_v}{1 + e_0} \qquad (2.1i)$$

where a_v is the coefficient of compressibility and e_0 is the initial void ratio. The coefficient of compressibility is defined by Equation (2.1j)

$$a_v = -\frac{de}{d\sigma'} \qquad (2.1j)$$

Equation (2.1j) expresses the slope of the void ratio - effective stress curve. The negative sign in Equation (2.1j) denotes positive compression, i.e. the negative sign in Equation (2.1j) ensures that the a_v value remains positive as the void ratio decreases.

2.1.4 Biot's Consolidation Theory

The classical theory of consolidation was developed by considering long-term deformations of a one-dimensional soil column. Biot (1940) extended the treatment of consolidation to three-

7

dimensions by considering equilibrium of the elastic porous medium and the flow equations governed by the Darcy's law. Hence, the Biot's consolidation theory is also referred to as the theory of poro-elasticity. Biot's (1940) formulation is based on the following assumptions; first, isotropy of the material; second, reversibility of stress-strain relations under final equilibrium conditions; third, linearity of stress-strain relations; fourth, small strains; fifth, the water contained in the pores is incompressible; sixth, the water may contain air bubbles; and seventh, the water flows through the porous skeleton according to Darcy's law. Due to restrictive formulation of the deformation properties, Biot's theory is generally not applicable for evaluating consolidation of soft soil materials.

2.2 Large Strain Consolidation

2.2.1 Shortcomings of Terzaghi's Theory

Terzaghi's consolidation theory assumes small strain deformations and is therefore valid for relatively stiff soil deposits. Deformations of soft and very soft soils are difficult to evaluate based on Terzaghi's approach, because the soil behavior of these deposits is often governed by large strain effects. For soft soils, the coefficient of permeability and the coefficient of volume compressibility typically exhibit significant changes during the consolidation process. These changes are difficult to capture by using Terzaghi's theory. In addition, Terzaghi's approach ignores the influence of the soil's self-weight which may be a significant factor for determining consolidation settlements of soft and very soft soil deposits. The large strain consolidation approach is often necessary to provide realistic settlement predictions for soft soil deposits.

Therefore, the major shortcoming of the numerical approach based on classical Terzaghi's formulation is its failure to update material parameters (soil permeability and compressibility) during the calculation process. Moreover, soil's material properties may depend not only on the vertical effective stress, but also on the rate of change of stress and strain during the consolidation process. Specifically, some soils are known to exhibit volumetric creep effects, i.e., a gradual decrease in the void ratio while the effective stresses are kept constant.

2.2.2 Finite Strain Theory

Gibson, England and Hussey (1967) developed the one-dimensional (1D) nonlinear consolidation theory that is unrestricted with respect to the magnitude of deformation. Differences between the small strain and the finite strain theories are explained in the following paragraphs.

9

When soil is restricted to "small deformations" during the consolidation process, the governing equation can be solved by using the small strain (also known as infinitesimal strain) approach, commonly applied when solving Terzaghi's equation (2.1a). In contrast, Gibson et al. (1967) developed the consolidation theory allowing for the "large-strain" or "finite strain" deformation.   Gibson et al. (1967) theory allows for the change in material properties during the consolidation process resulting in the non-linear governing equation. The governing equation for the classical consolidation theory, Equation (2.1a), is linear. Generally, both the linear and the non-linear differential equations can be solved by using either the small strain or the large strain approach. In practice, however, the classical (linear) equation of consolidation, Equation (2.1.a), is typically solved by using the small-strain approach while the non-linear consolidation equations are solved by using either the small-strain or the large strain methods.

The differences between the small strain and the large strain methods can be explained by considering the selected frame of reference, i.e. the use of the coordinate system. The small strain approach, commonly applied when using the classical consolidation theory, is based on the Eulerian coordinate system for which the reference coordinates are fixed in space. Thus, the excess pore pressure in a consolidating clay layer is measured at a point in a fixed reference frame. The movement of material particles (i.e. the soil's porous skeleton) is determined with respect to the initial reference frame (the Eulerian coordinate system).

The convective coordinate system refers to coordinates related to a fixed amount of solid material. The coordinate system is allowed to move with the movement (convection) of the solid particles which is tantamount to the definition of the Lagrangian coordinate system. In the Lagrangian coordinate system, the position coordinates and velocity components are all independent variables and they all refer to an initial $t = 0$ configuration. Unlike the Eulerian

coordinate system, the Lagrangian approach considers coordinates enclosing the same material particle, i.e. the coordinate system allows for movements and distortions of the control element as the time progresses. For the finite strain consolidation problems, the thickness of the soil sample is constantly changing, i.e. the problem domain boundary is always moving. The time dependent location of the top/surface boundary makes it inconvenient to follow in the Eulerian coordinate system. The use of Lagrangian coordinates overcomes this problem because the material spatial coordinate is fixed, i.e., it is always in its original location. The use of convective coordinates can be now viewed as the application of a modified Eulerian coordinate system with the advantages offered by the Lagrangian system. In numerical applications such as PLAXIS, the use of convective coordinates should be viewed as equivalent to the mesh updating approach.

The Lagrangian and the convective coordinate descriptions are illustrated in Fig 2.2a. The initial configuration ($A_0B_0C_0D_0$) indicates the control volume before start of the consolidation process. The bottom boundary of the layer is assumed to be fixed in space. The control volume ($A_0B_0C_0D_0$) has the coordinate position "a" and the thickness δa. The distance "a" is the Lagrangian coordinate. With time, the initial soil layer shown in Fig 2.2a (a), will change its configuration as shown in Fig 2.2a (b). While the datum plane remains fixed, the top surface has settled and the control volume has deformed to a new position (ABCD). The distance ξ defines position of a point in the soil domain as a function of time; the distance ξ is the convective coordinate. The concept of a convective coordinate system (ξ, t) system, presented in Figure 2.2a, was introduced by Gibson et al (1967).

11
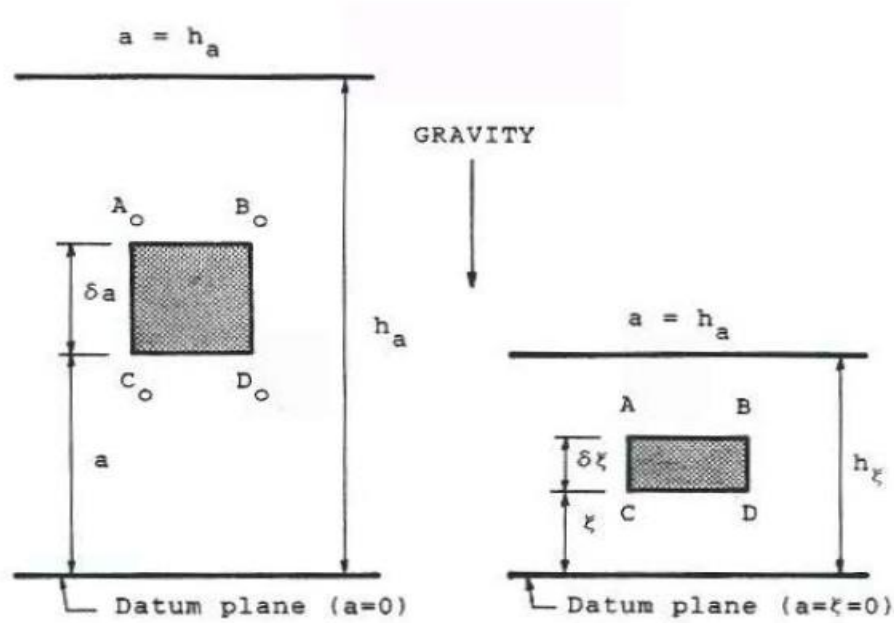
Figure 2.2a Lagrangian and Eulerian coordinates : (a) Initial configuration at t = 0; (b) configuration at time t

Another coordinate system, which is commonly referred to as a reduced or normalized Lagrangian coordinate system is especially useful for the consolidation analysis of soft soils, since it is based upon the volume of soil particles lying between the datum plane and the point being analyzed. Figure 2.2b outlines the differences between coordinate systems. Based on Figure 2.2b, the relationships between coordinates in different coordinate systems can be expressed as

$$\frac{\partial a}{\partial \xi} = \frac{1 + e_0}{1 + e} \tag{2.2a}$$

$$\frac{\partial \lambda}{\partial a} = \frac{1}{1 + e_0} \tag{2.2b}$$

$$\frac{\partial \xi}{\partial \lambda} = 1 + e \tag{2.2c}$$

12
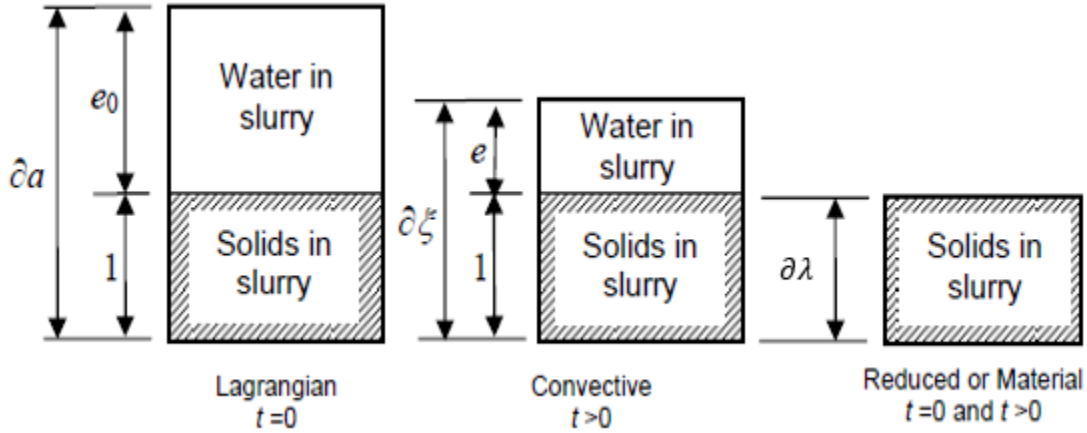
Figure 2.2b Void ratio for Lagrangian, Eulerian (convective), and material (reduced/normalized Lagrangian) coordinate.

Gibson et al. (1967) formulated the consolidation theory using the reference framework of a material coordinate system while allowing for the nonlinear compressibility and permeability relationships. The finite strain consolidation theory by Gibson et al. (1967) is formulated in terms of void ratios, i.e. it uses the void ratio as an independent variable. The basic continuity equation is expressed as

$$\frac{\partial e}{\partial t} = - \frac{\partial}{\partial \lambda}\left((v_w - v_s)\frac{e}{1+e}\right) , \tag{2.2d}$$

where t denotes time, λ is the spatial/material coordinate, v_w is the velocity of water and v_s is the solids velocity.

Darcy (1856) proposed an empirical law for the flow of water through a fixed porous skeleton. However, in large strain consolidation problems, solid particles move relative to water. Gersevanov (1934) modified the Darcy's law to take the relative movement of solid particles into account. The Darcy-Gersevanov's law can be expressed as

$$\frac{e}{1+e}(v_w - v_s) = -k\frac{1}{\gamma_w}\frac{\partial u_e}{\partial \xi} , \tag{2.2e}$$

13

where v_w is the water velocity, v_s is the solid velocity, k is the permeability, γ_w is the unit weight of water, and u_e is the excess pore pressure. The total stress gradient can be expressed by considering the equilibrium of a two-phase mixture. Assuming the positive upward orientation of the material coordinate (i.e., against the direction of gravity), the vertical equilibrium of a two-phase mixture is expressed as

$$\frac{\partial \sigma}{\partial \xi} = -\frac{e}{1+e}\gamma_w - \frac{1}{1+e}\gamma_s \ , \qquad (2.2f)$$

where σ is the total vertical stress and γ_s is the unit weight of solids. The total and effective stresses in a two-phase mixture can be expressed by employing the effective stress principle:

$$\sigma = \sigma' + u_w = \sigma' + u_h + u_e \ , \qquad (2.2g)$$

where σ' is the effective stress, u_w is the pore water pressure, u_h is the hydrostatic pore pressure and u_e is the excess pore water pressure.

After combining equations (2.2d) to (2.2g), the Gibson's consolidation equation can now be written as

$$\frac{\partial e}{\partial t} + \left(\frac{\gamma_s}{\gamma_w} - 1\right)\frac{d}{de}\left[\frac{k(e)}{1+e}\right]\frac{\partial e}{\partial \lambda} + \frac{\partial}{\partial \lambda}\left[\frac{k(e)}{\gamma_w(1+e)}\frac{d}{de}[\sigma'(e)]\frac{\partial e}{\partial \lambda}\right] = 0 \qquad (2.2h)$$

14

2.3 Secondary Compression

2.3.1 Overview of Secondary Compression

A conventional approach adopted in the majority of cases in today's engineering practice is to assume that the secondary compression occurs after the primary consolidation is largely completed, i.e. at the point at which the magnitude of excess pore pressures is negligible. The governing physical mechanisms responsible for the secondary compression are not fully understood. However, particle reorientation during the loading process, viscous creep, and decomposition of organic materials are some of the factors responsible for settlements in addition to those predicted by the consolidation theory. However, in contrast to the consolidation settlements, an additional deformation due to secondary compression is not caused solely by changes in the vertical effective stress; it will also occur at a constant effective stress. Therefore, the secondary compression is time-dependent and can lead to significant deformations in plastic clays, organic soils, and sanitary landfills, but is typically negligible in sands and gravels. The secondary compression index, also known as the coefficient of secondary compression, Ca, defines the rate of secondary compression. The Ca value can be defined in terms of the change in void ratio or the change in the volumetric strain as defined by Equation (2.3a) and Equation (2.3b)

$$C_a = -\frac{\Delta e}{\Delta \log t} \qquad (2.3a)$$

$$\frac{C_a}{1 + e_p} = -\frac{\Delta \varepsilon_z}{\Delta \log t} \qquad (2.3b)$$

where e stands for the void ratio, e_p is the void ratio at end of primary consolidation, ε_z denotes the vertical (oedometer) strain, and t is time.

15

2.3.2 Secondary Compression vs Secondary Consolidation

Among geotechnical practitioners, "secondary compression" if often referred to as "secondary consolidation". However, Lo (1961) stated that using the term "secondary consolidation" is misleading, since the secondary compression settlements are realized under non-measurable (i.e., negligible) excess pore pressures, and thus, can hardly be attributed to the consolidation process. Leonards (1977) provided further clarification on the meaning of consolidation and compression. He stated that, based on the Terzaghi's definition, the term "compression" implies any kind of volume reduction and "consolidation" is a particular type of compression that is accompanied by a significant increase in the effective stress due to the corresponding reduction in the pore pressure. The term "primary consolidation" is reasonable since a decrease in volume is due to an increase in effective stresses. However, the term "secondary consolidation" is not reasonable since in this case the volume decreases while the effective stress remains constant.

There are many studies in the geotechnical literature reporting the secondary compression phenomena. In some of these cases, the creep can be modeled reasonably well by using the theories of visco-elasticity or visco-plasticity. For these models, the creep is represented by a viscous element, i.e. the stress is functionally related to the rate of deformation. Although the soil deformation models can be developed by including rheological (viscous) components, the creep behavior is usually described by specialized models, developed by calibrating model predictions against the actual soil behavior observed during the laboratory and in-situ testing. The available creep models support the use of the term "secondary compression" instead of "secondary consolidation" when describing soil deformations at negligible excess pore pressures.

16

2.3.3 Buisman's Theory

In 1936, Keverling Buisman, the first professor of soil mechanics at the Delft University, found out that, during the long-duration consolidation experiments, the deformations of clay did not approach a constant final value. Instead, Buisman found that the soil deformations could be approximated well by a straight line on a semi-logarithmic (log time – deformation) scale as:

$$\varepsilon = \varepsilon_p + \varepsilon_s \, log\left(\frac{t}{t_o}\right) \tag{2.3c}$$

where ε_p denotes the primary strain, ε_s is the secondary strain, t_o is a reference time (usually 1 day), and t is time.

Buisman (1936) used the term "secular effect" to describe deformations after the dissipation of excess pore pressures (see e.g., Szavits-Nossan, 1988) and proposed a semi-empirical formula for estimating the amount of secondary compression on the basis of laboratory test data. Assuming that the deformation in (2.3c) is caused by an increase in effective stresses, Δσ', and after introducing primary and secondary compression constants, α_p and α_s, one can write:

$$\varepsilon = \Delta\sigma'\left[\alpha_p + \alpha_s \, log\left(\frac{t}{t_o}\right)\right] \tag{2.3d}$$

The total consolidation settlement at time t can now be expressed as

$$z_t = h\Delta\sigma'\left[\alpha_p + \alpha_s \, log\left(\frac{t}{t_o}\right)\right] \tag{2.3e}$$

where z_t denotes the settlement at time t, h is the initial thickness of layer, $\Delta\sigma'$ is the effective stress increment, α_p is the primary compression constant, α_s is the secular or secondary compression constant. The compression constants are to be calculated per unit thickness and unit pressure. Based on the Buisman's (1936) approach, the C_a value in equations (2.3a) and (2.3b) is constant. However, it was found that the application of Buisman's consolidation equation may lead to poor settlement predictions due to significant overestimation of the long-term

17

deformations. The theory implicitly assumes that the secondary compression starts at t = 1 day. For in-situ soil deposits with a significant thickness, the secondary compression may start much later, i.e. the Buisman's theory will yield artificially large settlement predictions in these cases. Additional limitation of the Buisman's approach is the use of constant values for α_p and α_s coefficients. The primary and secondary compression coefficients are reported to be dependent on time and the stress state (Houkes, 2016). E.g., Koppejan (1948) expressed the compression coefficients as a function of effective stresses in accordance with the Terzaghi's logarithmic compression law.

2.3.4 Koppejan's Theory

Koppejan (1948) combined Terzaghi's compression law with the Buisman's expression for secondary compression to determine the following expression for volumetric strain:

$$\varepsilon = \left(\frac{1}{C_p} + \frac{1}{C_s}\log t\right)ln\frac{\sigma'_{v0} + \Delta\sigma'}{\sigma'_{v0}} \qquad (2.3f)$$

Equation (2.3f) can now be used to determine the expression for total settlement as.

$$z_t = h\left(\frac{1}{C_p} + \frac{1}{C_s}\log t\right)ln\frac{\sigma'_{v0} + \Delta\sigma'}{\sigma'_{v0}} \qquad (2.3g)$$

where z_t denotes the settlement at time t, h is the initial thickness of the soil layer, C_p is the Koppejan's primary compression coefficient, C_s is the Koppejan's secondary compression coefficient, σ'_{v0} is the initial overburden pressure, and $\Delta\sigma'$ is the pressure increase due to loading. Limitations of the Koppejan's approach were discussed by Houkes (2016): first, the compression coefficients C_p and C_s may not be constant; second, if the initial effective stress is too small comparatively to the load increment, the calculated strains will be unrealistically high; third, Koppejan's approach is based on the implicit assumption that secular or secondary compression occurs after 1 day.

18

2.3.5 Mesri's Theory

Mesri and Godlewski (1977) conducted a detailed study on the relationship between *Ca* and *Cc* and concluded that the volume changes during secondary compression and primary consolidation are consistent with the Terzaghi's effective stress principle. They proposed the concept of *Ca/Cc*, where *Ca* stands for the secondary compression index and *Cc* is the compression index (the slope of the compression (e-log σ') curve in the normally consolidated range). Mesri and Godlewski (1977) pointed out that *Ca* is strongly dependent on the final effective stress. The value of *Ca* defines the slope of "e-log (t)" curve and is defined by Equation (2.3a) while the *Cc* value is defined as

$$C_c = -\frac{\Delta e}{\Delta \log \sigma'_v} \qquad (2.3h)$$

According to Mesri and Godlewski (1977), the *Ca/Cc* ratio is a constant value for the considered soil type, i.e. it does not change with time, the level of effective stress, or the void ratio. Therefore, for the known compression curve (e-log σ') relationship and for the known effective stress at the end of primary consolidation, one can evaluate effects of the secondary compression for a given *Ca/Cc* ratio.

Choi (1982) and Mesri and Castro (1987) presented more information supporting the use of a constant *Ca/Cc* value for different soil types and for a wide range of effective stresses, void ratios, and loading conditions. They notice that the value of *Ca* approaches its maximum for effective stresses close to the preconsolidation pressure, and that it may also change with time. However, these changes in *Ca* value are accompanied with similar changes in the *Cc* values, allowing to treat the ratio *Ca/Cc* as a constant value for investigated soils. Figure 2.3a illustrates the graphical procedure using the Mesri's creep model for three consolidation pressures. One can consider point "a" at the end of the primary consolidation line on the $e - \log \sigma'_v$ plot. By

19

projecting the void ratio on the $e - \log t$ plot, the rate at which the void ratio changes with time is determined by the gradient of the curve Ca. From point "a" onwards, the creep will reduce the void ratio at a constant effective stress to the void ratio corresponding to point "b". The rate at which the soil creeps, can again be found by projecting the void ratio to the $e - \log t$ curve. If the soil is re-compressed, it will follow a recompression line until reaching the primary compression line (EOP), as illustrated by point "c" in Figure 2.3a (see Bartholomeeusen, 2003).

Some researchers, however, discuss potential shortcomings of the Mesri's theory. Watabe et al. (2012) and Leroueil (2006) provide the evidence for the variable Ca/Cc value. Their evaluation of available laboratory and field data indicates that the Ca/Cc ratio decreases with the decrease in the visco-plastic strain rate. In addition, Kurz, Sharma, Alfaro, and Graham (2006) reported the increase in creep settlement values with the increase in soil temperature for normally consolidated soils. Therefore, Mesri and Godlewski's (1977) theory may require adjustments and/or revisions when considering specific loading and soil conditions.
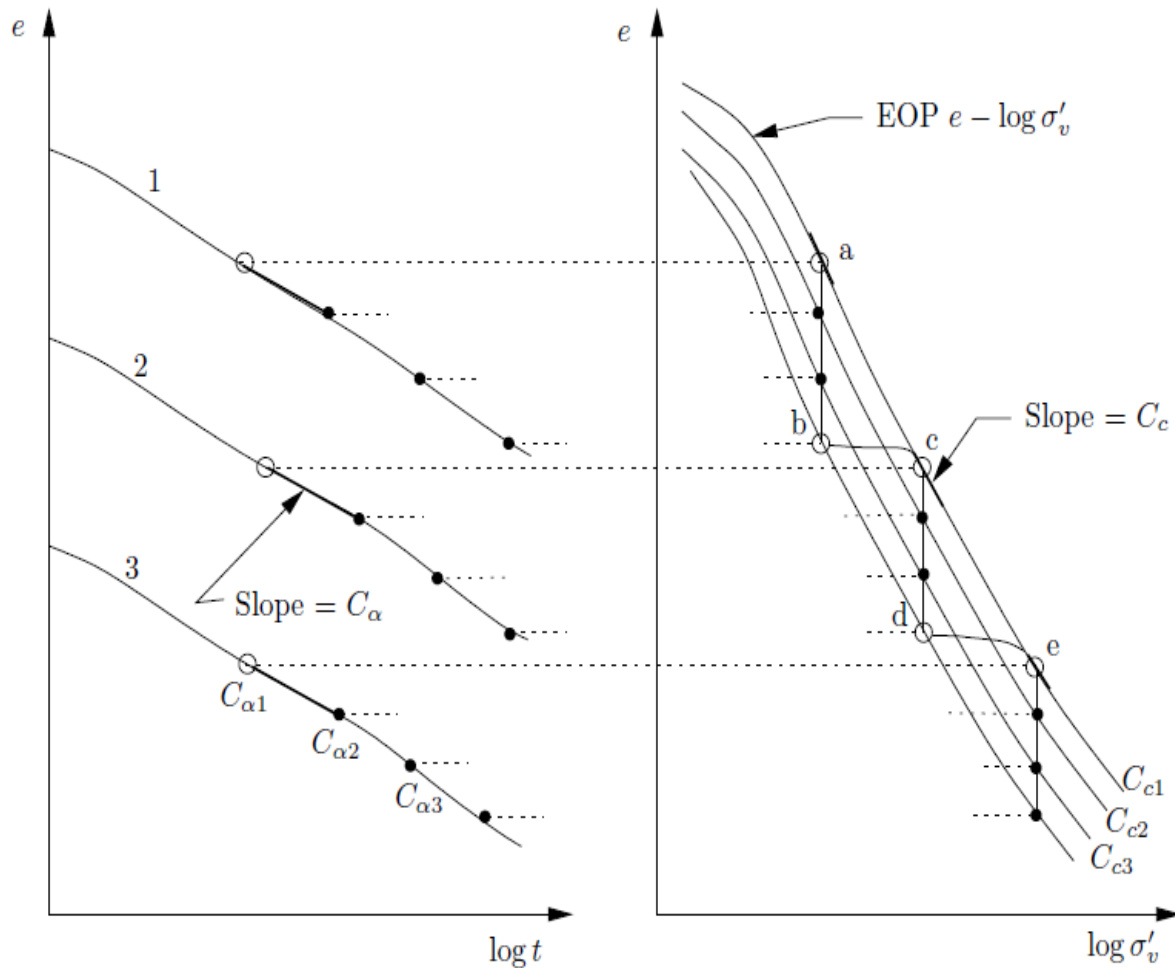
Figure 2.3a Corresponding values of Ca and Cc at any instant (e, σ′$_v$, t) during secondary compression (Mesri and Godlewski 1977; Mesri and Casto 1987) (Bartholomeeusen, 2003)

2.3.6 Bjerrum's Theory

Bjerrum (1967) presented results of the creep behavior of Drammen clay in Norway by introducing concepts of the instant compression and the delayed compression and compared these concepts to the framework of primary and secondary consolidation (see Figure 2.3b).

Instant compression occurs simultaneously with the increase in effective stress and causes a reduction in the void ratio until an equilibrium value is reached at which the structure effectively supports the overburden pressure, i.e. instant compression corresponds to the settlement and the

void ratio profile that would occur without water in the pores retarding the compression process. Delayed compression represents the reduction in volume at unchanged effective stresses.

The concepts of instant and delayed compression are illustrated in Figure 2.3b. The effective stress increases gradually due to the viscosity of water, and the compression occurs as represented by the solid line. The dashed line at the origin, at t = 0, represents the value of instant compression, assuming an immediate application of effective stress, which practically can't be achieved as it would imply a completely pervious soil structure. The division of compression into primary and secondary parts is considered to be rather arbitrary (Bjerrum 1967) as the time required for dissipation of excess pore water pressures is dependent on factors such as the thickness of the clay layer, its permeability and the drainage conditions.   Hence, Bjerrum (1967) declared the division of compression into primary and secondary parts to be unsuitable of describing the behavior of the soil structure with respect to effective stresses.

It should be noted that the delayed compression concept is similar to the approach initially introduced by Suklje (1957) who defined isotaches as graphs relating intergranular pressure σ_v' to void ratios e for a constant rate of change of the void ratio $\delta e/\delta t$. The timelines concept of Bjerrum (1967) and the isotache concept of Suklje (1957) are identical when the strain rate on the sedimentation line (i.e., the compression line that corresponds to a specific delay time), defined by Bjerrum (1967), is constant.

22
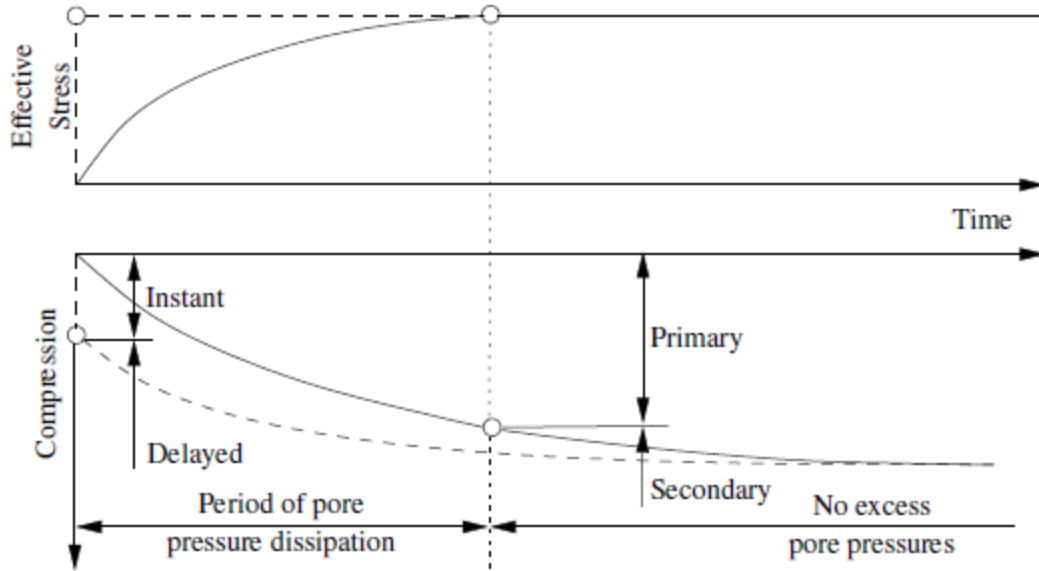
Figure 2.3b. Definition of instant and delayed compression compared to concept of primary and secondary compression, after Bjerrum (1967) (adopted from Bartholomeeusen, 2003)

2.3.7 Hypotheses A and B

As noted in the previous chapters, there is a controversy among the geotechnical engineers in the treatment of creep related to a question when does the creep occur. There are two hypotheses: Hypothesis A and Hypothesis B. In Hypothesis A, the secondary compression occurs only after the end of primary consolidation (EOP). Hypothesis A allows for the law of square of the drainage path length to be used when calculating the required time to reach the EOP consolidation, implying the same value of the compressive strain at the EOP in the field and in the laboratory. In contrast, Hypothesis B assumes that the secondary compression effects exist during the dissipation of excess pore pressures and are governed by some type of "structural" viscosity. I.e., Hypothesis B assumes that some type of creep mechanism is active during both the primary and the secondary compression, which may result in substantially larger compressive strains than predicted by Hypothesis A when considering deformations of a relatively thick soil

23

layer. The scale effects, however, have not been verified conclusively as different researchers report results supporting either Hypothesis A or Hypothesis B predictions.

Hypothesis A is supported by the research that validates constant *Ca/Cc* proposed by Mesri and Godlewski (1977), Mesri and Castro (1987), as well as the equivalent strain concept at the EOP proposed by Mesri & Choi (1985). The constant *Ca/Cc* concept can support both hypotheses A and B, but the same strain concept at the EOP supports only Hypothesis A. The research by Jamiolkowski et al. (1985) indicates that the process responsible for creep occurs only after the excess pore water pressures have dissipated, i.e., after the end of primary consolidation. Jamiolkowski et al. (1985) assume that the same mechanisms responsible for the increase in effective stresses are governing the secondary compression behavior.

The second approach, i.e. Hypothesis B, is supported by the research that validates the isotache concept initially proposed by Suklje (1957). Bjerrum (1973) reported that the creep occurs together with the primary consolidation and continues as a secondary compression process when the primary consolidation has ceased. Bjerrum (1973) assumes that the strain at the end of primary consolidation increases for thicker soil deposits.

Both hypotheses assume that the primary consolidation is governed by the dissipation of excess pore pressures. Figure 2.3c illustrates the conceptual differences between Hypotheses A and B by using the graph of void ratio vs. vertical effective stress, and the graph of strain vs. time.
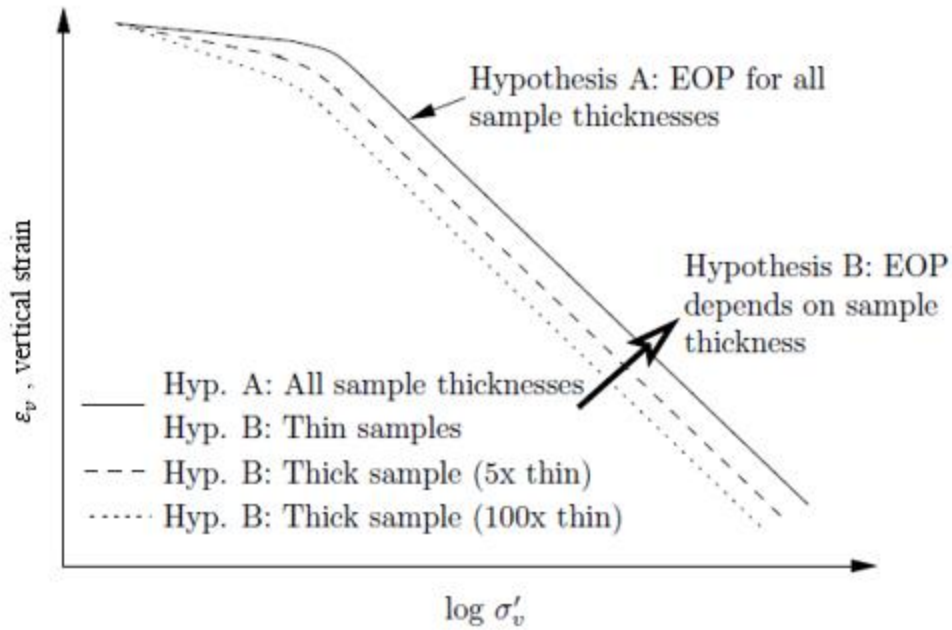
(a) Strain vs stress at end of primary consolidation
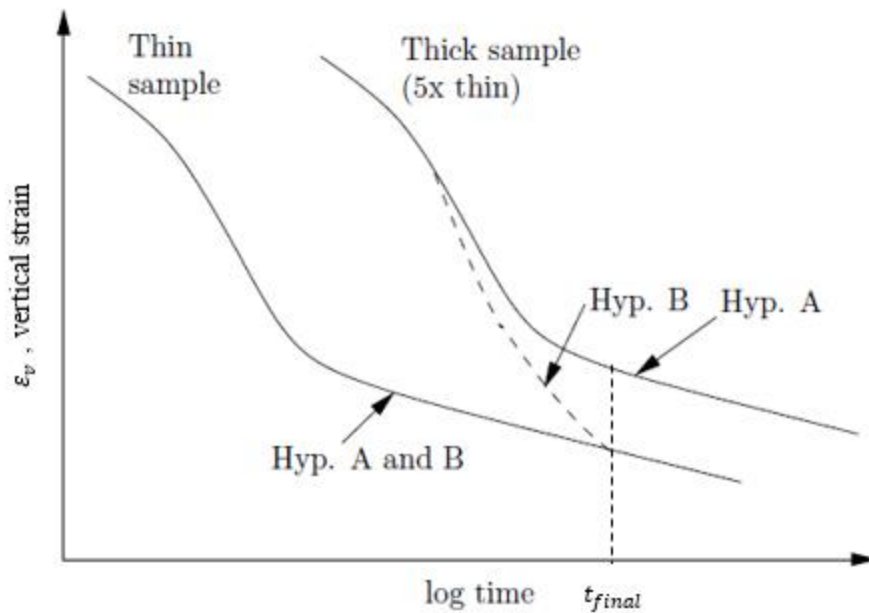
(b) Strain vs time for OCR of 1, samples having equal initial conditions and $\Delta\sigma_v$

Figure 2.3c. Comparison between hypotheses A & B in terms of (a) Strain vs vertical effective stress and (b) Strain vs time, after Jamiolkowski et al. (1985) (after Bartholomeeusen, 2003)

25

2.3.8 General Classification of Creep Models

Leroueil et al. (1985) categorized over 25 different rheological models into four categories, as defined by Equations (2.3i), (2.3j), (2.3k), and (2.3l).

$$R(\sigma_v', e) = 0 \tag{2.3i}$$

$$R(\sigma_v', e, t) = 0 \tag{2.3j}$$

$$R(\sigma_v', e, \dot{\sigma}_v', \dot{e}) = 0 \tag{2.3k}$$

$$R(\sigma_v', e, \dot{e}) = 0 \tag{2.3l}$$

In the above equations, e is the void ratio, σ_v' is the vertical effective stress, and t is time. The rates of change of the void ratio and the effective stress are defined as $\dot{e} = \partial e / \partial t$, and $\dot{\sigma}_v' = \partial \sigma_v' / \partial t$.

Equation (2.3i) is representative of models in which the effective stress-void ratio response of the soil is unique and independent of time or strain rate. This is the case for the classical Terzaghi's theory of consolidation in which a linear effective stress – void ratio relation is assumed. Buisman (1936) demonstrated that the constitutive model provided by Equation (2.3i) is not sufficient to provide a complete description of the clay behavior. Koppejan (1948), Bjerrum (1967), and Hansen (1969) have proposed models represented by Equation (2.3j) in which the void ratio is a function of the effective stress and time. However, a major difficulty with these models is to define a time origin for the secondary compression, particularly when the applied load varies with time. The creep formulation proposed by Equations (2.3k) and (2.3l) overcomes this difficulty since the behavior of the material is fully defined by state parameters in the current time step, i.e. the soil behavior is not a function of previous soil history. Taylor and Merchant (1940) were first to suggest a model of the type presented by Equation (2.3k) for which the rate of change of the void ratio is a function of the effective stress, the current value of

26

the void ratio itself and the rate of change of the effective stress. Equation (2.3l), indicates a unique relationship between the effective stress, the void ratio and the rate of change of the void ratio. This type of creep can be represented in the e - σ'_v diagram by $\dot{e}$ = constant lines called isotaches as initially proposed by Suklje (1957).

Leroueil et al. (1985) proposed two equations based on the rheological behavior of natural clays, expressed by Equation (2.3m) and Equation (2.3n). Equations (2.3m) and (2.3n) can be combined to obtain the general rheological Equation (2.3o), see e.g., Leroueil (1985).

$$\sigma'_p = f(\dot{\varepsilon}_v) \tag{2.3m}$$

$$\sigma'_v/\sigma'_p = g(\varepsilon_v) \tag{2.3n}$$

$$\dot{\varepsilon}_v = f^{-1}\left(\frac{\sigma'_v}{g(\varepsilon_v)}\right) \tag{2.3o}$$

2.3.9 Leroueil's Theory

Leroueil et al. (1985) proposed the model for which the creep rate is expressed as a function of the pre-consolidation pressure, see Equation (2.3m). The creep formulation with the constant *Ca* value, is unrealistic as it eventually yields negative values of the void ratio. Watabe et al. (2012) reported decreasing trend of the *Ca/Cc* values as the visco-plastic strain rates decrease (see Figure 2.3e).

Watabe et al. (2012) formulation relies on the constitutive model initially proposed by Leroueil et al. (1985). Watabe et al. (2012) employed the $\varepsilon_{vp} - \log p'$ relationship, where ε_{vp} is the visco-plastic strain, which is defined as the difference between total strain ε, obtained from the consolidation tests, and elastic strain ε_e as illustrated in Figure 2.3d.

$$\varepsilon_{vp} = \varepsilon - \varepsilon_e \tag{2.3p}$$

27

The relationship between the effective stress and the viscoplastic strain is defined by the reference compression curve (see Figure 2.3d)

$$\frac{p'}{p'_c} = f(\varepsilon_{vp}) \tag{2.3q}$$

In Equation (2.3q), p' is the vertical effective stress (σ'_v) and p'_c is the consolidation yield stress (preconsolidation pressure σ'_p). The preconsolidation pressure, p_c', is defined as a function of the strain rate, $\dot{\varepsilon}_{vp} = d\varepsilon_{vp}/dt$ (see Figure 2.3e)

$$p'_c = g(\dot{\varepsilon}_{vp}) \tag{2.3r}$$

In order to define the relationships expressed by Equation (2.3q) and Equation (2.3r), constant rate of strain (CRS) consolidation tests and long-term (LT) consolidation tests must be performed (Watabe et al., 2012). The reference compression curve (Figure 2.3d) and the three isotache parameters (p'_{cL}, c_1, and c_2) are required to define the Watabe et al. (2012) creep model.
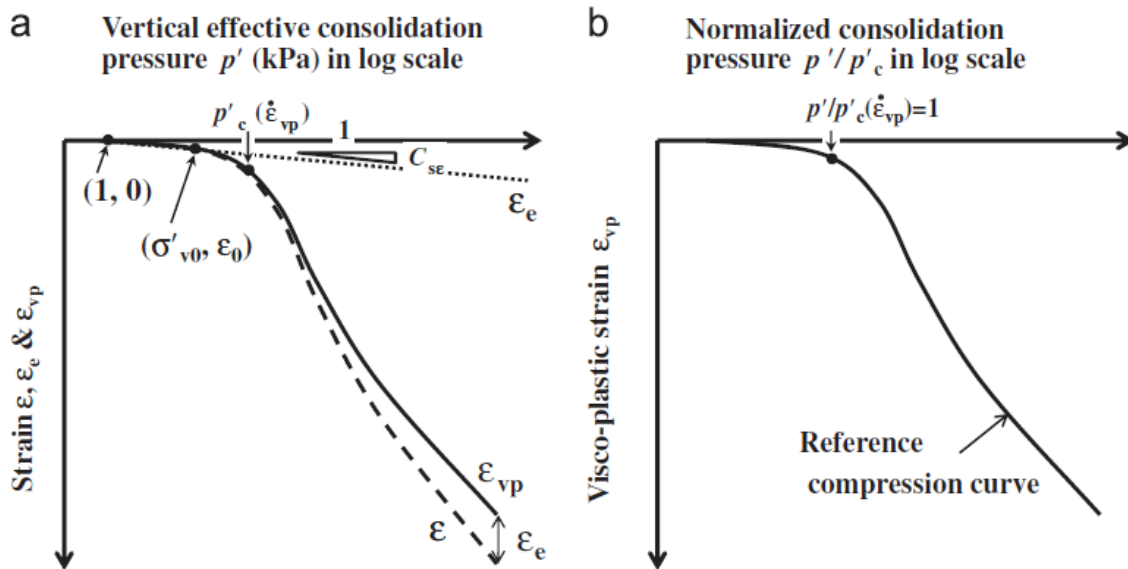
Figure 2.3d Compression curve ($\varepsilon - \log p'$ curve) : (a) definition of ε_e and ε_{vp} (b) reference compression curve.

28

The strain rate dependency defined by Equation (2.3r) can be expressed as

$$ln\frac{p'_c - p'_{cL}}{p'_{cL}} = c_1 + c_2 \, ln \, \dot{\varepsilon}_{vp} \qquad (2.3s)$$

In Equation (2.3s), parameters p'_{cL}, c_1 and c_2 are determined as a "best-fit" to the available experimental data. In addition, parameter p'_{cL} represents the lower limit of p'_c. When $\dot{\varepsilon}_{vp}$ decreases towards zero, p'_c converges towards p'_{cL}. Equation (2.3s) is similar to $p'_c = g(\dot{\varepsilon}_{vp})$ relationship previously proposed by Leroueil (2006) in which the slope α (defined as $\Delta \, log \, p'_{cL} / \Delta \, log \, \dot{\varepsilon}_{vp}$) decreases when $\dot{\varepsilon}_{vp}$ decreases to a very small value. Parameter c_1 is equal to $ln \, \{(p'_c - p'_{cL})/p'_{cL}\}$ at $\dot{\varepsilon}_{vp} = 1$. Parameter c_2 represents the level of strain-rate dependency.

Figure 2.3e (a) presents a comparison between the integrated fitting curve required for the Watabe et al. (2012) model and a constant C_a/C_c with $\alpha = 0.04$. Figure 2.3e (b) presents the relationship between α and the strain rate calculated from the integrated fitting curve. As seen in Figure 2.3e (b), $\alpha = C_a/C_c$ is not a constant and decreases when $\dot{\varepsilon}_{vp}$ decreases. In Figure 2.3e, p'_{c0} is p'_c corresponding to $\dot{\varepsilon}_{vp} = 1.0 \times 10^{-7} \, s^{-1}$.
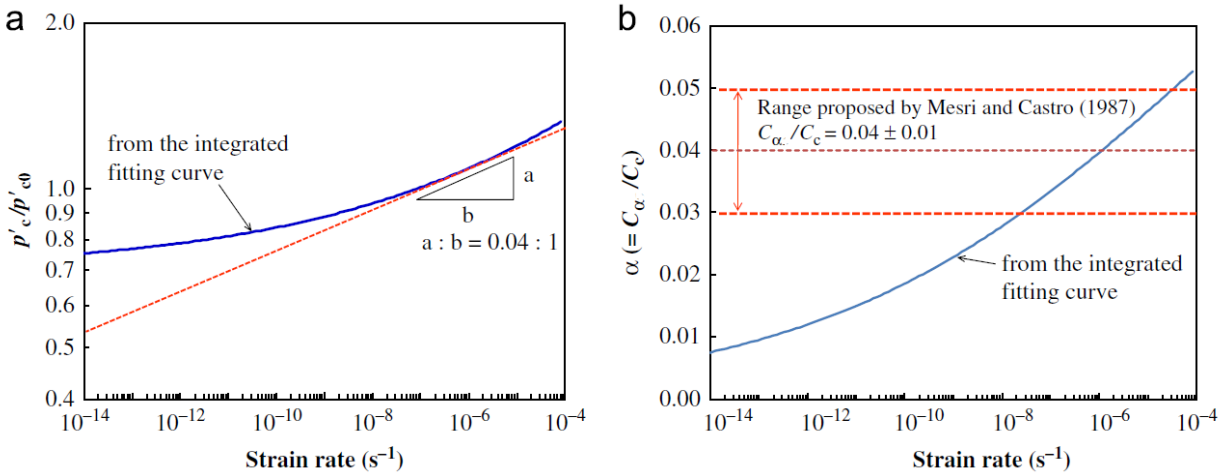
Figure 2.3e Comparison of the integrated fitting curve with the constant Ca/Cc concept : (a) relationship between p'_c/p'_{c0} and strain rate and (b) relationship between $\alpha \, (= C_a/C_c)$ and strain rate.

29

3. HOW EACH MODEL WORKS

3.1 CONDES

CONDES is a one-dimensional finite strain consolidation model developed at the University of Colorado at Boulder (Yao and Znidarcic, 1997). The code provides a numerical solution for the one-dimensional large strain consolidation problem by solving Gibson's et al (1967) equation.

Constitutive models used in CONDES define the relationship between the void ratio and the effective stress (Equation 3.1a) and the relationship between the hydraulic conductivity and the void ratio (Equation 3.1b). Parameters A, B, Z, C and D are obtained by fitting the proposed constitutive models to available experimental data. Parameters A, B, and Z define the compressibility curve, e-σ', i.e. the void ratio - effective stress relationship. Parameters C and D define the permeability curve, e-k, i.e. the void ratio - hydraulic conductivity relationship. Some useful relationships for fitting parameters A, B, and Z to experimental data are presented by Equation 3.1c. Similarly, useful relationships for fitting parameters C and D to experimental data are expressed as Equation 3.1d. Parameter A has the unit of $1/\text{stress}^B$ or stress^{-B}, B is unit-less, Z has the units of stress, C has the desired unit for the hydraulic conductivity, and D is unit-less. In Equations (3.1c) and (3.1d), e_1 is the void ratio at the end of consolidation, k_1 is the hydraulic conductivity at the end of consolidation, and e_0 is the initial void ratio.

$$e = A(\sigma' + Z)^B \tag{3.1a}$$

$$k = Ce^D \tag{3.1b}$$

$$A = \frac{e_0}{Z^B} \qquad B = \frac{ln\frac{e_1}{e_0}}{ln\frac{\sigma_1' + Z}{Z}} \qquad Z = \frac{\sigma_1'}{\left(\frac{e_1}{e_0}\right)^{\frac{1}{B}} - 1} \tag{3.1c}$$

30

$$C = \frac{k_1}{e_1^D} \qquad D = \frac{ln\frac{k_1}{C}}{ln \ e_1} \qquad\qquad (3.1d)$$

Based on Equation (2.1h), defining the coefficient of consolidation, Equation (3.1a),

defining the void ratio-effective stress relationship, and Equation (3.1e), defining the coefficient

of volume compressibility, the coefficient of consolidation can be expressed as Equation (3.1f)

by using parameters A, B, Z, C, and D (Yao and Znidarcic, 1997).

$$m_v = \frac{d\varepsilon}{d\sigma'} = -\frac{de}{d\sigma'}\frac{1}{1+e} \qquad\qquad (3.1e)$$

$$C_v = -\frac{C}{\gamma_w B} A^{D-1}(\sigma' + Z)^{1+B(D-1)}[1 + A(\sigma' + Z)^B] \qquad\qquad (3.1f)$$

The initial height of soil, H_i, can be expressed by Equation (3.1g)

$$H_i = H_s(1 + e_0) \qquad\qquad (3.1g)$$

During the consolidation process, the height of a soil column can be determined from the

calculated void ratio profile expressed as function of the height of solids

$$H = \int_0^{Hs} (1 + e)dz \qquad\qquad (3.1h)$$

$$H = H_s + \frac{A}{(G_s - 1)\gamma_w(B + 1)}\{[(G_s - 1)\gamma_w H_s + Z]^{B+1} - Z^{B+1}\} \qquad\qquad (3.1j)$$

Steady-state solutions for a variety of boundary conditions are evaluated numerically and are

reported in CONDES output files. The large-strain consolidation and constitutive equations are

implemented in CONDES without accounting for the creep mechanism.

31

3.2 Mathematica

Mathematica is a computer program for technical computing that allows for both numerical and symbolic evaluations. To facilitate comparisons between different consolidation programs available in engineering practice, a simplified finite-difference program for nonlinear consolidation and secondary compression was developed in Mathematica. Both, the explicit and implicit versions of the program were developed.

The governing equations used to develop finite difference schemes in Mathematica are presented by Equations (3.2a) and (3.2b).

$$\frac{1}{\gamma_w}\left(k\frac{\partial^2 u}{\partial z^2}+\frac{\partial u}{\partial z}\frac{\partial k}{\partial z}\right)-\frac{av}{1+e_0}\frac{\partial u}{\partial t}=0 \ (t<t_{ref}) \tag{3.2a}$$

$$\frac{1}{\gamma_w}\left(k\frac{\partial^2 u}{\partial z^2}+\frac{\partial u}{\partial z}\frac{\partial k}{\partial z}\right)-\frac{av}{1+e_0}\frac{\partial u}{\partial t}+\frac{\alpha}{t(1+e_0)}=0 \ (t\geq t_{ref}) \tag{3.2b}$$

Equation (3.2a) accounts for the non-linear consolidation without creep, i.e. Equation (3.2a) is used to evaluate soils behavior during the period of primary consolidation ($t<t_{ref}$). Equation (3.2b) accounts for the secondary compression of soil, i.e. it is used for times larger than t_{ref}. Alternatively, factor 1/t can be eliminated from Equation (3.2b) by using Equation (3.2c) as proposed by Brandenberg (2016).

$$\frac{1}{t}=\frac{1}{t_{ref}}exp\left(\frac{e-e_{ca,ref}}{\alpha}+\frac{C_c}{\alpha}log_{10}\left[\frac{\sigma_v'}{\sigma_{vca,ref}'}\right]\right) \tag{3.2c}$$

The explicit finite difference scheme used to calculate excess pore pressures in Mathematica

is expressed by Equation (3.2d).

32

$$u_i^{j+1} = \frac{\Delta t(1+e_{0_i}^j)}{av_i^j}\frac{1}{\gamma_w}\left[\frac{k_i^j}{0.5(\Delta z_i + \Delta z_{i-1})}\left(\frac{u_{i+1}^j - u_i^j}{\Delta z_i} - \frac{u_i^j - u_{i-1}^j}{\Delta z_{i-1}}\right)\right.$$

$$+ \frac{1}{2}\left(\frac{u_{i+1}^j - u_i^j}{\Delta z_i} + \frac{u_i^j - u_{i-1}^j}{\Delta z_{i-1}}\right)\frac{1}{2}\left(\frac{k_{i+1}^j - k_i^j}{\Delta z_i} + \frac{k_i^j - k_{i-1}^j}{\Delta z_{i-1}}\right) + \left.\frac{\alpha}{t(1+e_{0_i}^j)}\right]$$

$$+ u_i^j \quad (3.2d)$$

The implicit scheme was constructed after re-arranging the following equation for non-linear consolidation and creep:

$$u_i^j = u_i^{j+1} - \frac{\Delta t(1+e_{0_i}^j)}{av_i^{j+1}}\frac{1}{\gamma_w}\left[\frac{k_i^{j+1}}{0.5(\Delta z_i + \Delta z_{i-1})}\left(\frac{u_{i+1}^{j+1} - u_i^{j+1}}{\Delta z_i} - \frac{u_i^{j+1} - u_{i-1}^{j+1}}{\Delta z_{i-1}}\right)\right.$$

$$+ \frac{1}{2}\left(\frac{u_{i+1}^{j+1} - u_i^{j+1}}{\Delta z_i} + \frac{u_i^{j+1} - u_{i-1}^{j+1}}{\Delta z_{i-1}}\right)\frac{1}{2}\left(\frac{k_{i+1}^{j+1} - k_i^{j+1}}{\Delta z_i} + \frac{k_i^{j+1} - k_{i-1}^{j+1}}{\Delta z_{i-1}}\right)$$

$$+ \left.\frac{\alpha}{t(1+e_{0_i}^j)}\right]. \quad (3.2e)$$

Required input parameters for the Mathematica model are the initial height and the initial void ratio distribution before start of the consolidation process, increase in the vertical stress (applied at the top of the model), parameters defining the virgin compression curve, i.e. the compression index Cc and the reference void ratio, the specific gravity of soil solids, parameters defining permeability curve, i.e. the coefficient of permeability C_k and the reference void ratio, the secondary compression index Ca, time defining the beginning of secondary compression t_{ref}, the number of nodes required for the spatial discretization, and the output times.

The time increment used for explicit scheme calculations, Δt, is defined by Equation (3.2f).

33

$$\Delta t = \frac{CO * \Delta z^2}{cv_i} \qquad\qquad (3.2f)$$

Based on the Courant–Friedrichs–Lewy (CFL) condition, the constant CO value must be smaller than 0.5 for the numerical scheme stability (Courant, Friedrichs, & Lewy, 1967). In Equation (3.2f), cv_i is the value of the coefficient of consolidation at the beginning of the numerical simulation, and Δz is the distance between two nodes in the finite difference grid. The time step selection defined by Equation (3.2f) affects both the precision and the stability of numerical scheme. The magnitude of numerical errors was found to depend on the selection of the nodal distance and on the selected time step. The program execution time significantly increases by increasing the number of nodes and by decreasing the time step value. A trend between the simulation time and the adopted Δt value is illustrated in Table 3.2.

Table 3.2 Simulation Time vs. Time Step

Δt (year)	7.912E-04	3.956E-04	3.493E-04
Simulation time (sec)	8.335E+02	3.104E+03	5.480E+03

A comparison between the explicit and implicit schemes implemented in Mathematica is illustrated in Figure 3.2a and Figure 3.2b. Input parameters for these figures are discussed in more detail in Chapter 6 (Research Case). Figure 3.2a illustrates the solution without creep while Figure 3.2b presents the case that includes the secondary compression. In Figures 3.2a and 3.2b, the implicit scheme results are denoted as MI, while the explicit scheme solution is denoted as ME. The number next to MI and ME in the legend of Figures 3.2a and 3.2b denotes the value of the CO coefficient in Equation (3.2f). Figures 3.2a and 3.2b demonstrate that the explicit scheme requires smaller time steps for the numerical convergence than required for the implicit scheme, i.e. the implicit scheme is more stable.

34
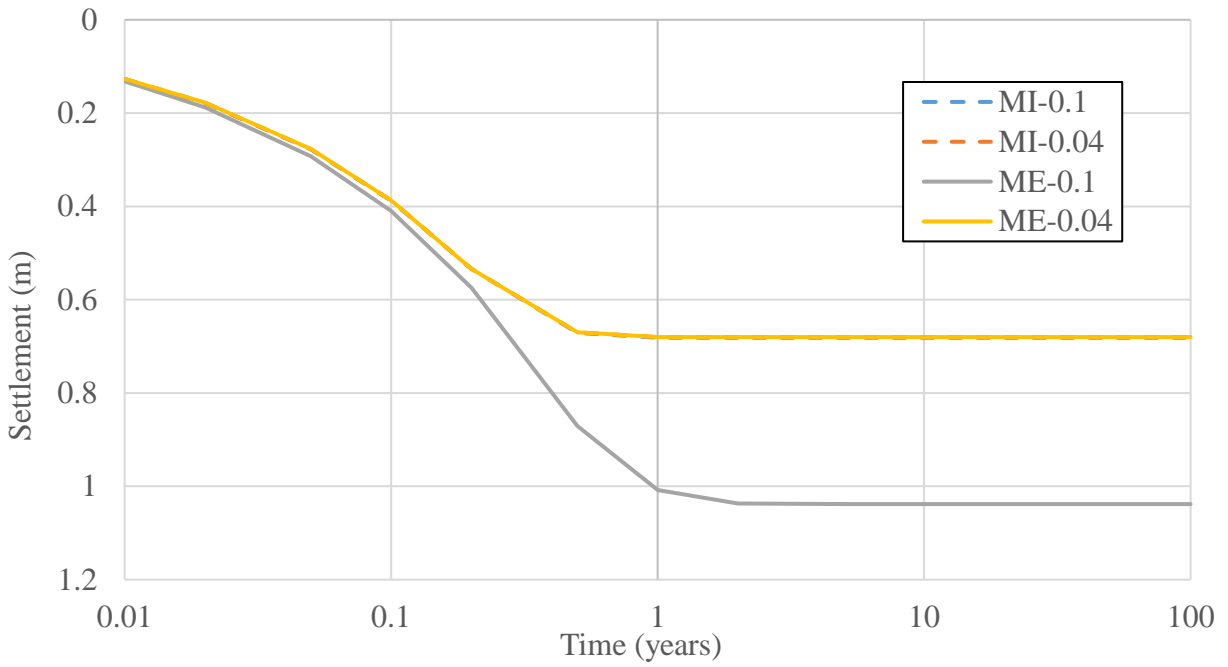
Figure 3.2a Settlement graph for Mathematica schemes (MI=Implicit, ME = Explicit) w/out creep
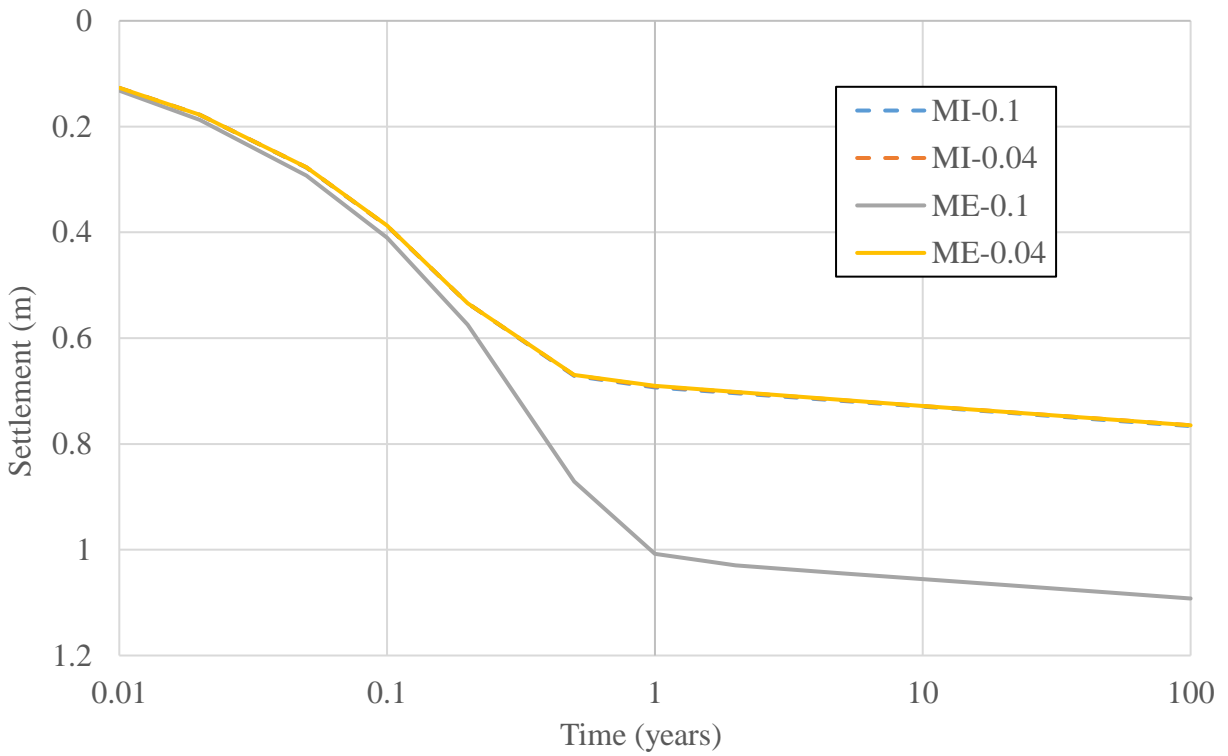
Figure 3.2b Settlement graph for Mathematica schemes (MI=Implicit, ME = Explicit) w/ creep

35

3.3 iConsol.js

Program iConsol.js is an implicit finite-difference code for solving one-dimensional problems of nonlinear consolidation and secondary compression that was developed by Brandenberg (2016) as a JavaScript and deployed through an HTML interface (http://www.uclageo.com/Consolidation/).

Brandenberg (2016) stated that the traditional approach for evaluating secondary compression is problematic for two fundamental reasons. First, the primary consolidation and the secondary compression occur simultaneously rather than occurring in distinct regions of time. The second problem with the traditional approach is that the benchtop clock provides an arbitrary time reference that is not fundamentally related to the state of the soil. Brandenberg (2016) proposed the approach that includes time reference, t_{ref}, parameter for the start of secondary compression but eliminates the benchtop clock effects, i.e. eliminates time variable by utilizing substitution defined by Equation (3.2c).

To calculate excess pore pressures and settlements resulting from the primary consolidation and the secondary compression process, Brandenberg (2016) utilized the form of the governing differential equations presented by Equation (3.3a).

$$\frac{1}{\gamma_w}\left(k\frac{\partial^2 u}{\partial z^2} + \frac{\partial u}{\partial z}\frac{\partial k}{\partial z}\right) - \frac{av}{1+e_0}\frac{\partial u}{\partial t}$$

$$+ \frac{\alpha}{t_{ref}(1+e_0)}exp\left[\frac{e-e_{c\alpha,ref}}{\alpha} + \frac{C_c}{\alpha}log\left(\frac{\sigma_v'}{\sigma_{vc\alpha,ref}'}\right)\right] = 0 \quad (3.3a)$$

Equation (3.3.a) was developed by additive decomposition of the volumetric strain rate, $\dot{\varepsilon}_v$, by considering components for the primary consolidation, $\dot{\varepsilon}_{v,pc}$ and for the secondary compression $\dot{\varepsilon}_{v,sc}$, as indicated in Equation (3.3b).

$$\dot{\varepsilon}_v = \dot{\varepsilon}_{v,pc} + \dot{\varepsilon}_{v,sc} \quad (3.3b)$$

36

The volumetric strain rate can be defined by combining the equation of continuity and the Darcy's law

$$\dot{\varepsilon}_v \ = \ \frac{\dot{Q}_{out} - \dot{Q}_{in}}{dx\,dy\,dz} = \ -\frac{1}{\gamma_w}\left(k\frac{\partial^2 u}{\partial z^2} + \frac{\partial u}{\partial z}\frac{\partial k}{\partial z} \right) \qquad (3.3c)$$

The volumetric strain rate due to secondary compression can be defined by using material constants t_{ref}, $e_{ca,ref}$, $\sigma'_{vca,ref}$, and C_a, all of which can be measured in a traditional oedometer test for which the secondary compression behavior is linear in $e - log_{10}(t)$ space.

$$\dot{\varepsilon}_{v,sc} = \frac{\alpha}{t_{ref}(1 + e_0)}exp\left[\frac{e - e_{c\alpha,ref}}{\alpha} + \frac{C_c}{\alpha}log\left(\frac{\sigma'_v}{\sigma'_{vc\alpha,ref}} \right) \right] \qquad (3.3d)$$

The volumetric strain rate due to primary consolidation can be expressed in terms of the coefficient of compressibility, as demonstrated by Equation 3.3e

$$\dot{\varepsilon}_{v,pc} = \ -\frac{a_v}{1 + e}\frac{du}{dt} \qquad (3.3e)$$

where $du/dt = -d\sigma'_v/dt$, $\varepsilon_{v,pc} = -de/(1 + e)$, and $a_v = -de/d\sigma'_v$.

To solve Equation (3.3a), Brandenberg (2016) employed the implicit finite-difference scheme utilizing the midpoint rule, i.e. the Crank and Nicolson (Crank and Nicolson, 1947) method. The approach is summarized by Equation (3.3f).

37

$$\frac{(a_v)_{i,j}}{1 + e_{i,j-1}} \frac{u_{i,j} - u_{i,j-1}}{t_j - t_{j-1}} + \frac{k_{i,j}}{2}\left[\frac{(u_{i+1,j} - 2u_{i,j} + u_{i-1,j})}{\Delta z_{i,j}^2}\right]$$

$$+ \frac{k_{i,j-1}}{2}\left[\frac{(u_{i+1,j-1} - 2u_{i,j-1} + u_{i-1,j-1})}{\Delta z_{i,j}^2}\right]$$

$$+ \frac{1}{2}\left[\frac{(u_{i+1,j} - u_{i-1,j})(k_{i+1,j} - k_{i-1,j})}{\Delta z_{i,j}^2} + \frac{(u_{i+1,j-1} - u_{i-1,j-1})(k_{i+1,j} - k_{i-1,j})}{\Delta z_{i,j-1}^2}\right]$$

$$+ \frac{0.5a}{t_{ref}(1 + e_{i,j-1})}\left(exp\left\{\frac{e_{i,j} - e_{ca,ref}}{a} + \frac{c_c}{a}log\left[\frac{(\sigma_v')_{i,j}}{\sigma_{vca,ref}'}\right]\right\}\right.$$

$$\left. + exp\left\{\frac{e_{i,j-1} - e_{ca,ref}}{a} + \frac{c_c}{a}log\left[\frac{(\sigma_v')_{i,j-1}}{\sigma_{vca,ref}'}\right]\right\}\right) = 0 \ (3.3f)$$

Brandenberg's (2016) implementation [see Equations (12) and (13) in the reference paper] resulted in a solution that deviates from the benchmark solution by Fox and Pu (2015). While it is difficult to distinguish between typos in the Brandenberg's (2016) paper and the errors in the actual numerical implementation, potential discrepancies between the Brandenberg's (2016) approach and the Fox and Pu's (2015) benchmark solution are due to: 1) failure to include the unit weight of water in the formulation defined by Equation (3.3f), see e.g. corresponding residual estimate by Equation (12) in Brandenberg (2016); 2) inconsistent use of hydraulic conductivity values in the finite difference implementation defined by Equation (3.3f) and the corresponding residual formulation defined by Equation (12) in Brandenberg (2016); and 3) inconsistent use of finite difference estimates when formulating derivatives for the grid with non-equidistant spacing.

Inputs for the Brandenberg (2016) model are similar to inputs for the model developed in Mathematica. However, Brandenberg's (2016) model accounts for the re-compression and

38

swelling and, therefore, requires additional inputs: the recompression index Cr, and the over-consolidation ratio OCR.

Brandenberg's (2016) model accounts for the secondary compression. However, it assumes that the Ca value defining creep deformations is constant. While commonly used in practice, this assumptions may lead to unrealistically large creep rates (or even negative void ratio values). Research by Watabe et al. (2012) supports the assumption that the *Ca/Cc* ratio decreases with the decreasing visco-plastic strain rate, i.e. by expressing the secondary compression model parameters as a function of the strain rate is likely to lead to more realistic physical models.

3.4 PLAXIS

PLAXIS is a finite element software for geotechnical analysis of stability and deformation of soil structures. PLAXIS is available as a two-dimensional (2D) and three-dimensional (3D) software. PLAXIS 2D, i.e. a two-dimensional version (supporting both plane strain and axisymmetric simulations) was used for the consolidation analyses presented in this study. In this study, terms PLAXIS and PLAXIS 2D are equivalent.

PLAXIS supports the use of different constitutive models: Linear Elastic model, Mohr-Coulomb model, Hardening Soil model, Hardening Soil model with small-strain stiffness, Soft Soil model, Soft Soil Creep model, Jointed Rock model, and Modified Cam-Clay model. Numerical simulations presented in this study were conducted by using the Soft Soil model and the Soft Soil Creep model. The Soft Soil model is a Cam-Clay type model capable of evaluating primary compression of normally-consolidated and near-normally consolidated clay-type soils. The Soft Soil Creep model is an extension of the Soft Soil model that accounts for viscous effects, i.e. it is capable of modeling creep and stress relaxation.

Material models in PLAXIS are defined by a set of mathematical equations providing the relationship between stresses and strains. Material models are often expressed in a form in which infinitesimal increments of stress (or 'stress rates') are related to infinitesimal increments of strain (or 'strain rates'). All material models implemented in PLAXIS are based on a relationship between the effective stress rates, $\dot{\sigma}'$, and the strain rates, $\dot{\varepsilon}$.

In the Soft Soil model, it is assumed that there is a logarithmic relation between changes in the volumetric strain ε_v, and changes in the mean effective stress p'. This relationship is expressed as Equation (3.4a). The parameter λ^* is the modified compression index, which determines the compressibility of the material in primary loading. During isotropic unloading

40

and reloading, the constitutive behavior can be expressed as Equation 3.4b. The parameter φ denotes the friction angle, and C is the effective cohesion. The parameter k^* is the modified swelling index, which determines the compressibility of the material for unloading and reloading conditions.

$$\varepsilon_v - \varepsilon_v^0 = -\lambda^* \ln\left(\frac{p' + C * \cot\varphi}{p^0 + C * \cot\varphi}\right) \quad (virgin\ compression) \qquad (3.4a)$$

$$\varepsilon_v^e - \varepsilon_v^{e0} = -k^* \ln\left(\frac{p' + C * \cot\varphi}{p^0 + C * \cot\varphi}\right) \quad (unloading\ and\ reloading) \qquad (3.4b)$$

In the Soft Soil Creep model, the end-of-consolidation strain ε_c is defined by Equation (3.4c); where ε is a logarithmic strain, σ_0' is the initial effective pressure before loading, and σ' is the final effective pressure. σ_{p0} and σ_{pc} represent the pre-consolidation pressures corresponding to before-loading and to end-of-consolidation states, respectively. Parameters a and b are defined by Equation (3.4d). C_s is the recompression index and C_c is the compression index. Based on Equation (3.4c), it is possible to formulate the differential creep equation, which is expressed as Equation (3.4e). Parameter c is defined by Equation (3.4f), where C_a is the creep index for secondary compression, σ_p is the pre-consolidation pressure defined by Equation (3.4g), and τ stands for the time period.

$$\varepsilon_c = \varepsilon_c^e + \varepsilon_c^c = -a \ln\left(\frac{\sigma'}{\sigma_0'}\right) - (b - a) \ln\left(\frac{\sigma_{pc}}{\sigma_{p0}}\right) \qquad (3.4c)$$

$$a = \frac{C_s}{(1 + e_0) * \ln 10} \qquad b = \frac{C_c}{(1 + e_0) * \ln 10} \qquad (3.4d)$$

$$\dot{\varepsilon} = \dot{\varepsilon}^e + \dot{\varepsilon}^c = -a\frac{\dot{\sigma}'}{\sigma'} - \frac{c}{\tau}\left(\frac{\sigma'}{\sigma_p}\right)^{\frac{b-a}{c}} \qquad (3.4e)$$

$$c = \frac{C_a}{(1 + e_0) * \ln 10} \qquad (3.4f)$$

41

$$\sigma_p = \sigma_{p0} \, exp\left(\frac{-\varepsilon^c}{b - a}\right) \qquad\qquad (3.4g)$$

Input parameters for the Soft Soil model include: effective cohesion, friction angle, dilatancy angle, Poisson' ratio for unloading-reloading, stress ratio of horizontal and vertical effective stress in a state of normal consolidation, slope of the critical state line, modified swelling index, modified creep index, compression index, swelling index, secondary compression index, initial void ratio, saturated unit weight of soil, overconsolidation ratio (OCR), and pre-overburden pressure (POP). Some of the above parameters are redundant allowing for multiple input options.

Input parameters for the Soft Soil Creep model are the same as for the Soft Soil model, with the additional parameter, Ca, required to define creep behavior.

PLAXIS may produce erroneous results for the secondary compression index values approaching the threshold of Ca= 0.0001, i.e. the minimum value allowed as an input in the Soft Soil Creep model.

42

4. PRIMARY CONSOLIDATION CASE STUDY

4.1 Benchmark Case – Introduction

This chapter provides a comparison between iConsol.js (Web), Mathematica (Math), and CONDES programs for the benchmark case of non-linear consolidation (Fox and Pu 2015). This case is referred to as Benchmark 1 in this thesis. Benchmark 1 case considers a one-dimensional large strain consolidation problem involving saturated normally consolidated soil layer subjected to surcharge loading. The problem geometry is depicted in Figure 4.1a. A soil layer with the initial height of 10 meters is assumed to be fully consolidated (i.e. exhibiting zero excess pore pressures) when subjected to the initial effective overburden stress of 40 kPa. An instantaneous vertical stress increment of 400 kPa is applied at the top of the soil layer at time $t = 0$ and remains constant thereafter. The initial void ratio distribution is a function of the effective stress conditions immediately prior to the application of the surcharge load of 400 kPa. The top and bottom boundaries are drained, i.e. the excess pore pressures are set to zero at both boundaries during the consolidation process.
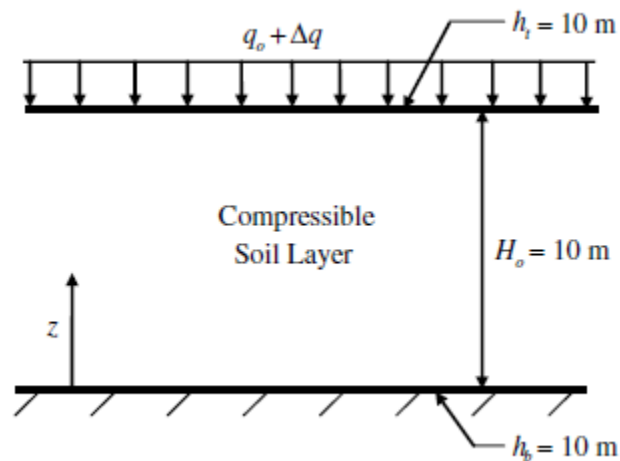
Figure 4.1a Initial geometry Benchmark 1 case (Fox and Pu 2015)

4.2 Input Parameters

Based on the imposed boundary conditions, the initial increase in total stresses results in an immediate increase of pore water pressures resulting in the fluid flow towards top and bottom boundaries. Changes in effective stresses and hydraulic conductivities can be expressed by employing constitutive equations providing the relationships between these quantities and the changes in soil volume. Constitutive equations defining the compressibility (e-σ_v') and the hydraulic conductivity (e-k) relationships (see Equations 4.2a and 4.2b) are non-linear functions of the void ratio. Consequently, the coefficient of consolidation for the Benchmark 1 problem (Fox and Pu 2015) varies during the consolidation process. The compressibility and the permeability relationships used for the Benchmark 1 problem are

$$e = 2.7 - log\left(\frac{\sigma'}{40\ kPa}\right) \tag{4.2a}$$

$$e = 4.3 + 1.3\ log\left(\frac{k}{2 \times 10^{-8}\frac{m}{s}}\right) \tag{4.2b}$$

General expressions for the compressibility and hydraulic conductivity functions are defined by Equation (4.2c) and (4.2d).

$$e = e_{v,ref} - Cc\ log_{10}\left(\frac{\sigma'}{\sigma'_{v,ref}}\right) \tag{4.2c}$$

$$k = k_{ref}10^{\left(\frac{e-e_{k,ref}}{C_k}\right)} \tag{4.2d}$$

Benchmark 1 input parameters defining the compressibility and permeability relationships are summarized in Table 4.2a and Table 4.2b.

Table 4.2a Compressibility Parameters

	Web	Math	CONDES
C_c	1	1	NA
C_r	0.1	0.1	NA
$\sigma'_{v,ref}$ (kPa)	40	40	NA
$e_{v,\,ref}$ (-)	2.608	2.608	NA
A $(1/kPa)^B$	NA	NA	8.1499
B (-)	NA	NA	-0.2597
Z (kPa)	NA	NA	31.4691

Table 4.2b Permeability Parameters

	Web	Math	CONDES
C_k	1.3	1.3	n/a
$e_{k,\,ref}$	4.3	4.3	n.a
k_{ref} (m/s)	2E-08	2E-08	n/a
C (m/s)	NA	NA	2.959E-11
D	NA	NA	3.63

Initial loading conditions are illustrated in Figure 4.1a and summarized in Table 4.2c.

Table 4.2c Initial Parameters (Upper Boundary Loading Conditions)

	Web	Math	CONDES
dq (kPa)	400	400	400
q0 (kPa)	40	40	40

The initial void ratio profile and initial densities were determined for the surface load q0=40

kPa applied at the top boundary (Table 4.2c) and by assuming the phreatic surface at the top of

the soil model. Effective stresses and void ratios were then determined by using constitutive

parameters in Table 4.2a for the specific gravity value of 2.78. The calculated range of initial

void ratios and densities is summarized in Table 4.2d.

Table 4.2d Specific Gravity, Void Ratios and Bulk Densities prior to Loading

	Web	Math	CONDES
e0	varies	varies	varies
Gs	2.78	2.78	2.78
γ_{sat} (kN/m^3)	varies	varies	varies

Parameters in Table 4.2a define compressibility relationships for different models used to conduct Benchmark 1 simulations. Employed compressibility relationships are shown in Figure 4.2a.
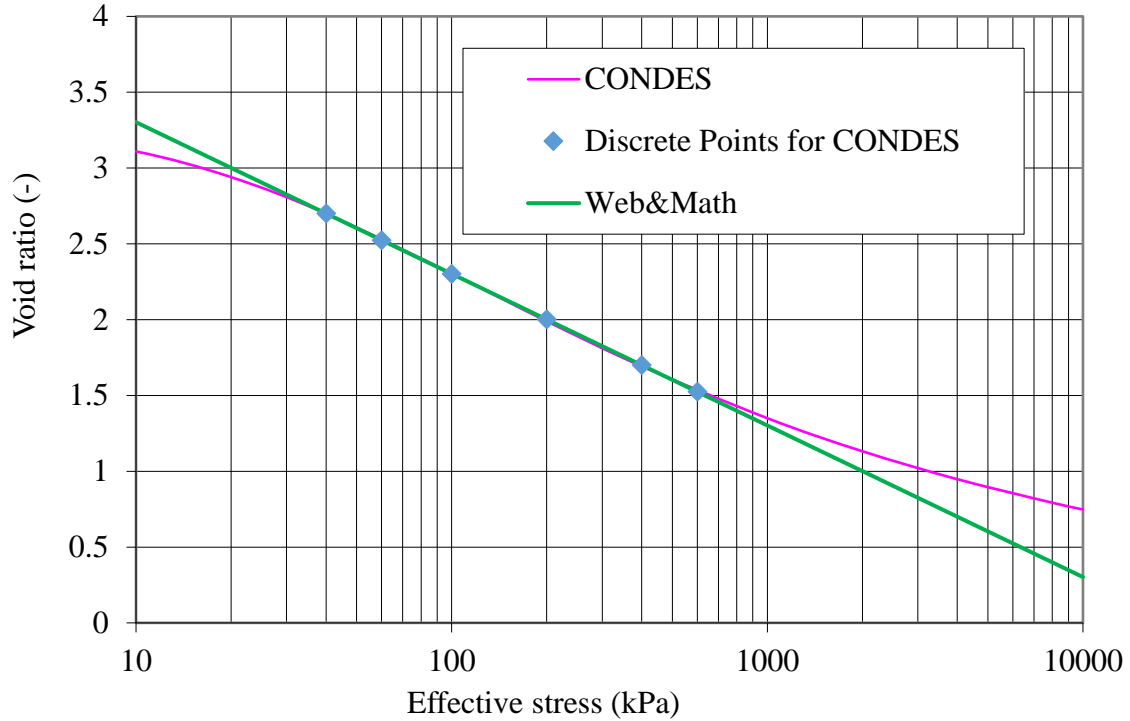
Figure 4.2a Compressibility relationships - Benchmark 1

Parameters in Table 4.2b define permeability (hydraulic-conductivity) relationships for different models used to conduct Benchmark 1 simulations. These relationships are shown in Figure 4.2b.
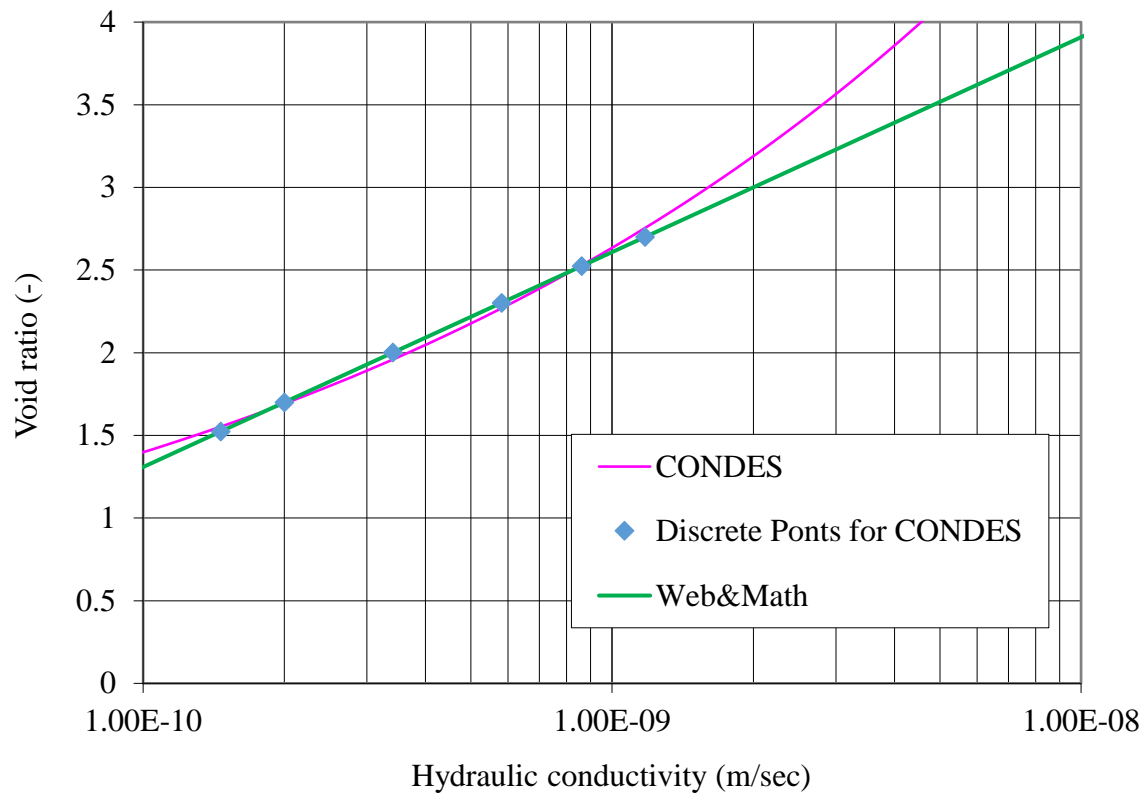
Figure 4.2b Hydraulic conductivity relationships - Benchmark 1

4.3 Output Results

Fox and Pu (2015) solved the Benchmark 1 problem by using a piecewise-linear consolidation model (Fox and Berles 1997) with 1000 elements. Fox and Pu (2015) solution is compared to solutions obtained by iConsol.js (Web), Mathematica (Math), and CONDES programs. Additional simulations were conducted by running the Benchmark No. 1 problem while allowing for the secondary compression, i.e. by adding creep parameters.

4.3.1 Benchmark No. 1 Results w/out Creep

Surface settlement values for the large strain consolidation problem (Benchmark No. 1) by Fox and Pu (2015) are presented in Figure 4.3.1a. The Fox and Pu (2015) solution is compared to model results by Mathematica (Math), iconsol.js (Web) and CONDES in terms of surface settlements in Figure 4.3.1a.
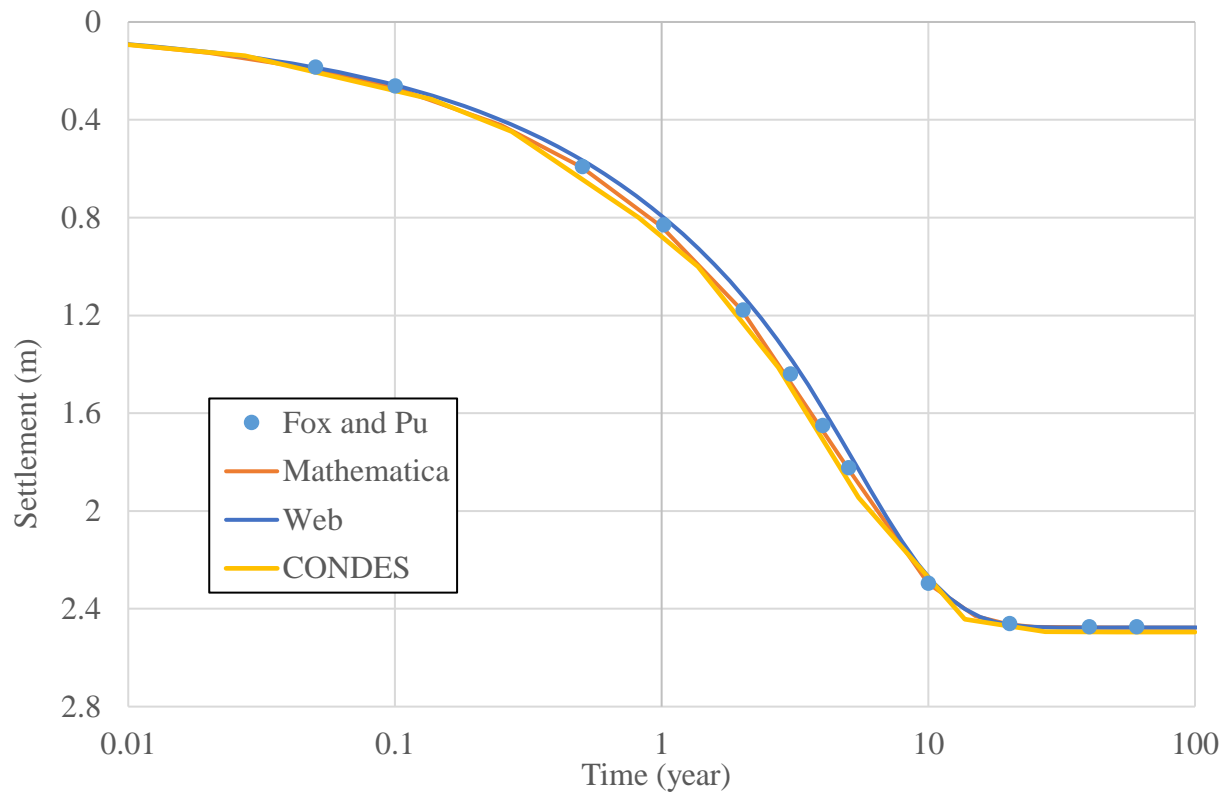
Figure 4.3.1a Settlement vs. time for Benchmark 1

Calculated void ratio profile determined by Fox and Pu (2015) is compared to model results by Mathematica (Math), iConsol.js (Web) and CONDES in Figure 4.3.1b.
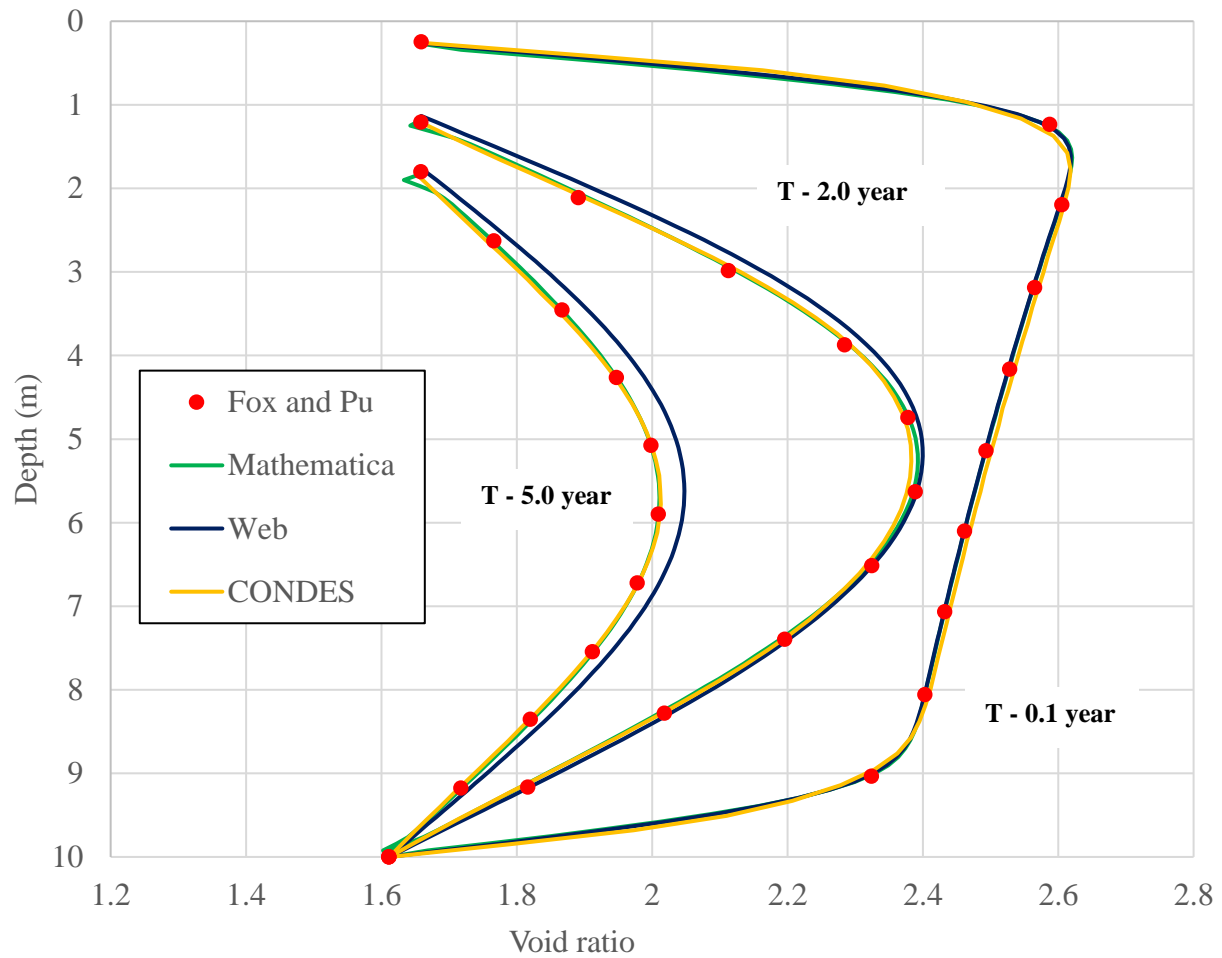
Figure 4.3.1b Void ratio profiles for Benchmark 1 – t = 0.1, 2 and 5 years

Excess pore pressures calculated by Fox and Pu (2015) are compared to model results by Mathematica (Math), iconsol.js (Web) and CONDES in Figure 4.3.1c.
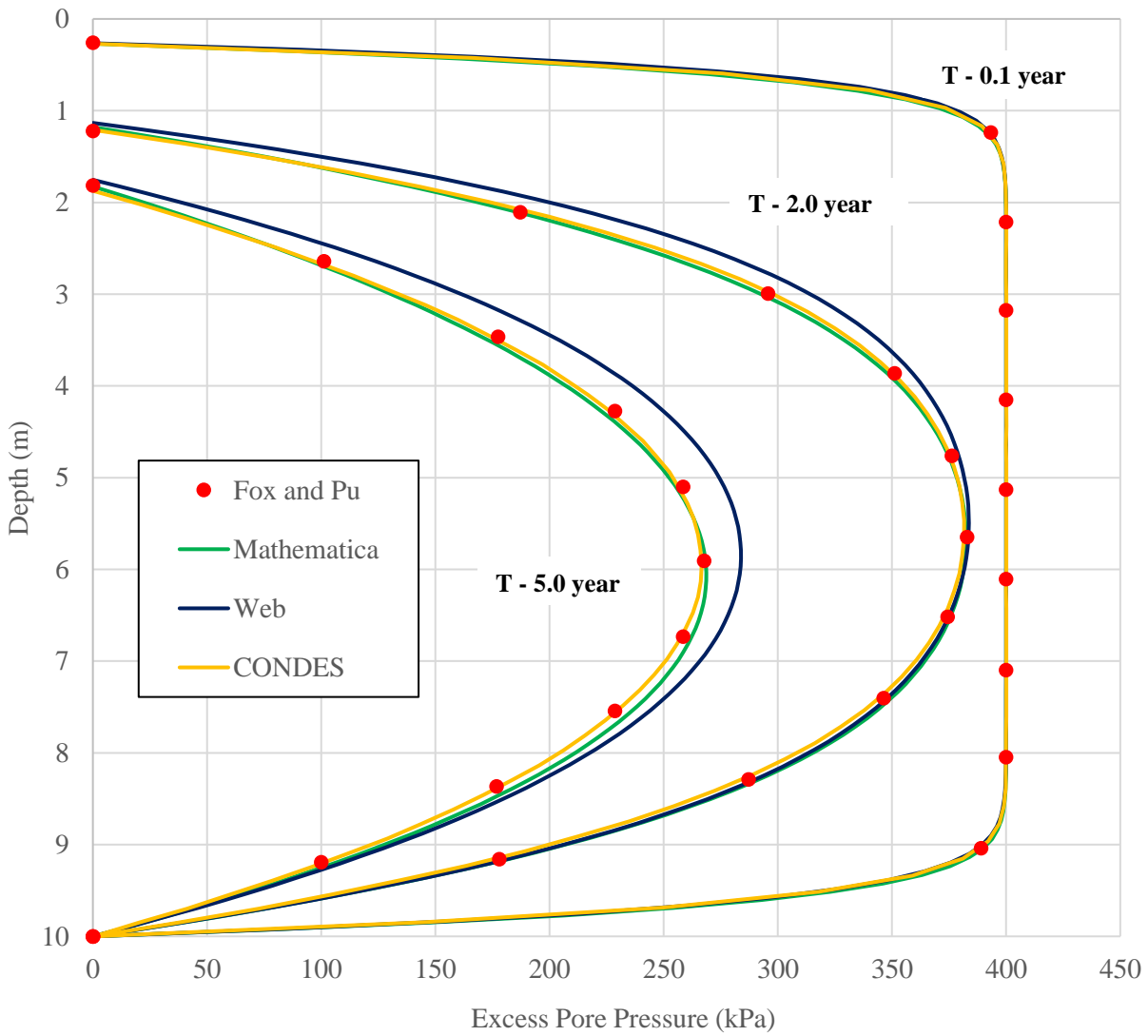
Figure 4.3.1c Excess pore pressure profiles for Benchmark 1 - t = 0.1, 2 and 5 years

Figures 4.3.1a, 4.3.1b, and 4.3.1c display favorable agreement between Benchmark 1 results by Fox and Pu (2015) and other programs. The calculated settlement values in Figure 4.3.1a indicate relatively minor differences between Benchmark 1 solution and iConsol.js before year=0.1 and after year =10. The difference in calculated settlements between these two programs is more significant for the time interval 0.1 year < time < 10 year. Void ratio profiles determined by iConsol.js demonstrate somewhat slower consolidation (time lag) than other

50

models. E.g., Figure 4.3.1b illustrates that iConsol.js model consistently predicts higher void ratios than the CS2 numerical model (Fox and Pu 2015) and other utilized models at 2 and 5 years. The void ratio profile predictions by iConsol.js (Figure 4.3.1b) are consistent with the settlement values in Figure 4.3.1a), i.e. iConsol.js/Web model predicts smaller settlements than other models between 1 and 10 years. The predicted settlement and void ratio values are also consistent with the calculated excess pore pressures displayed in Figure 4.3.1c. Specifically, the average excess pore pressures predicted by iConsol.js/Web are higher than the pore pressures predicted by Fox and Pu (2015), CONDES and Mathematica at 2 and 5 years.

Results presented in Figures 4.3.1a and 4.3.1c are summarized in Tables 4.3a, 4.3b and 4.3c. The reported average excess pore pressures were determined from calculated excess pore pressure profiles by numerical integration of Equation (4.3a).

$$u_{avg} = \frac{1}{2H_{dr}} \int\limits_{0}^{2H_{dr}} u_e(z,t)dz \qquad (4.3a)$$

In Equation (4.3a), u_{avg} denotes the average excess pore pressure, H_{dr} is the longest drainage path, and u_e stands for the excess pore pressure. At any given time, the height of soil layer, H, is equal to H=2Hdr. The degree of consolidation, U, is determined from Equation (2.1c).

Table 4.3a Benchmark 1 Solution Summary - Mathematica

Time (year)	Height of soil (m)	u_{avg} (kPa)	U (%)
0.1	9.73	376	5.9
2	8.82	282	29.5
5	8.17	182	54.4

Table 4.3b Benchmark 1 Solution Summary – iConsol.js/Web

Time (year)	Height of soil (m)	u_{avg} (kPa)	U (%)
0.1	9.74	377	5.8
2	8.87	288	28.0
5	8.25	196	50.9

51

Table 4.3c Benchmark 1 Solution Summary - CONDES

Time (year)	Height of soil(m)	u_{avg} (kPa)	U (%)
0.1	9.73	376	6.0
2	8.79	282	29.5
5	8.13	182	54.6

Discrepancies between the Brandenberg (2016) solution and other models are likely due to inconsistencies in the numerical implementation of the iConsol.js model as explained in Chapter 3.3.

4.3.2 Benchmark 1 Case Final Remarks

Numerical and analytical investigations of the Benchmark 1 simulations indicate the importance of consistent implementation of numerical schemes when solving large strain non-linear consolidation problems. A numerical approach that may be adequate for small strain analyses, may result in unacceptable errors when solving large strain consolidation problems. The Benchmark 1 output results confirm that iConsol.js calculations yield settlements that are smaller than computed by other models for the time range between 0.1 and 10 years. Consequently, the iConsol.js model predicts higher void ratios and higher excess pore pressures for the same period.

52

5. COMPARISON BETWEEN TERZAGHI'S AND NON-LINEAR CONSOLIDATION MODELS

5.1 Motivation

This chapter presents a comparison between Benchmark 1 results based on the Terzaghi's theory and the results from the non-linear consolidation model developed in Mathematica. To illustrate limitations of the classical consolidation model, Benchmark 1 results were also analyzed by using the coefficient of consolidation determined by graphical methods proposed by Cassagrande and Taylor (see e.g., Coduto, 2010). The motivation to compare results from the one-dimensional Terzaghi's model and from the model based on the nonlinear consolidation theory was to evaluate differences between these two models and to investigate potential errors occurring in engineering practice when applying the classical (i.e., linear) theory of consolidation to solve large strain consolidation problems.

5.2 Analyzed Case Scenarios

Case scenarios used to compare linear and non-linear theories of consolidation are based on the material properties for Benchmark 1 case (Fox and Pu 2015) discussed in Chapter 4. To evaluate sensitivity of results to applied vertical stress increments, case scenarios with the vertical stress increment of 400 kPa, 40 kPa, and 4 kPa were analyzed. All analyzed scenarios utilize the initial soil height of 0.02 m, i.e. model scenarios are based on the height that is typical for laboratory samples. The coefficient of consolidation used for linear analyses was determined by using Cassagrande and Taylor graphical methods (see Appendix A) and by using the time corresponding to 50 percent settlement for Cassagrande and 90 percent settlement for Taylor as follows:

$$c_v = \frac{0.196 * H_{dr}^2}{t_{50}} \qquad (5.2a)$$

$$c_v = \frac{0.848 * H_{dr}^2}{t_{90}} \qquad (5.2b)$$

where t50 is the time required to reach 50 percent of the final settlement and Hdr is the corresponding drainage length, both values determined from settlement curves for the non-linear model scenario as calculated by Mathematica. The t50, t90, and t100 values, representing times with the degree of settlement (consolidation) equal to 50, 90, and 100 percent, were determined as applicable. The degree of consolidation based on settlements, i.e. the degree of settlement, was determined from Equation 2.1b. The degree of consolidation based on excess pore pressures, i.e. the degree of excess pore pressure dissipation, was determined from Equation 2.1c.

54

5.3 Linear and Non-Linear Model Comparison

5.3.1 Surface Load Increment = 400 kPa

Times required to reach the degree of consolidation of 50, 90 and 100 percent and the

coefficient of consolidation for consolidation models with the surface load increment of 400

kPa are presented in Table 5.3.1a. Model simulations were terminated at 5 x 10^{-4} years.

Table 5.3.1a Calculated t50, t90, t100 and c_v values - 400 kPa case

	Cassagrande	Taylor	Terzaghi	Nonlinear
t50 (year)	8.37E-06	8.36E-06	8.33E-06	8.30E-06
t90 (year)	3.71E-05	3.60E-05	3.60E-05	3.70E-05
t100 (year)	5.42E-05	N/A	N/A	N/A
c_v (m^2/year)	2.343	2.356	2.354	see Figure 5.3.1a

The coefficient of consolidation profiles for the case scenario with the applied surface

load increment of 400 kPa are displayed Figure 5.3.1a. During the consolidation process, the

average coefficient of consolidation increases from 1.288 to 1.746 m^2/year with the

equivalent Terzaghi's coefficient of consolidation varying between 2.34 and 2.36 m^2/year as

summarized in Table 5.3.1a.

55
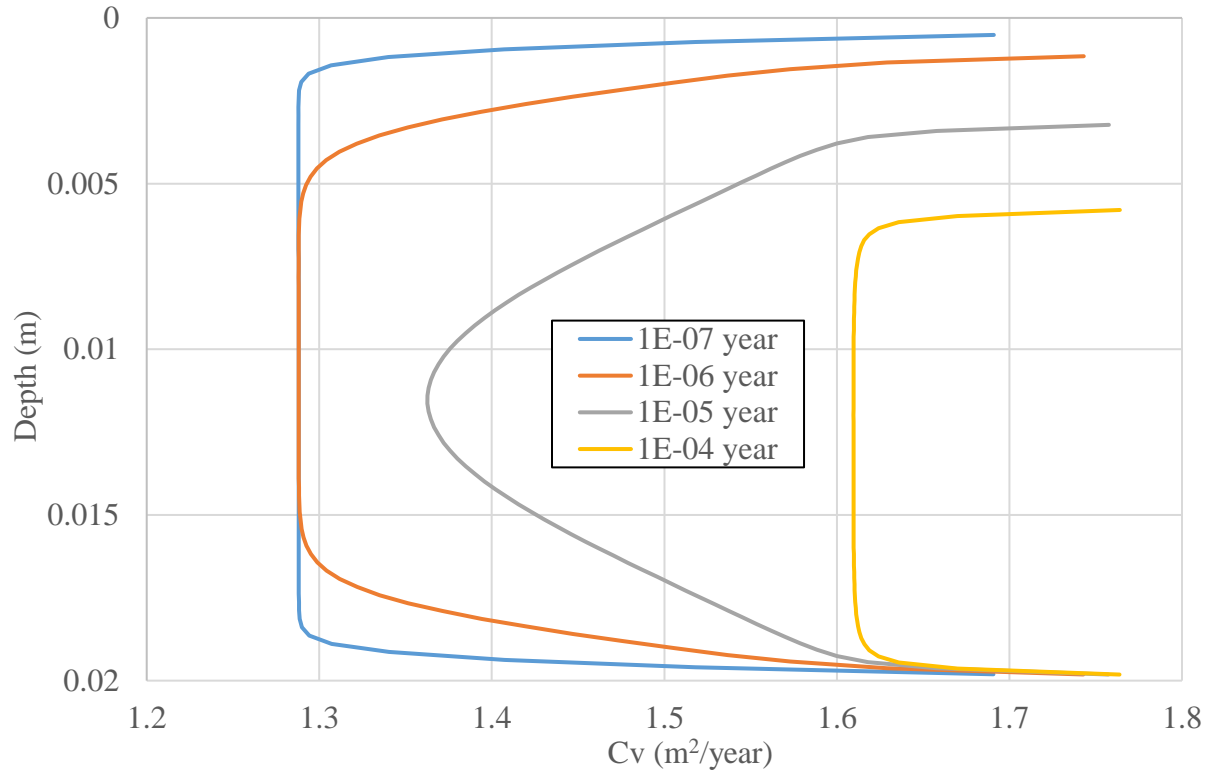
Figure 5.3.1a Mathematica c_v profiles for 400 kPa – t = 1E-07, 1E-06, 1E-05, and 1E-04 years

Figure 5.3.1a demonstrate that c_v values based on the linear theory are larger than the corresponding average c_v values calculated by Mathematica. I.e., when using the coefficient of consolidation based on material properties from Mathematica, Terzaghi's model predicts significantly larger consolidation times than estimated from the corresponding non-linear model. A major driver for this discrepancy is the model's drainage length which remains constant in the Terzaghi's model while being continuously reduced in the non-linear consolidation models. Since c_v values in Table 5.3.1a are based on the consolidation times and settlement values from the non-linear model, the "effective" Terzaghi's coefficient of consolidation (required to match the observed behavior) is significantly larger than the average c_v values determined from the compressibility and permeability parameters in Figure 5.3.1a.

56

Calculated excess pore pressures and settlements for the degree of consolidation of 10, 50, 90 and 99 percent are presented in Table 5.3.1b and Table 5.3.1c. Values in Table 5.3.1b and 5.3.1c correspond to model times: t10, t50, t90 and t99 matching the appropriate degree of settlement, i.e. the degree of settlement and the degree of excess pore pressure dissipation are equivalent when applying the classical Terzaghi's model and different if accounting for the non-linear consolidation effects.

Table 5.3.1b displays average excess pore pressures for the degree of consolidation of 10, 50, 90 and 99 percent. Average excess pore pressures, for the selected degrees of consolidation, were determined from calculated average pore pressures and the corresponding output times by using linear interpolation of pore pressures and logarithmic interpolation between time increments.

Table 5.3.1b Excess Pore Pressures at 10,50,90 and 99 Percent Consolidation - 400 kPa

	u_{avg} (Terzaghi)	u_{avg} (Nonlinear)	Difference (%)
U (10%)	360 kPa	360 kPa	0
U (50%)	200 kPa	198 kPa	1.01
U (90%)	40.0 kPa	32.8 kPa	22.0
U (99%)	4.00 kPa	1.01 kPa	296

Table 5.3.1c displays settlement values for the degree of consolidation of 10, 50, 90 and 99 percent. Settlement values in Table 5.3.1c were determined from calculated settlements and the corresponding output times by using linear interpolation of settlements and logarithmic interpolation between calculated time increments.

Table 5.3.1c Settlement at 10,50,90 and 99 percent consolidation - 400 kPa

	Terzaghi	Nonlinear	Difference (%)
U (10%)	5.63E-04 m	5.54E-04 m	1.62
U (50%)	2.81E-03 m	2.78E-03 m	1.08
U (90%)	5.07E-03 m	5.02E-03 m	1.00
U (99%)	5.57E-03 m	5.56E-03 m	0.18

57

Results in Table 5.3.1d illustrate differences in the calculated degree of consolidation based on settlement values and excess pore pressures. Noting that the calculated excess pore pressures and displacements are dependent on the applied material properties, average values for the hydraulic conductivity and for the coefficient of volume compressibility are included for comparison. Table 5.3.1d indicates the hydraulic conductivity decreasing from 1.07e-9 to 1.87e-10 m/sec and the coefficient of volume compressibility decreasing from 2.65e-3 to 3.73e-4 1/kPa during the time of consolidation between 1e-7 and 1e-4 years.

Table 5.3.1d Calculated U, k and mv values for t=1e-7, 1e-6, 1e-5 and 1e-4 years for non-linear consolidation model - 400 kPa

Time (year)	U_settlement (-)	U_excess_pore_pressure (-)	Hydraulic Conductivity (m/s)	Coefficient of Volumetric Compressibility (kPa^{-1})
1.00E-07 year	0.057	0.030	1.07E-09	2.65E-03
1.00E-06 year	0.173	0.091	8.92E-10	2.14E-03
1.00E-05 year	0.542	0.320	4.50E-10	9.87E-04
1.00E-04 year	0.999	0.998	1.87E-10	3.73E-04

Results in Table 5.3.1d indicate a relatively large discrepancy between the calculated degree of consolidation values based on settlements and based on excess pore pressures. The difference between two methods can be traced to the variability of material parameters. I.e. the hydraulic conductivity and the coefficient of volume compressibility display an order of magnitude changes during the model simulation emphasizing non-linearity of the calculated flow rates and deformations throughout the consolidation process.

Results in Table 5.3.1a, indicate favorable agreement between the coefficient of consolidation determined by graphical methods (Cassagrande and Taylor) and Terzaghi's approach. To reconcile differences in the calculated coefficient of consolidation between

58

Terzaghi's (linear) and non-linear models, one can introduce the correction factor, COF, defined by Equation 5.3b. Based on Equation 5.3c, the updated coefficient of consolidation value can be used to scale material parameters from the non-linear models to Terzaghi's 1D consolidation theory:

$$t_{50}(Terzaghi) = \frac{T_{50} * H_{dr}^2}{c_v(Mathematica)} \tag{5.3a}$$

$$\frac{t_{50}(Terzaghi)}{t_{50}(Mathematica)} = COF \tag{5.3b}$$

$$c_v(Terzaghi) = c_v(Mathematica) * COF \tag{5.3c}$$

5.3.2 Surface Load Increment = 40 kPa

Times required to reach the degree of consolidation of 50, 90 and 100 percent and the coefficient of consolidation for the case scenario with the surface load increment of 40 kPa are presented in Table 5.3.2a. The t100 value for the classical (Terzaghi) and the non-linear (Mathematica) consolidation models were not reported because, theoretically, the time required to reach 100 percent consolidation is infinite.

Table 5.3.2a Calculated t50, t90, t100 and c_v values - 40 kPa case

	Cassagrande	Taylor	Terzaghi	Mathematica
t50 (year)	1.28 E-05	1.28E-05	1.27E-05	1.27E-05
t90 (year)	5.70E-05	5.63E-05	5.50E-05	5.63E-05
t100 (year)	7.87E-04	N/A	N/A	N/A
c_v (m^2/year)	1.508	1.508	1.541	see figures

The coefficient of consolidation profiles for the case scenario with the applied surface load increment of 40 kPa are displayed Figure 5.3.2a. During the consolidation process, the average coefficient of consolidation increases from 1.288 to 1.395 m^2/year with the equivalent Terzaghi's coefficient of consolidation varying between 1.51 and 1.54 m^2/year as summarized in Table 5.3.2a
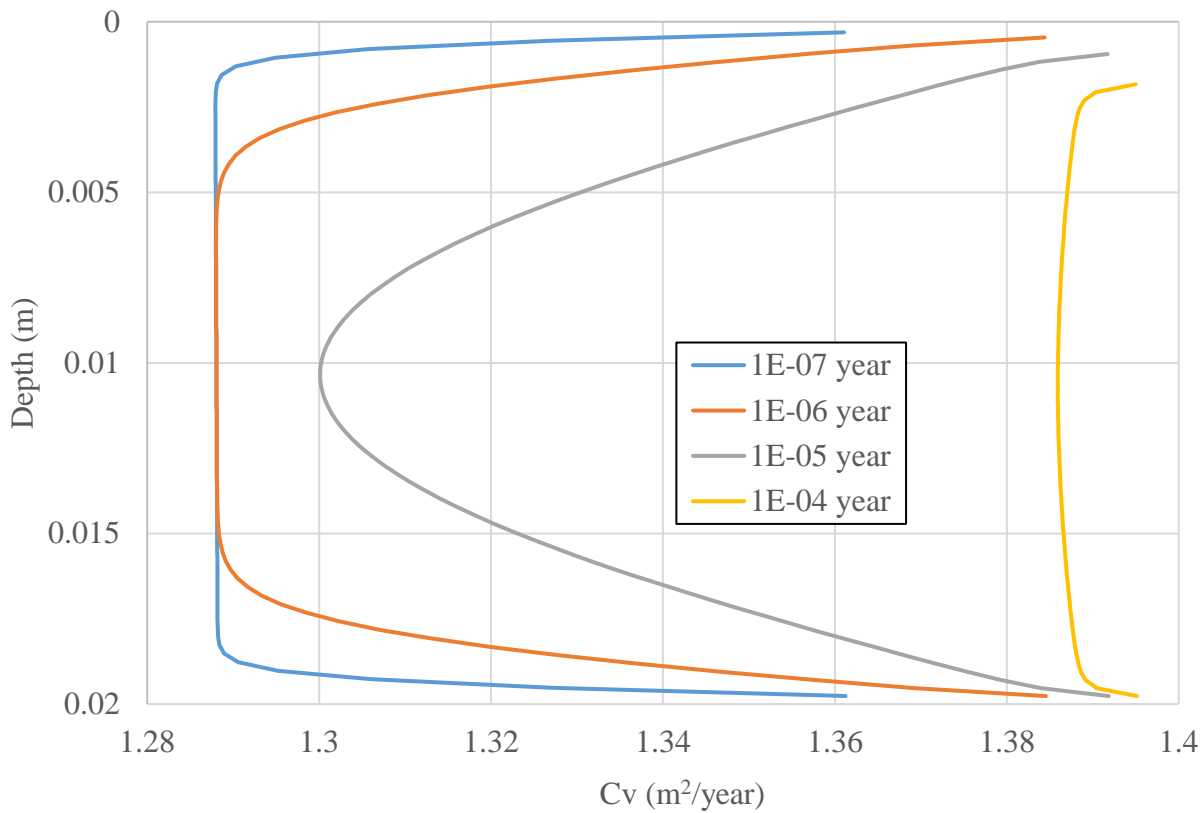
59

Figure 5.3.2a Mathematica c_v profiles for 40 kPa - t = 1E-07, 1E-06, 1E-05, and 1E-04 years

Figure 5.3.2a demonstrate that c_v values based on the linear theory are larger than the corresponding average c_v values calculated by Mathematica. I.e., when using the coefficient of consolidation based on material properties from Mathematica, Terzaghi's model predicts significantly larger consolidation times than estimated from the corresponding non-linear model. As noted previously, a major driver for this discrepancy is the model's drainage length which remains constant in the Terzaghi's model while being continuously reduced in the non-linear consolidation models. Since c_v values in Table 5.3.2a are based on the consolidation times and settlement values from the non-linear model, the "effective" Terzaghi's coefficient of consolidation (required to match the observed behavior) is larger

60

than the average c_v values determined from the compressibility and permeability parameters in Figure 5.3.2a.

Calculated excess pore pressures and settlements for the degree of consolidation of 10, 50, 90 and 99 percent are presented in Table 5.3.2b and Table 5.3.2c. Values in Table 5.3.2b and 5.3.2c correspond to model times: t10, t50, t90 and t99 matching the appropriate degree of settlement, i.e. the degree of settlement and the degree of excess pore pressure dissipation are equivalent when applying the classical Terzaghi's model and different if accounting for the non-linear consolidation effects. The method for Table 5.3.2.b and Table 5.3.2c is same as Chapter 5.3.1 and this goes same to the Chapter 5.3.3.

Table 5.3.2b Excess Pore Pressures at 10,50,90 and 99 Percent Consolidation - 40 kPa

	Terzaghi	Nonlinear	Difference (%)
U (10%)	36.0 kPa	36.0 kPa	0
U (50%)	20.0 kPa	19.8 kPa	1.01
U (90%)	4.00 kPa	2.73 kPa	46.5
U (99%)	0.40 kPa	0.09 kPa	344

Table 5.3.2c Settlement at 10,50,90 and 99 percent consolidation - 40 kPa

	Terzaghi	Nonlinear	Difference (%)
U (10%)	1.63E-04 m	1.59E-04 m	2.52
U (50%)	8.14E-04 m	8.02E-04 m	1.50
U (90%)	1.46E-03 m	1.46E-03 m	0.00
U (99%)	1.61E-03 m	1.61E-03 m	0.00

Results in Table 5.3.2d illustrate differences in the calculated degree of consolidation based on settlement values and excess pore pressures. Noting that the calculated excess pore pressures and displacements are dependent on the applied material properties, average values for the hydraulic conductivity and for the coefficient of volume compressibility are included for comparison. Table 5.3.2d indicates the hydraulic conductivity decreasing from 1.15e-9 to

61

6.96e-10 m/sec and the coefficient of volume compressibility decreasing from 2.85e-3 to

1.61e-3 1/kPa during the time of consolidation between 1e-7 and 1e-4 years.

Table 5.3.2d Calculated U, k and mv values for t=1e-7, 1e-6, 1e-5 and 1e-4 years for non-linear consolidation model - 40 kPa

Time (year)	U_settlement (-)	U_excess_pore_pressure (-)	Hydraulic Conductivity (m/s)	Coefficient of Volumetric Compressibility (kPa^{-1})
1.00E-07	0.045	0.038	1.15E-09	2.85E-03
1.00E-06	0.139	0.116	1.09E-09	2.70E-03
1.00E-05	0.438	0.374	9.33E-10	2.25E-03
1.00E-04	0.984	0.978	6.96E-10	1.61E-03

Results in Table 5.3.2d indicate a poor agreement between the calculated degrees of

consolidation based on settlement values and based on excess pore pressures. Analogous to

the previous case (with the surface load increment of 400 kPa), the difference between two

methods is due to variability of material parameters. I.e. changes in the hydraulic

conductivity and the coefficient of volume compressibility are relatively significant, although

smaller than for the case scenario with the surface load of 400 summarized in Table 5.3.1d.

5.3.3 Surface Load Increment = 4 kPa

Times required to reach the degree of consolidation of 50, 90 and 100 percent and the

coefficient of consolidation for the case scenario with the surface load increment of 4 kPa are

presented in Table 5.3.3a. The t100 value for the classical (Terzaghi) and the non-linear

(Mathematica) consolidation models were not reported because, theoretically, the time required

to reach 100 percent consolidation is infinite.

Table 5.3.3a Calculated t50, t90, t100 and c_v values - 4 kPa case

	Cassagrande	Taylor	Terzaghi	Mathematica
t50 (year)	1.50 E-05	1.50E-05	1.49E-05	1.50E-05
t90 (year)	6.95E-05	6.50E-05	6.46E-05	6.88E-05
t100 (year)	8.39E-05	N/A	N/A	N/A
c_v (m²/year)	1.306	1.305	1.312	Graph

The coefficient of consolidation profiles for the case scenario with the applied surface load increment of 4.0 kPa are displayed Figure 5.3.3a. During the consolidation process, the average coefficient of consolidation increases from 1.288 to 1.302 m²/year with the equivalent Terzaghi's coefficient of consolidation of approximately 1.31 m²/year as summarized in Table 5.3.3a.
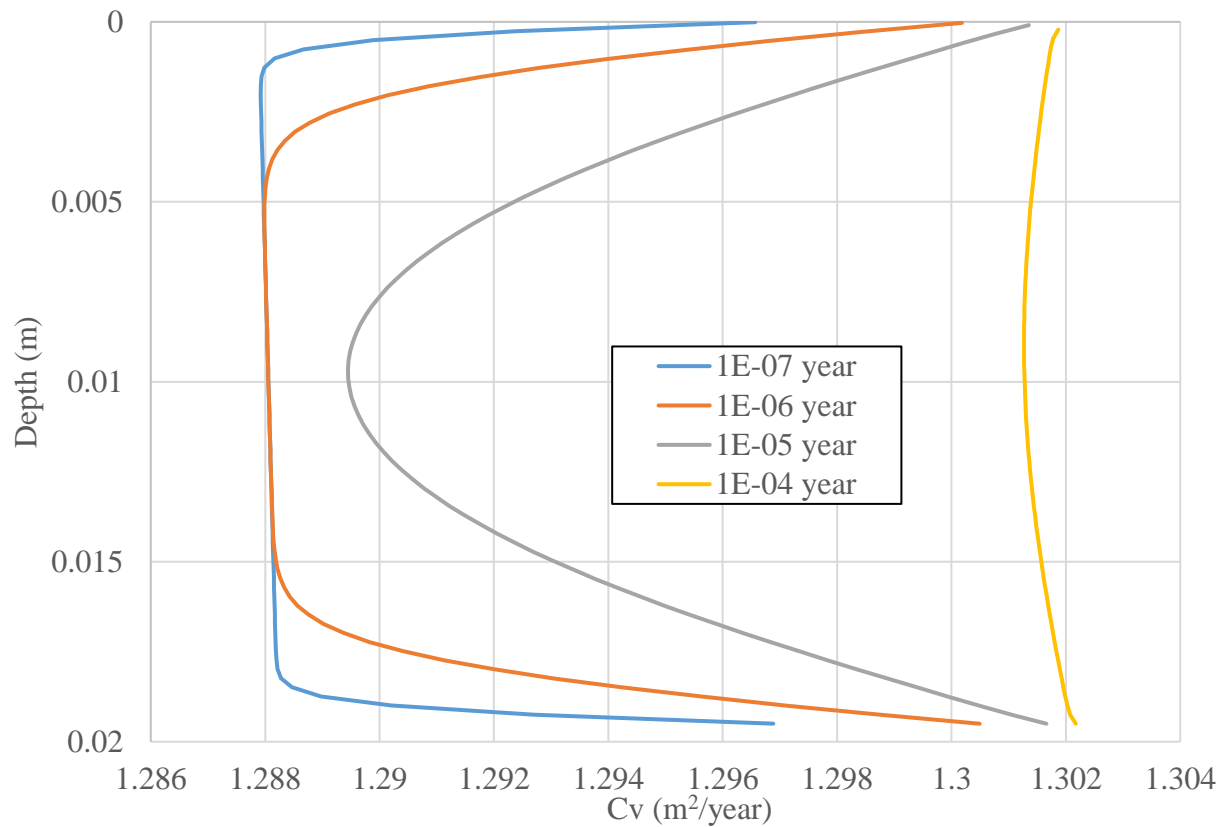

Figure 5.3.3a Mathematica c_v profiles for 4 kPa - t = 1E-07, 1E-06, 1E-05, and 1E-04 years

63

Figure 5.3.3a demonstrate that c_v values based on the linear theory (Table 5.3.3a) are somewhat larger than the corresponding c_v values used in Mathematica. In comparison to the case scenarios evaluating surface load increments of 400 and 40 kPa, differences in the coefficient of consolidation used to evaluate linear and non-linear models for the surface load of 4 kPa are relatively insignificant. However, the "effective" Terzaghi's coefficient of consolidation (Table 5.3.3a) remains larger than the average c_v values for the non-linear model (Figure 5.3.2a).

Calculated excess pore pressures and settlements for the degree of consolidation of 10, 50, 90 and 99 percent are presented in Table 5.3.3b and Table 5.3.3c. Values in Table 5.3.3b and 5.3.3c correspond to model times: t10, t50, t90 and t99 matching the appropriate degree of settlement, i.e. the degree of settlement and the degree of excess pore pressure dissipation are equivalent when applying the classical Terzaghi's model and different if accounting for the non-linear consolidation effects. Absolute differences between the Terzaghi's and the non-linear model are significantly smaller than for the case scenarios considering the surface load increment of 400 and 40 kPa (see e.g., Table 5.3.1b and Table 5.3.2b).

Table 5.3.3b Excess Pore Pressures at 10, 50, 90 and 99 Percent Consolidation - 4 kPa

	Terzaghi	Nonlinear	Difference (%)
U (10%)	3.60 kPa	3.60 kPa	0
U (50%)	2.00 kPa	1.97 kPa	1.52
U (90%)	0.40 kPa	0.30 kPa	33.3
U (99%)	0.04 kPa	0.01 kPa	300

Table 5.3.3c Settlement at 10, 50, 90 and 99 percent consolidation - 4 kPa

	Terzaghi	Nonlinear	Difference (%)
U (10%)	2.24E-05 m	2.18E-05 m	2.75
U (50%)	1.12E-04 m	1.10E-04 m	1.82
U (90%)	2.01E-04 m	2.01E-04 m	0.00
U (99%)	2.22E-04 m	2.22E-04 m	0.00

64

Results in Table 5.3.3d illustrate differences in the calculated degree of consolidation based on settlement values and excess pore pressures. Noting that the calculated excess pore pressures and displacements are dependent on the applied material properties, average values for the hydraulic conductivity and for the coefficient of volume compressibility are included for comparison. Table 5.3.3d indicates the hydraulic conductivity decreasing from 1.17e-9 to 1.09e-9 m/sec and the coefficient of volume compressibility decreasing from 2.92e-3 to 2.70e-4 1/kPa during the time of consolidation between 1e-7 and 1e-4 years.

Table 5.3.3d Calculated U, k and mv values for t=1e-7, 1e-6, 1e-5 and 1e-4 years for non-linear consolidation model - 4 kPa

Time	U_settlement (-)	U_excess_pore_pressure (-)	Hydraulic Conductivity (m/s)	Coefficient of Volumetric Compressibility (kPa^{-1})
1.00E-07 year	0.042	0.041	1.17E-09	2.92E-03
1.00E-06 year	0.130	0.127	1.16E-09	2.90E-03
1.00E-05 year	0.409	0.401	1.14E-09	2.83E-03
1.00E-04 year	0.969	0.968	1.09E-09	2.70E-03

Results in Table 5.3.3d indicate favorable agreement between the calculated degrees of consolidation based on settlement values and based on excess pore pressures. Small differences between the two methods are due to (relatively small) changes in material parameters. I.e. changes in the hydraulic conductivity and the coefficient of volume compressibility are significantly smaller than for the case scenario with the surface load of 400 and 40 kPa summarized in Table 5.3.1d and Table 5.3.2d

5.3.4 Comparison between Linear and Non-Linear Consolidation Models - Final Remarks

A comparison between Terzaghi's (linear) and non-linear consolidation models was conducted by considering a laboratory-size sample and a set of consolidation properties for the Benchmark 1 (Fox and Pu 2015) scenario analyzed in Chapter 4. For completeness, model

65

results were also analyzed utilizing graphical methods that are commonly used in practice to determine the "effective" coefficient of consolidation.

Analyzed case scenarios considered the surface load application of 4, 40 and 400 kPa to provide a sufficient range of stresses for evaluating the impact of non-linear material properties and potential errors to due linearization of the governing equation.

In comparison to scenarios with larger surface load application, model scenario with the surface load increment of 4 kPa resulted in relatively minor changes of material properties during the consolidation process. Consequently, a favorable agreement was observed between linear and non-linear model results. However, differences between linear and non-linear consolidation model results became larger as the changes in the hydraulic conductivity and the coefficient of volume compressibility (as observed during the consolidation process) increased.

For a case scenario with the surface load of 400 kPa, the hydraulic conductivity and the coefficient of volume compressibility change by an order of magnitude during the consolidation process. Consequently, the Terzaghi's model (based on "average" material properties) predicts significantly larger consolidation times than the corresponding non-linear model. A major driver for this discrepancy is the "effective" drainage length which remains constant in the Terzaghi's model while being continuously reduced in the non-linear consolidation models.

The use of graphical methods by Cassagrande and Taylor provided favorable agreement with the corresponding non-linear model when estimating times of consolidation. However, the estimated coefficient of consolidation (predicted by graphical methods when analyzing time-settlement curve from a non-linear model) may be significantly larger than the average c_v value based on the actual (non-linear) compressibility and permeability parameters. E.g., the "effective" Terzaghi's coefficient of consolidation, obtained by matching the non-linear model

66

with the surface load of 400 kPa, was 35 to 83 percent larger than the coefficient of consolidation calculated from the permeability and compressibility parameters in a non-linear model. Changes (non-linearity) of material parameters during the consolidation process result in non-linearity of flow rates and deformation rates. Consequently, the calculated degree of consolidation in terms of settlements is going to differ from the calculated degree of consolidation expressed in terms of excess pore pressures. I.e. when describing effects of non-linear consolidation, the degree of settlement and the degree of excess pore pressure dissipation need to be defined as separate items.

Based on the above, the use of Terzaghi's consolidation theory should be restricted to small strain applications characterized by relatively small changes in material properties during the consolidation process.

6. SECONDARY COMPRESSION CASE STUDY

6.1 Research Case – Introduction

This chapter presents results from numerical models developed to investigate the large strain consolidation and creep behavior for soft soil deposits. The goal was to investigate the behavior of a clayey soil with the known engineering properties. Initially, the soil is subjected to stresses dominated by the material self-weight followed by the application of a surface load. The soil selected for the Research Case was Kaolin clay. This material is readily available, i.e. it is relatively easy to obtain samples with the controlled material properties. The kaolin clay used for the Research Case was purchased in a dry form and then reconstituted into a slurry through the addition of water and by mixing action. Kaolin represents a relatively stiff fine-grained slurry. Tap water was added to the dry clay in sufficient quantities to achieve a water content 2.5 times greater than the clay's liquid limit. The consolidation parameters for Kaolin clay used for the Research Case analyses were determined from seepage-induced consolidation tests (SICTs) conducted by Brink (2012).

Research Case analyses were conducted using iConsol.js (Web), CONDES, Mathematica, and PLAXIS. One dimensional model scenarios considered the initial height of soil equal to 4 meters. A vertical load of 100 kPa was applied at the soil surface in addition to stresses due to self-weight consolidation. Research Case scenarios were evaluated with and without accounting for secondary compression effects. E.g., CONDES does not account for the secondary compression effects. Since PLAXIS is a two-dimensional model, the width of the model is a required input parameter. All PLAXIS simulations were conducted for the model width of 4 meters. Based on the adopted initial conditions, i.e. based on stresses immediately prior to application of the design load increment, the initial height of 4.4 meters was used for PLAXIS

68

simulations and the initial height of 4.003 meters was used for CONDES model runs. The initial

height of 4.4 meters used in PLAXIS was required to reach the equilibrium while allowing for

the self-weight consolidation, i.e. prior to applying the specified surface load increment of 100

kPa. Furthermore, the initial height correction, applied to CONDES and PLAXIS models, was

necessary to ensure that the volume of solids is the same for all models.

69

6.2 Input Parameters

Inputs parameters used for the Research Case modeling scenarios are summarized in Tables 6.2a to 6.2d.

Table 6.2a Compressibility Parameters

	Web	Math	CONDES	PLAXIS
Cc	0.555	0.555	NA	0.555
Cr	0.05	0.05	NA	0.05
$\sigma'_{v,ref}$ (kPa)	2.84	2.84	NA	2.84
$e_{v, ref}$ (-)	2.608	2.608	NA	2.608
A $(1/kPa)^B$	NA	NA	3.1718	NA
B (-)	NA	NA	-0.1296	NA
Z (kPa)	NA	NA	1.6883	NA

Table 6.2b Permeability Parameters

	Web	Math	CONDES	PLAXIS
Ck	1.212	1.212	NA	1.212
$e_{k, ref}$	2.608	2.608	NA	2.608
k_{ref} (m/s)	1.42E-08	1.42E-08	NA	1.42E-08
C (m/s)	NA	NA	3.17E-10	NA
D	NA	NA	3.91	NA

Table 6.2c Initial Parameter (initial and boundary condition)

	Web	Math	CONDES	PLAXIS
dq (kPa)	100	100	100	100
q0 (kPa)	2.84	2.84	2.84	2.84

Table 6.2d Soil Weight and Porosity Parameters

	Web	Math	CONDES	PLAXIS
e0	varies	varies	varies	2.608
Gs	2.66	2.66	2.66	NA
γ_{sat} (kN/m^3)	varies	varies	varies	14.32

70

Parameters in Table 6.2a define compressibility relationships for different models used to conduct Research Case simulations. These relationships are presented graphically in Figure 6.2a.
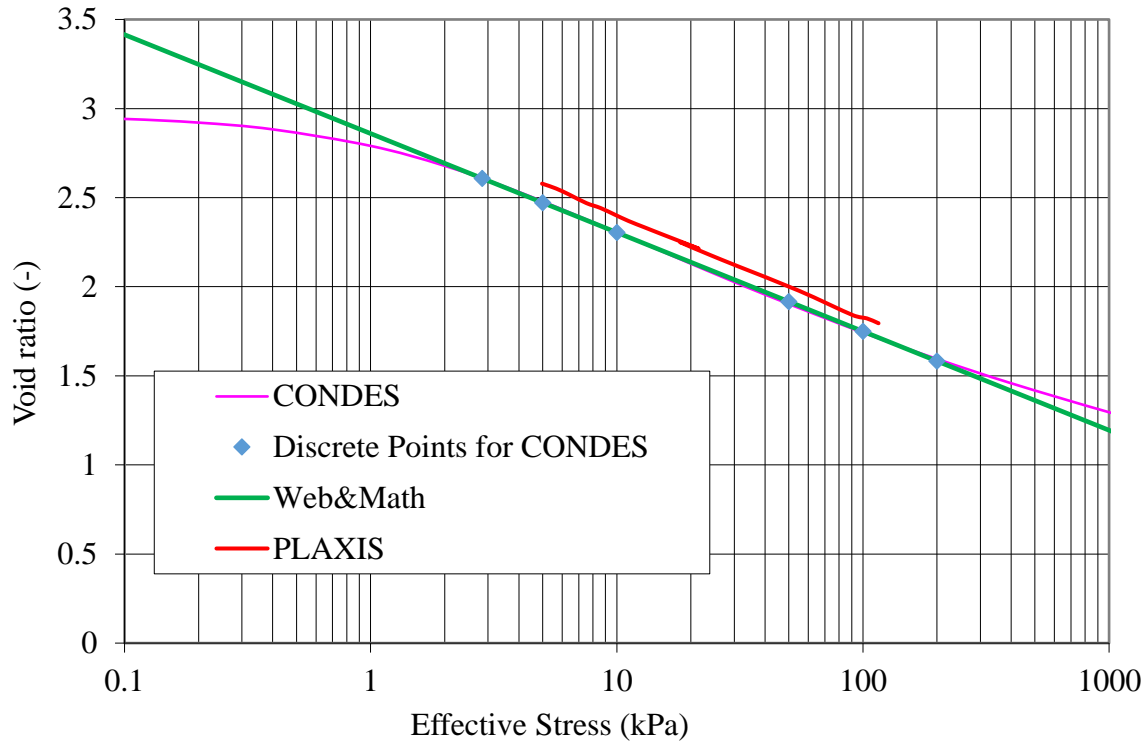

Figure 6.2a Compressibility relationships – Research Case

In Figure 6.2a, the presented compressibility relationship for PLAXIS model is based on the Research Case simulation results, i.e. PLAXIS results in Figure 6.2a display calculated void ratios and the corresponding vertical effective stresses. The apparent discrepancy between PLAXIS and other numerical models is due to the constitutive model formulation, specifically, the void ratio in PLAXIS is calculated by the using mean effective stresses. Results in Figure 6.2a demonstrate that the mean effective stress calculated by PLAXIS is lower than the corresponding vertical effective stress (resulting in higher void ratios). Therefore, PLAXIS

71

model will exhibit higher void ratio than one-dimensional models at the same magnitude of vertical effective stresses when conducting Research Case simulations.

The hydraulic conductivity relationships for Research Case, defined by parameters in Table 6.2b, are shown in Figure 6.2a.
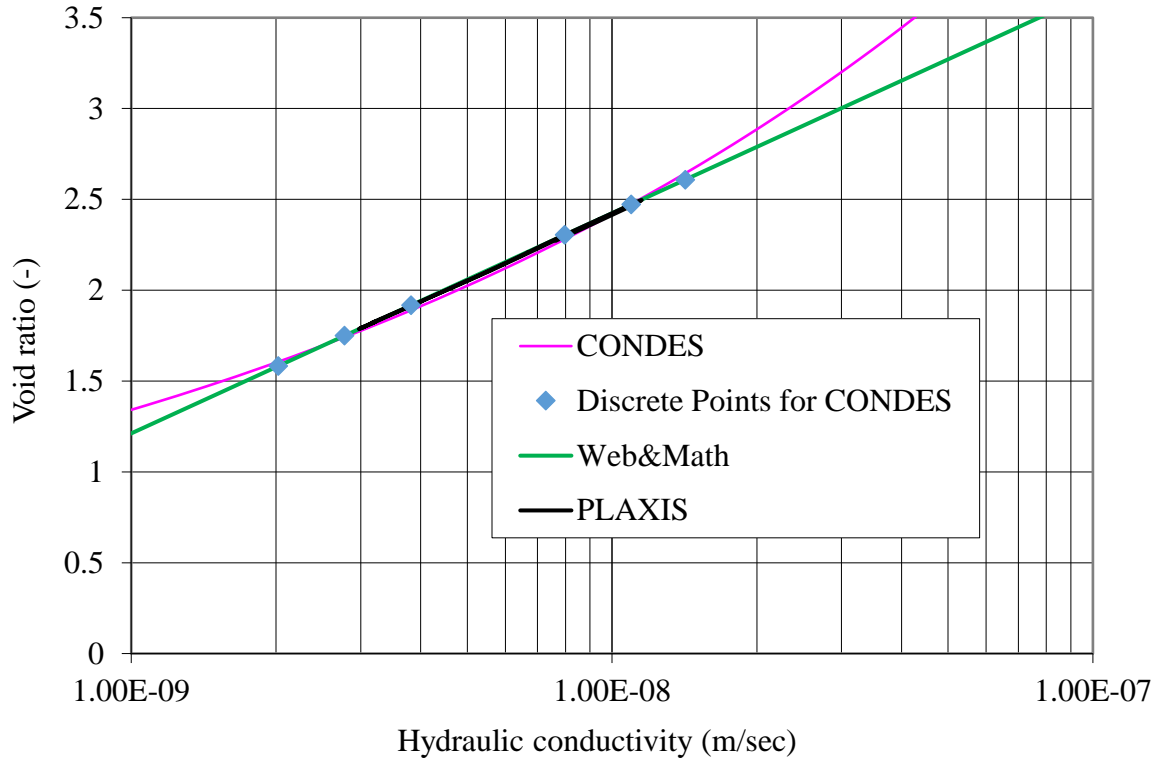
Figure 6.2b Hydraulic conductivity relationships – Research Case

6.3 Output Results - Research
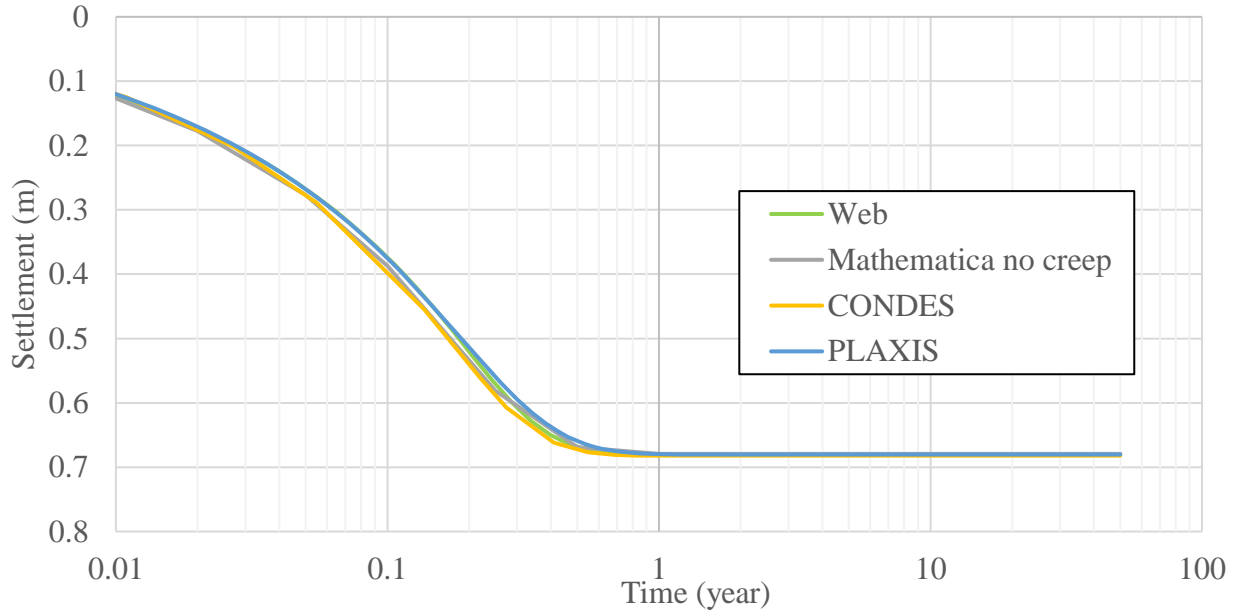
6.3.1 Research Case w/out Creep
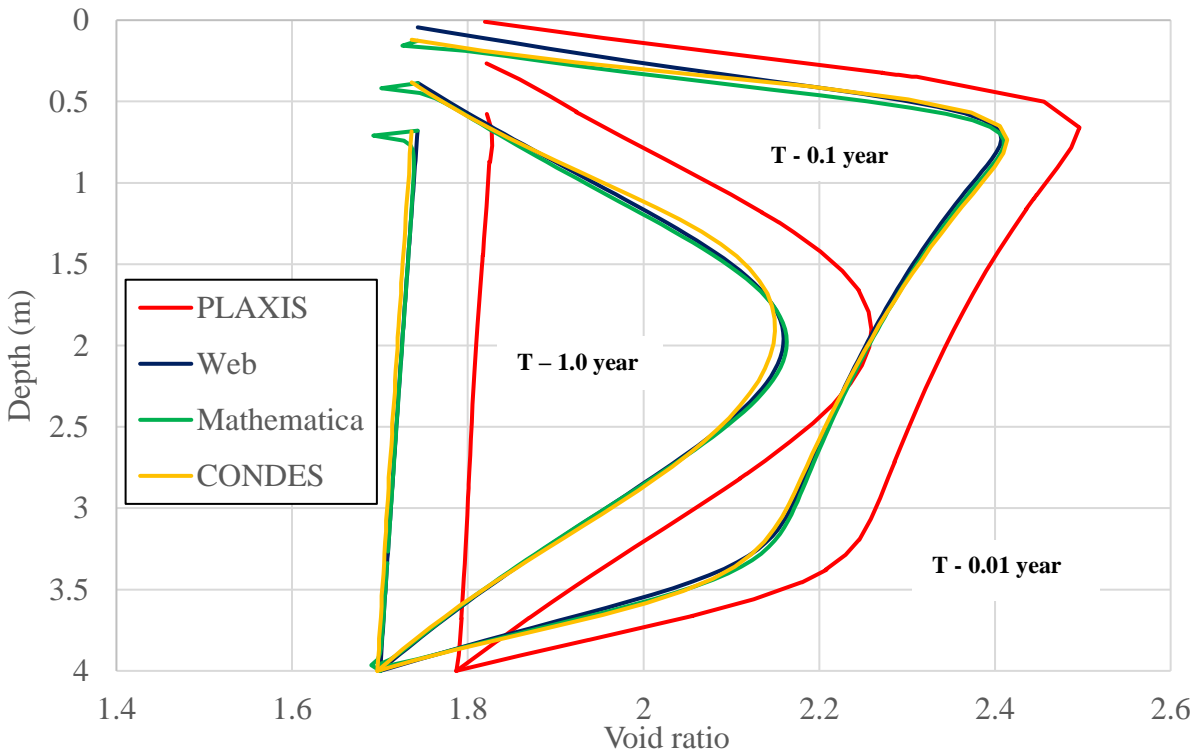

Figure 6.3.1a Settlement curve for Research Case w/out Creep

Figure 6.3.1b Void ratio profiles for Research Case w/out Creep, t = 0.01, 0.1, and 1 years

73
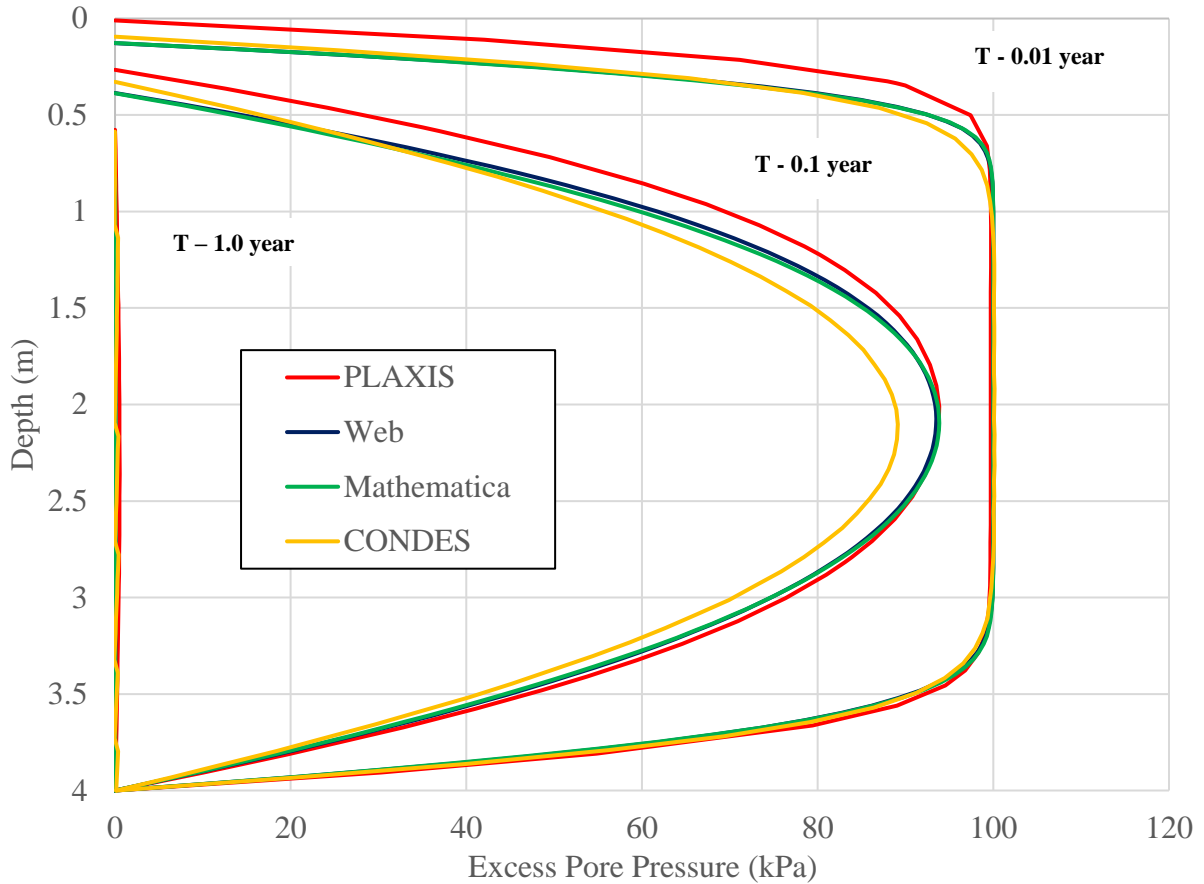
Figure 6.3.1c Excess pore pressure profiles for Research Case w/out Creep, t = 0.01, 0.1, and 1 years

Figure 6.3.1a indicates a reasonably good match between calculated settlement values for different numerical models. The settlement values calculated by PLAXIS, however, are consistently lower than determined by other models. Results in Figure 6.3.1b and 6.3.1c are consistent with results in Figure 6.3.1a displaying higher void ratios and higher excess pore pressures determined by PLAXIS than calculated by other models. In PLAXIS, calculated settlements are a function of the void ratio. The void ratio is a function of the mean effective stress, i.e. unlike the one-dimensional models (CONDES, iConsol.js and Mathematica), both horizontal and vertical stresses affect the magnitude of PLAXIS settlements. Results from

74

CONDES and Mathematica display favorable agreement except for pore pressures calculated in CONDES as the degree of consolidation approaches 100 percent. For these conditions, the use of CONDES outputs may result in negative excess pore pressure for individual layers.

6.3.2 Research Case w/ Creep, Ca = 0.003

Calculated settlements for the Research Case scenarios with the secondary compression index of Ca=0.003 are displayed in Figure 6.3.2a.
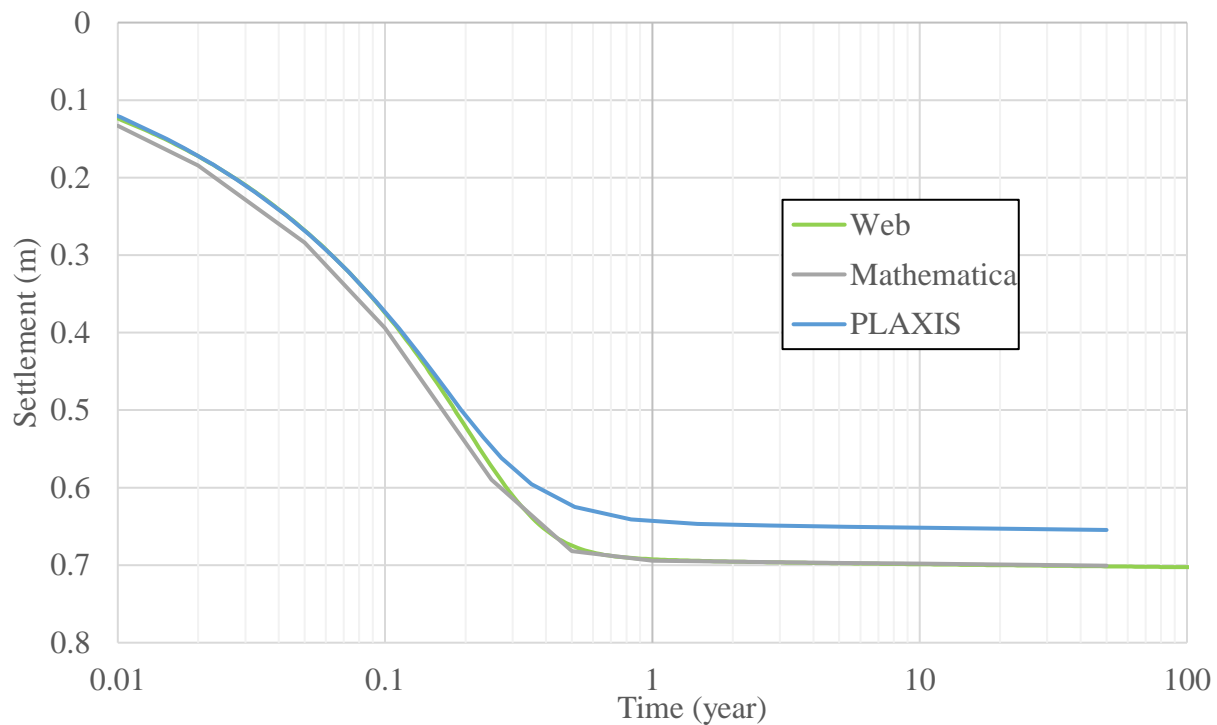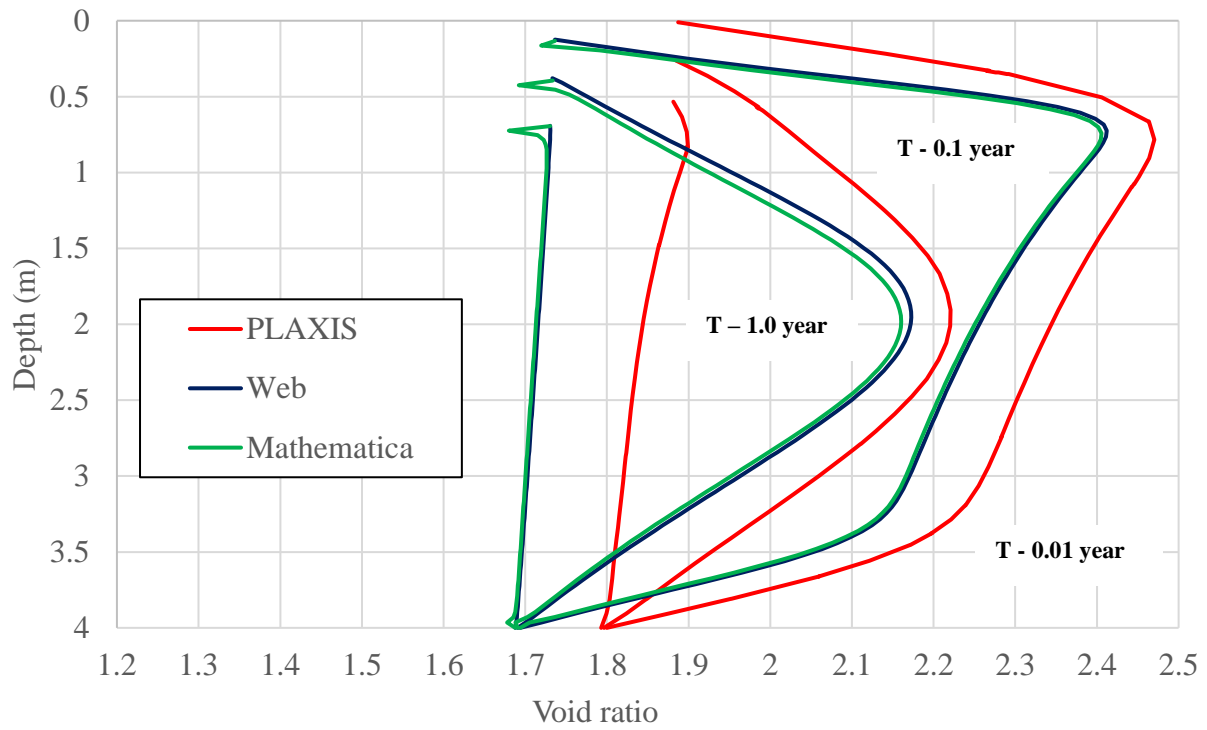

Figure 6.3.2a Settlement curve for Research Case w/ Creep, Ca = 0.003

Figure 6.3.2b Void ratio profiles for Research Case w/ Creep, Ca = 0.003, t = 0.01, 0.1, and 1 years
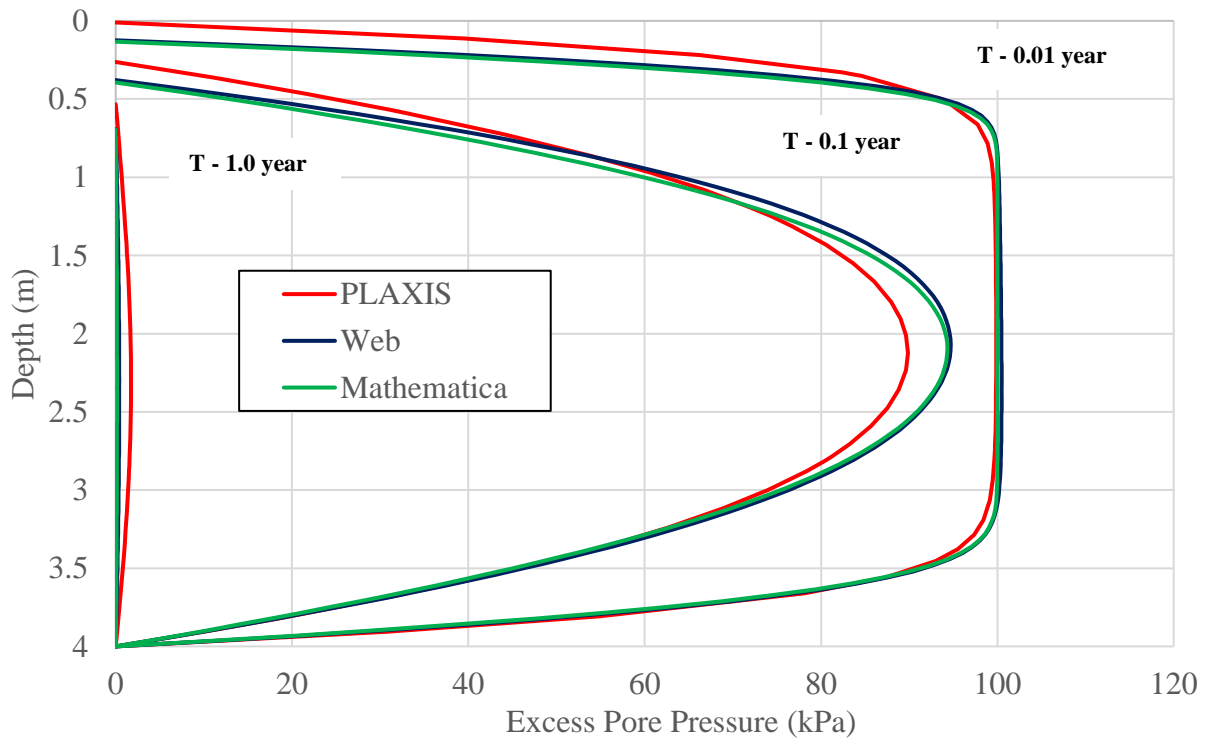

Figure 6.3.2c Excess pore pressure profiles for Research Case w/ Creep, Ca = 0.003, t = 0.01, 0.1, and 1 years

Results in Figure 6.3.2a raise a concern about conducting PLAXIS simulations using the Soft Soil Creep models for relatively low values of the secondary compression index Ca. Calculated PLAXIS settlements in Figure 6.3.2a are lower than the corresponding settlements in Figure 6.3.1a without creep. I.e., the Soft Soil Creep model with Ca=0.003 appears to be stiffer than the Soft Soil model using the same compressibility parameters. The current implementation of PLAXIS does not allow input for the secondary compression index, Ca, smaller than 0.001. PLAXIS used in this thesis is version 2012.01, which means the first version in year of 2012.

Results obtained by iConsol.js and Mathematica display favorable agreement. Consistent with the findings in Chapter 4, Mathematica exhibits higher settlements at earlier times with the difference between iConsol.js and Mathematica model results decreasing at larger times. The selected time reference value of t_{ref}=1.227E+07 seconds, used for iConsol.js and Mathematica simulations, corresponds to the settlement value of 95 percent for the case scenario without creep discussed in Chapter 6.3.1. The required PLAXIS inputs for the Soft Soil Creep model do not include t_{ref}. I.e., PLAXIS does not require specific inputs defining the end of primary consolidation.

6.3.3 Research Case w/ Creep, Ca = 0.03

Calculated settlements for the Research Case scenarios with the secondary compression index of Ca=0.03 are displayed in Figure 6.3.3a.
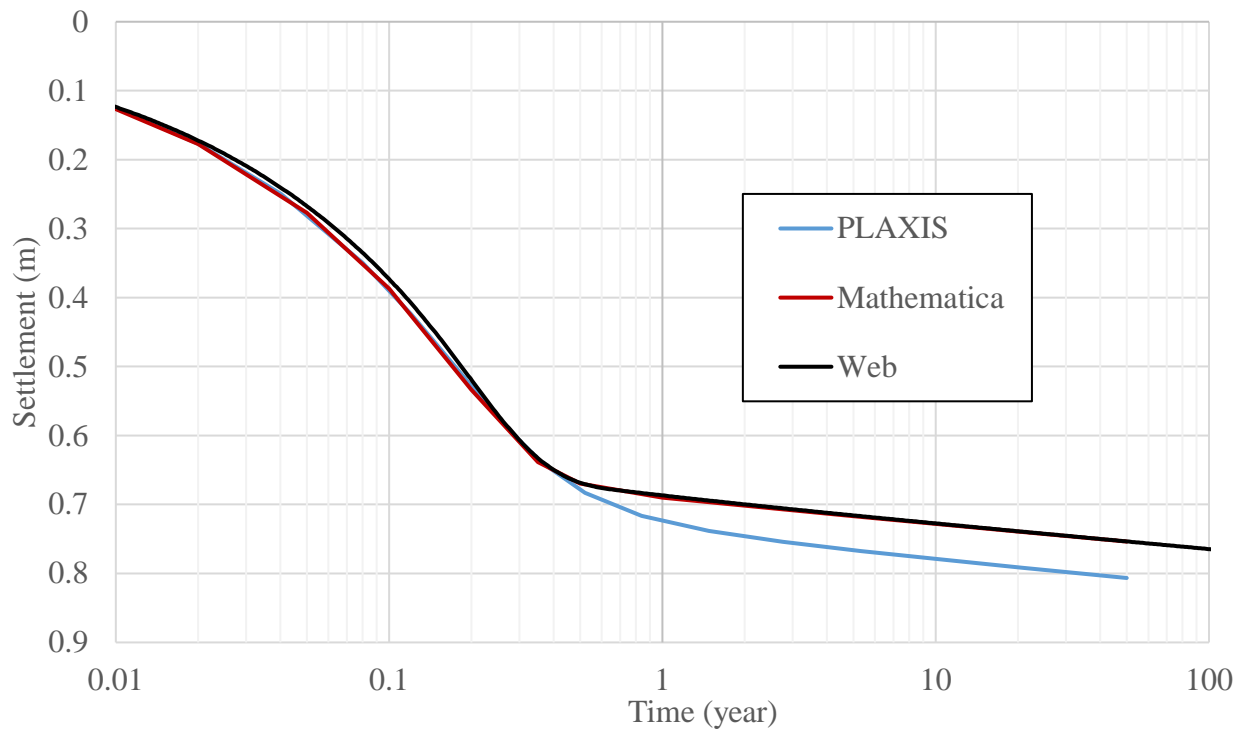
77

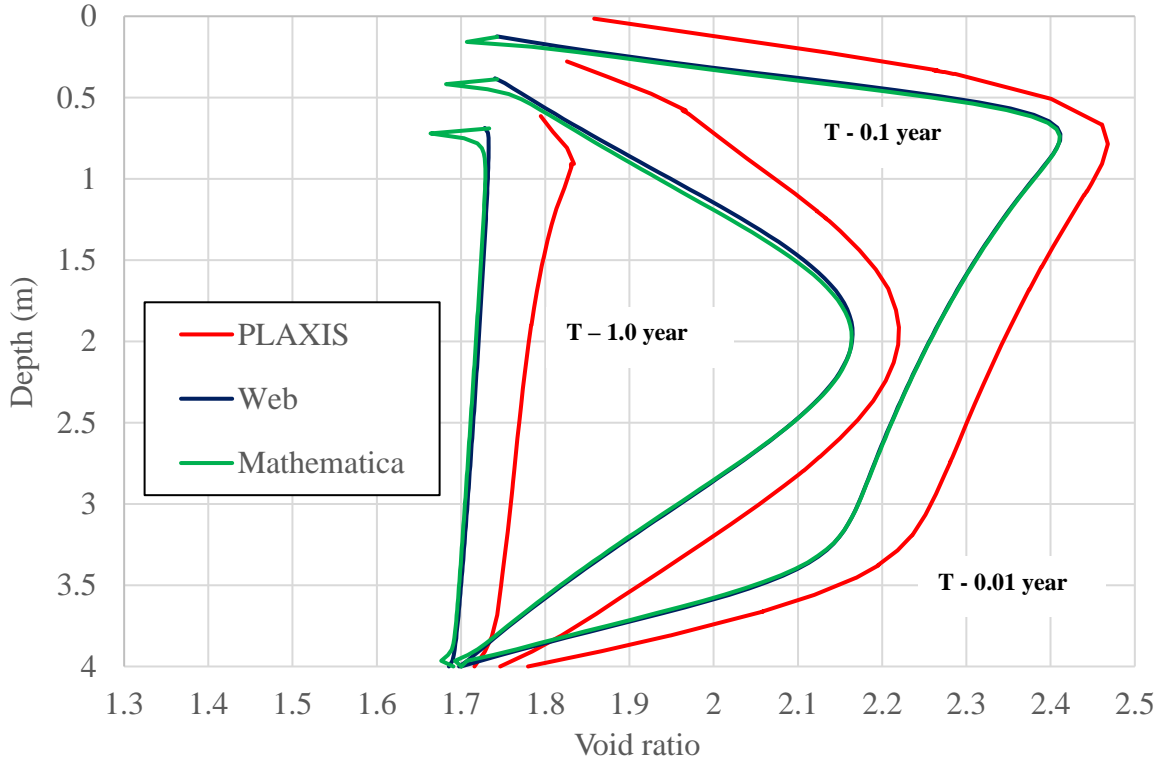Figure 6.3.3a Settlement curve for Research Case w/ Creep, Ca = 0.03

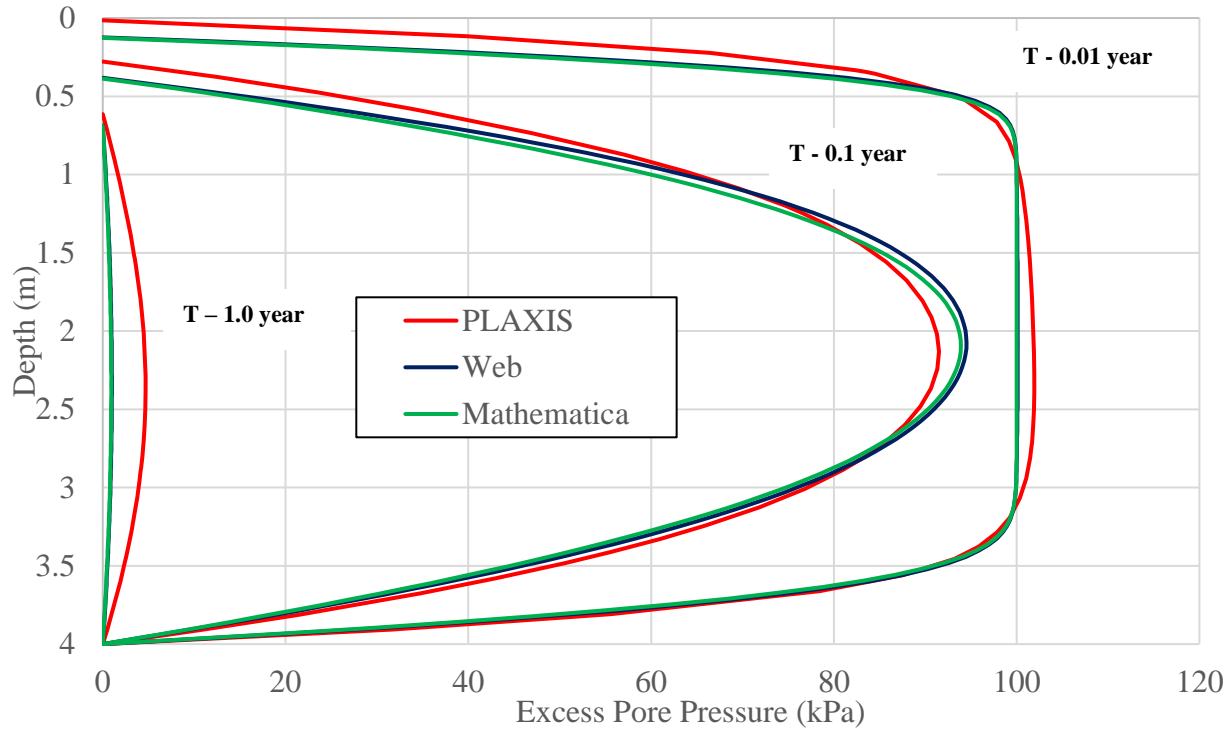Figure 6.3.3b Void ratio profiles for Research Case w/ Creep, Ca = 0.03, t = 0.01, 0.1, and 1 years

78

Figure 6.3.3c Excess pore pressure profiles for Research Case w/ Creep, Ca = 0.03, t = 0.01, 0.1, and 1 years

Figure 6.3.3a demonstrates significantly larger long-term settlements calculated by the

PLAXIS model than determined by iConsol.js and Mathematica. Therefore, PLAXIS results

indicate that the creep mechanism is activated prior to the end of primary consolidation (i.e.

the Soft Soil model appears to exhibit "artificial" stiffness only for low Ca values).

Consequently, PLAXIS results are likely to display larger settlements than models for which

the creep is activated at the end of the primary consolidation period. The void ratio profile

displayed in Figure 6.3.3b follows the same trend observed for the previously discussed

Research Case simulations discussed in Chapters 6.3.1 and 6.3.2. Creep effects affecting the

excess pore pressure distribution are illustrated in Figure 6.3.3c. Results in Figure 6.3.3c for

time= 0.01 year, illustrate excess pore pressures larger than 100 kPa for iConsol.js and

PLAXIS models.

79

6.3.4 Range of Secondary Compression Settlements

Figure 6.3.3a indicates that the model allowing for the activation of creep mechanism throughout the consolidation process (PLAXIS) is likely to exhibit larger overall settlements than the models accounting for the secondary compression only after the primary consolidation is largely completed (iConsol.js, Mathematica). However, a match between models allowing for the creep to occur throughout the consolidation process and the models requiring information about the end of primary consolidation is still possible. E.g., one can adjust the value of t_{ref} for models in this study (iConsol.js and Mathematica) until achieving acceptable match with PLAXIS (see Table 6.3a).

Table 6.3a displays t_{ref} values determined for the degrees of consolidation from 10 to 95 percent. Corresponding consolidation settlements allowing for the comparison between iConsol.js and PLAXIS models are displayed in Figure 6.3.4a. Results in Figure 6.3.4a indicate a good match between iConsol.js and PLAXIS results for the t_{ref} value equal to $t_{25} = 6.12 \times 10^5$ seconds (=0.0194 years).

Table 6.3a Range of t_ref Values for iConsol.js Comparison w/ PLAXIS

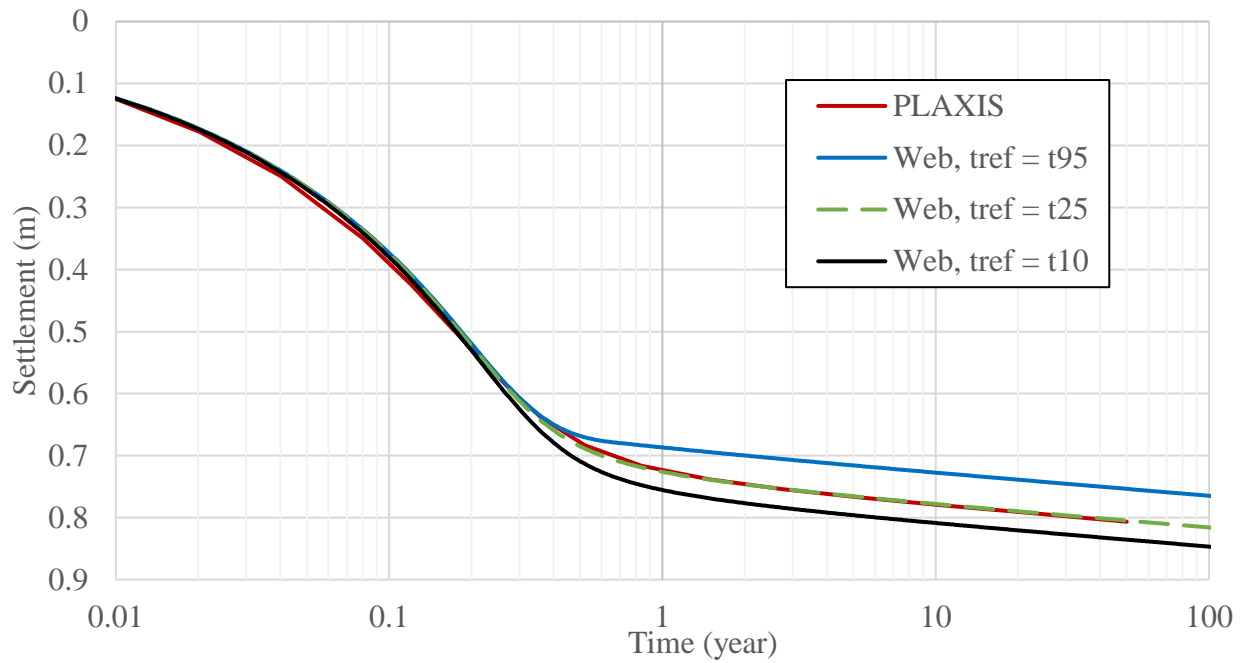|	t_{95}	t_{25}	t_{10}
t_{ref} (sec)	1.227E+07	6.120E+05	8.808E+04
t_{ref} (year)	3.891E-01	1.941E-02	2.793E-03

Figure 6.3.4a Comparison between iConsol.js and PLAXIS for t10 ≤ t_{ref} ≤ t95, Ca=0.03.

6.3.5 Research Case - Final Remarks

Research Case simulations were conducted to investigate consolidation behavior of a soft soil deposit for which the initial settlements are largely governed by the material self-weight. The non-linear consolidation process was simulated by using CONDES, Mathematica, iConsol.js, and PLAXIS models. A favorable match in the calculated consolidation settlements was observed between one-dimensional (CONDES, Mathematica, iConsol.js) and two-dimensional models (PLAXIS). The Soft Soil Creep model exhibits "artificial" stiffness when using very low values of the secondary compression index, i.e. for Ca values in 10^{-3} range.

For case scenarios where the degree of consolidation approaches 100%, the interpretation of CONDES outputs may result in negative pore pressures. A favorable match between PLAXIS and iConsol.js can be achieved by adjusting the t_{ref} value. For the

81

Research Case scenario considered in this study, a favorable match between PLAXIS and iConsol.js result was obtained for $t_{ref} = t_{25}$.

A comparison of void ratio profiles between PLAXIS and other models indicates the significance of lateral confinement to the overall settlement behavior. The void ratio calculated in PLAXIS is a function of mean effective stress. For conditions where horizontal stresses are smaller than the corresponding vertical stress, the resulting void ratio in two-dimensional or three-dimensional model will be larger than the void ratio determined in a one-dimensional (vertical) model. This is due to PLAXIS model that doesn't allow stiffness to be the same in horizontal direction and vertical direction. Typically, consolidation models used for one-dimensional simulations, (including the models in this study), do not account for lateral stresses.

6.4 Output Results – Benchmark Case

For the other case study about the secondary compression, the Benchmark 1 case will be
analyzed. To compare numerical predictions reported by Brandenberg (2016) for the Benchmark
1 scenarios with creep, a new set of numerical models with the secondary compression index of
C_a=0.025 and the initial soil heights of H= 2 m and H=20 m was evaluated in iConsol.js and
Mathematica.

6.4.1 Benchmark No. 1 Results w/ Creep

Results of these models are displayed in Figure 6.4.1a in terms of normalized settlements.
I.e. the settlement obtained from numerical models with creep was divided by the ultimate
settlement at the end of primary consolidation (i.e. the ultimate settlements for the corresponding
numerical model without creep was used to normalize calculated settlements). In addition, time
values in Figure 6.4.1a were normalized by using the t50 parameter. The t50 parameter
represents time at which 50% of the primary consolidation settlement was realized. All models in
Figure 6.4.1a were evaluated using the t_{ref} value of 2200 seconds to match model inputs for the
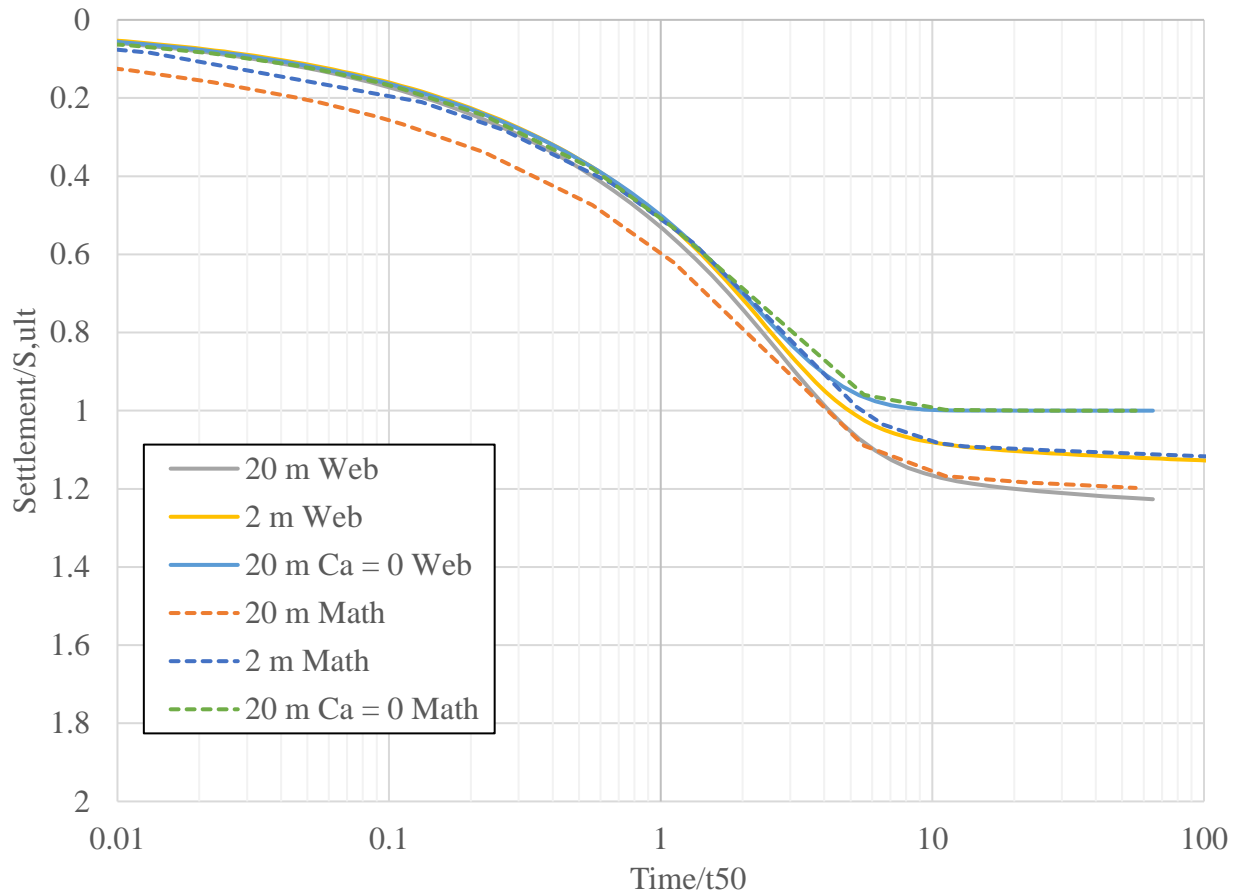Benchmark 1 scenarios with creep reported by Brandenberg (2016).

Figure 6.4.1a Normalized settlement values for Benchmark 1 models w/ creep

Figure 6.4.1a demonstrates that the initial settlements calculated by Mathematica are larger than the initial settlements (settlements at earlier times) determined by the iConsol.js model. The difference between two models decreases at later times.

To explain the difference between iConsol.js and Mathematica, calculated settlements are compared for three time intervals denoted by A, B, and C as illustrated in Figure 6.4.1b. Time interval A represents the period for which the settlements are governed by hydro-dynamic dissipation of excess pore pressures, i.e. before activating creep. In contrast, time interval C corresponds to the period with negligible excess pore pressures during which the settlements are dominated by the secondary compression. Time interval B indicates the

period between A and C during which both the hydrodynamic dissipation of excess pore pressures and the creep mechanism are governing the settlement process.
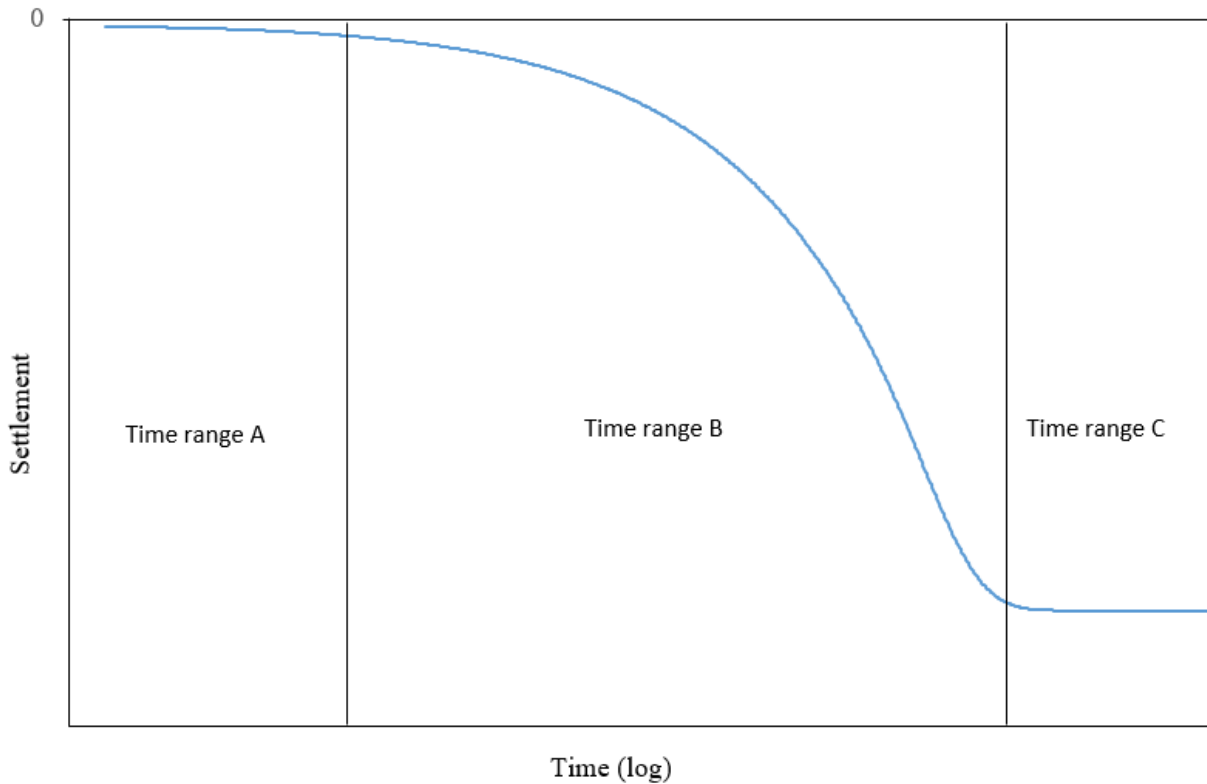

Figure 6.4.1b. Time intervals A, B, and C for model scenarios w/out creep

In Mathematica, the rate of creep is set to zero for times smaller than t_{ref}. For times larger than t_{ref}, the creep rate occurs in accordance with the defined secondary compression index as indicated by Equation (3.2b). I.e., for times larger than t_{ref}, the volumetric creep rate is defined as

$$\dot{\varepsilon}_{v,sc} = \frac{C_\alpha}{ln(10)\, t\, (1 + e)} = \frac{\alpha}{t\, (1 + e)} \qquad (6.4a)$$

85

Based on the secondary creep rate defined by Equation (6.4a), the change in void ratio vs. time plots as a straight line on e-log t plot with the slope equal to the secondary compression index Ca.

For the time range A, it was noted that iConsol.js reports small settlements due to creep. These values are attributed to errors in the implementation and are considered negligible as the inferred secondary compression settlement values are relatively small. Both iConsol.js and Mathematica implementations report similar final settlement values and display favorable agreement in predicted creep rates for the time range C (i.e. at times when the soil settlement is governed by creep). For the time range B, Mathematica displays larger settlements than iConsol.js with the difference in predicted settlements between the two models becoming smaller towards the end of primary consolidation. Figure 6.4.1a displays somewhat larger final settlements predicted by iConsol.js than predicted by Mathematica.

6.4.2 Differences between Model Results and Brandenberg (2016) Data

Normalized settlement curves for the Benchmark 1 scenario with creep reported by Brandenberg (2016) are displayed in Figure 6.4.2a. These results are markedly different from values reported in Figure 4.3.2a. E.g., for H = 20 m, Brandenberg (2016) reports the settlement at the end of primary consolidation of approximately $1.8 * S_{c,ult}$ (see Figure 6.4.2a), while Figure 6.4.1a demonstrates the settlement of $1.2 * S_{c,ult}$ for the same input parameters. A similar discrepancy between Brandenberg (2016) results for the Benchmark 1 model with creep and iConsol.js values reported in Figure 6.4.1a is noted for the shorter column i.e. for H = 2.0 m.
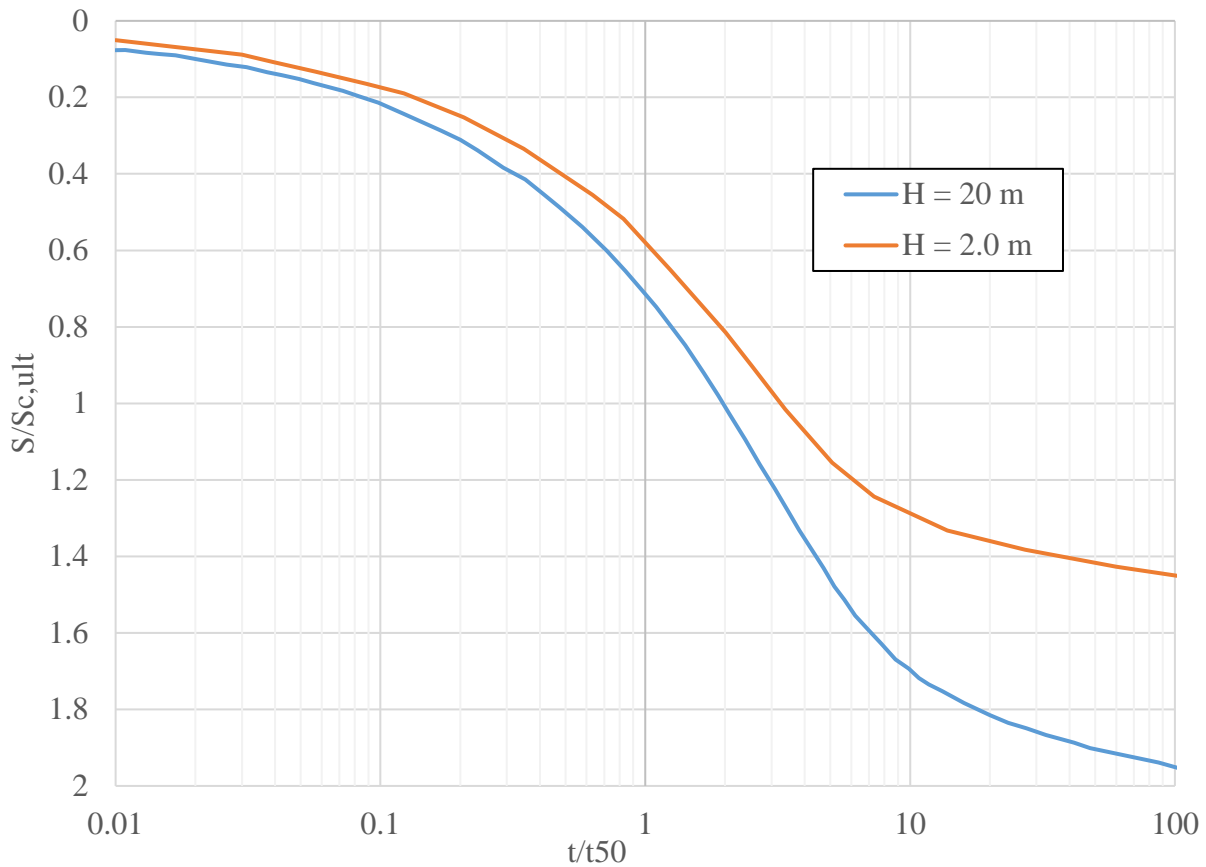
86

Figure 6.4.2a. Normalized settlements for Benchmark 1 scenario with creep - Brandenberg (2016)

The observed differences in Figure 6.4.1a and Figure 6.4.2a demonstrate gross errors in the interpretation of secondary compression results by Brandenberg (2016). In practice, it is customary to define the on-set of secondary compression, t_{ref}, as the time that corresponds to a state at which the primary consolidation is largely completed, i.e. the t_{ref} value is set to coincide with the time at which the magnitude of pore water pressures becomes negligible. In the absence of pore water pressure measurements, Mesri and Choi (1985) recommend the selection of time corresponding to a 95% settlement to identify the end of primary consolidation. To evaluate the sensitivity of settlement predictions to t_{ref}, additional numerical simulations were conducted by using t_{ref} corresponding to t_{90}, t_{95}, and

87

t_{99} values determined from calculated settlements for the Benchmark 1 scenarios without creep. The updated t_{ref} values are shown in Table 6.4a.

Table 6.4a Updated t_ref Values for Benchmark 1 Solution Based on Soil Height

	t_{90} (sec)	t_{95} (sec)	t_{99} (sec)
H = 20 m	2.246E+09	2.580E+09	3.332E+09
H = 2.0 m	2.132E+07	2.388E+07	3.060E+07
H = 0.02 m	2.089E+03	2.316E+03	2.831E+03

Values in Table 6.4a demonstrate that the t_{ref} value of 2200 sec reported by Brandenberg (2016) corresponds to the soil height of 0.02 m, i.e. this is a representative value for a laboratory-size sample. Re-calculated settlement plots for the Benchmark 1 scenarios with creep utilizing updated t_{ref} values from Table 6.4a are presented Figures 6.4.2b, 6.4.2c, and 6.4.2d.
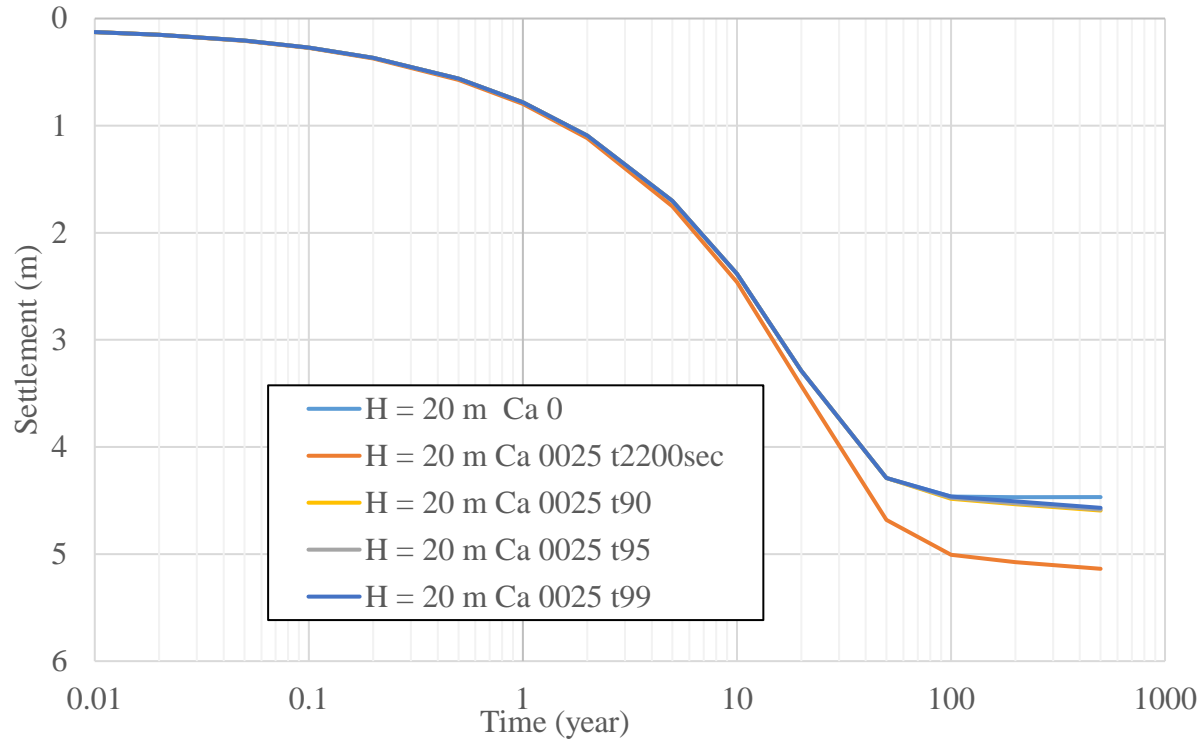
Figure 6.4.2b Settlements for Benchmark 1 w/ creep, H=20 m, updated t_{ref} values
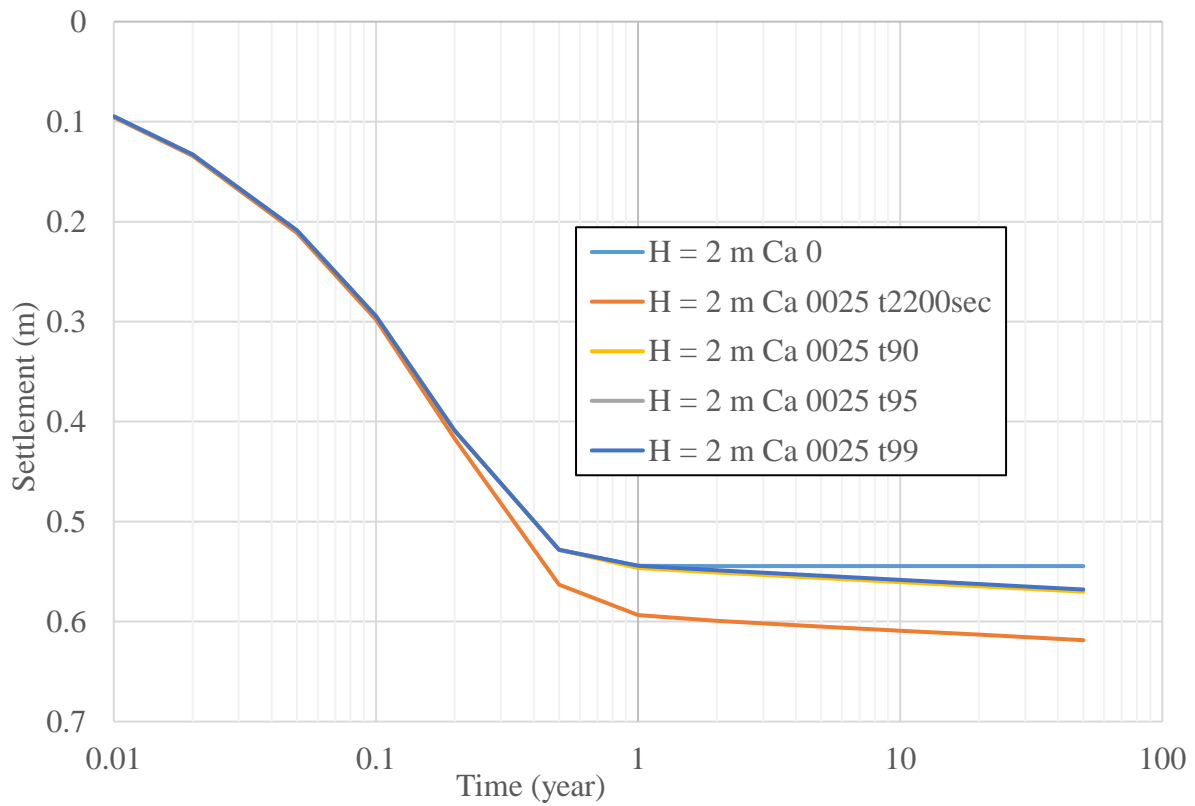

Figure 6.4.2c Settlements for Benchmark 1 w/ creep, H=2.0 m, updated t_{ref} values
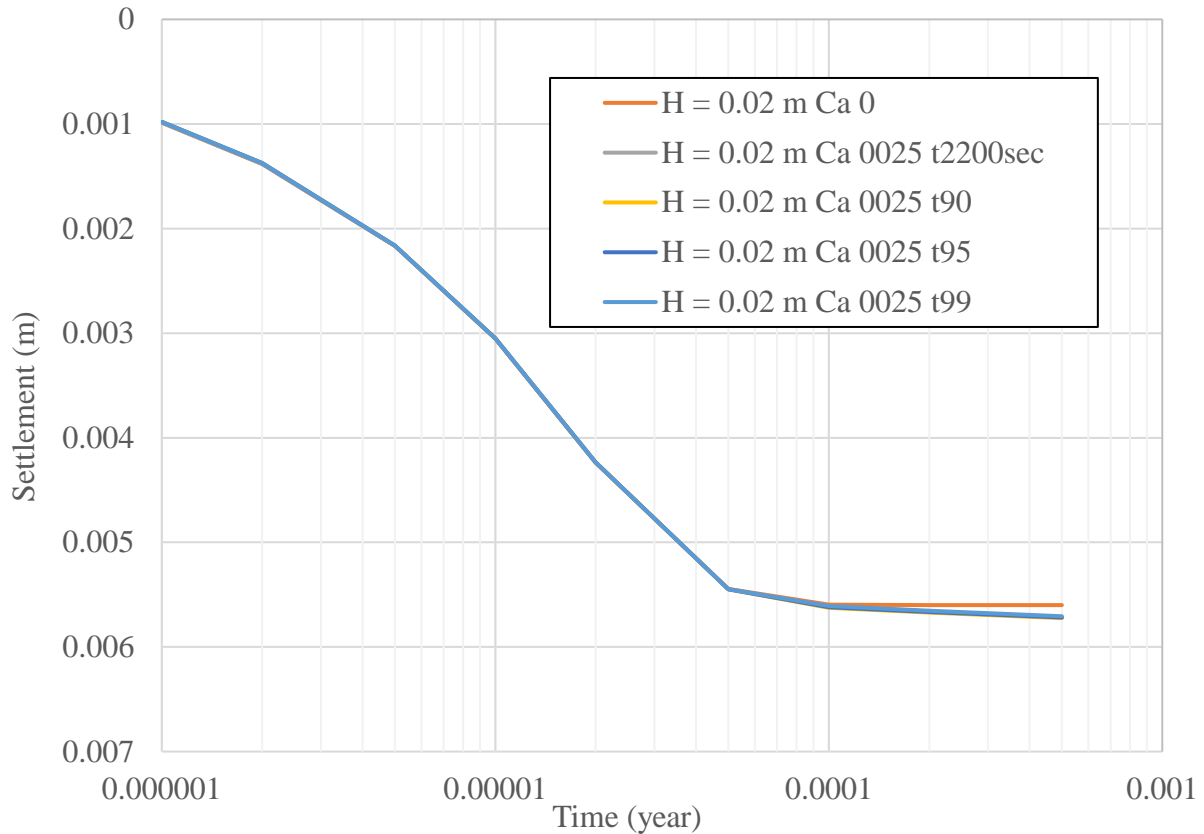
89

Figure 6.4.2d Settlements for Benchmark 1 w/ creep, H=0.02 m, updated t_{ref} values

Figures 6.4.2b, 6.4.2c, and 6.4.2d demonstrate larger settlements and longer consolidation times for the soil layer with larger initial thickness. In addition, the predicted total settlements will be larger for smaller values of t_{ref}, i.e. as the t_{ref} value increases, the predicted soil settlement decreases. Normalized settlement graphs based on the updated t_{ref} values are presented in Figures 6.4.2e, 6.4.2f, 6.4.2g, 6.4.2h, 6.4.2i, and 6.4.2j.
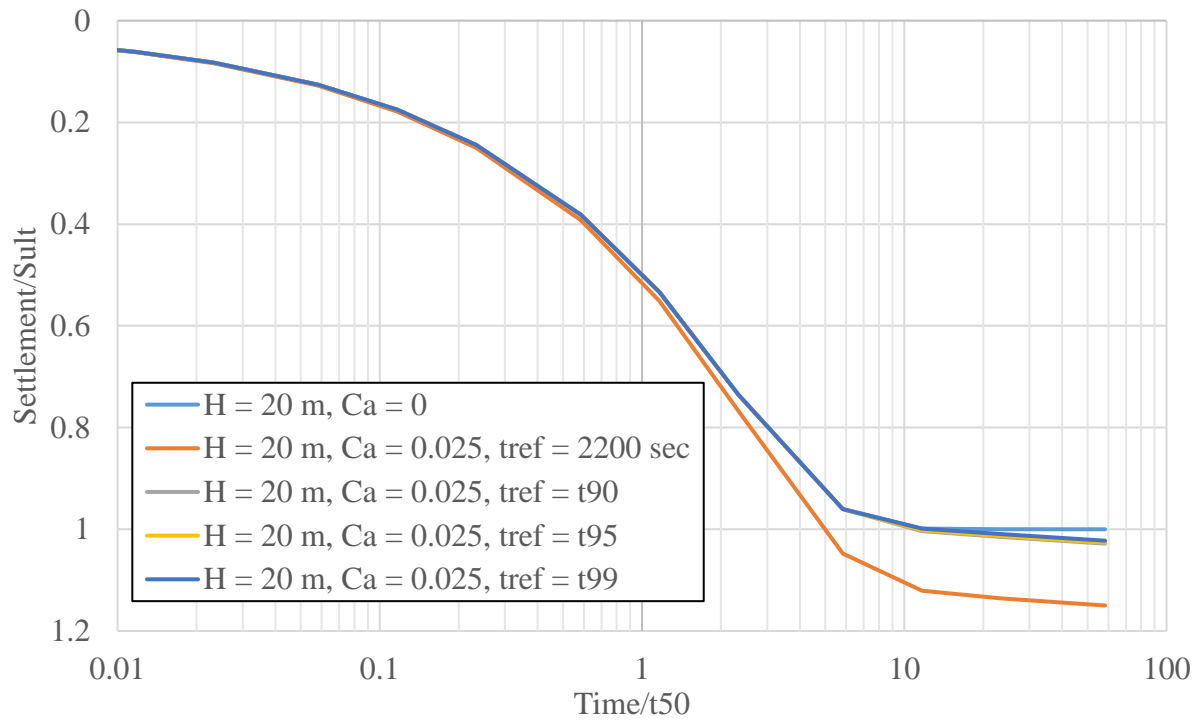
Figure 6.4.2e Normalized settlements for Benchmark 1 w/ creep, H=20 m, updated t_{ref} values
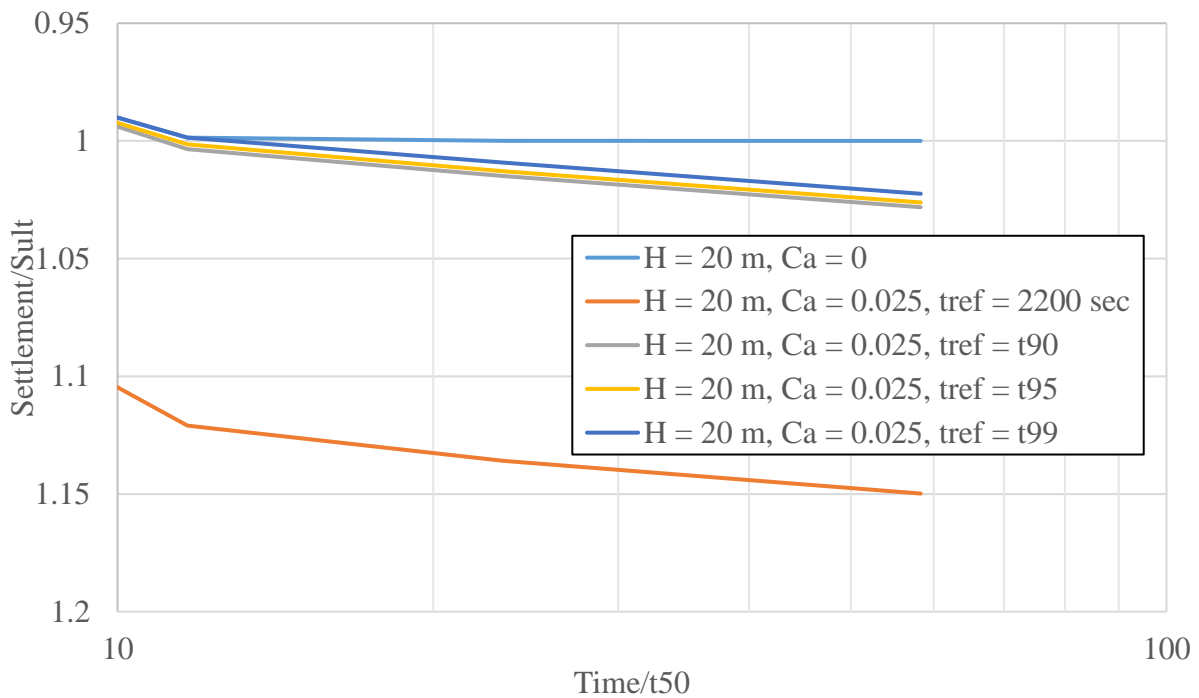

Figure 6.4.2f Magnified normalized settlement for Benchmark 1 w/creep, H=20 m, updated t_{ref} values

91

Figure 6.4.2g Normalized settlement for Benchmark 1 w/creep, H=2.0 m, updated t_{ref} values

Figure 6.4.2h Magnified normalized settlement for Benchmark 1 w/creep, H=2.0 m, updated t_{ref} values
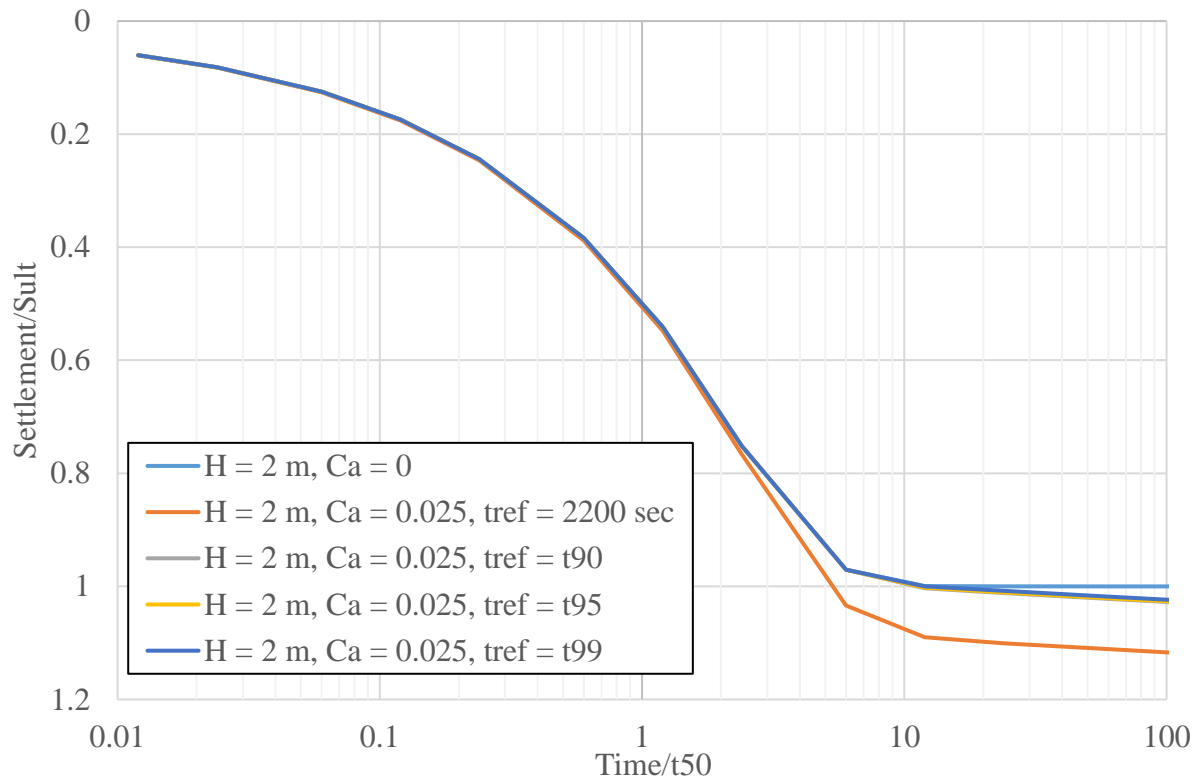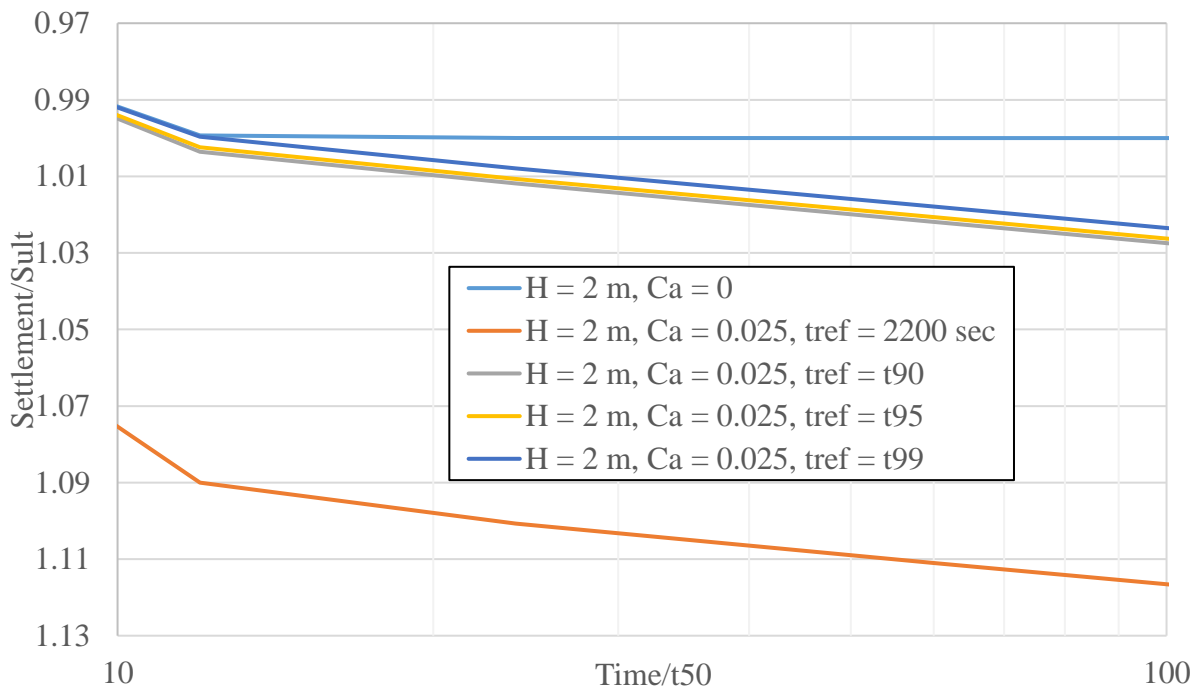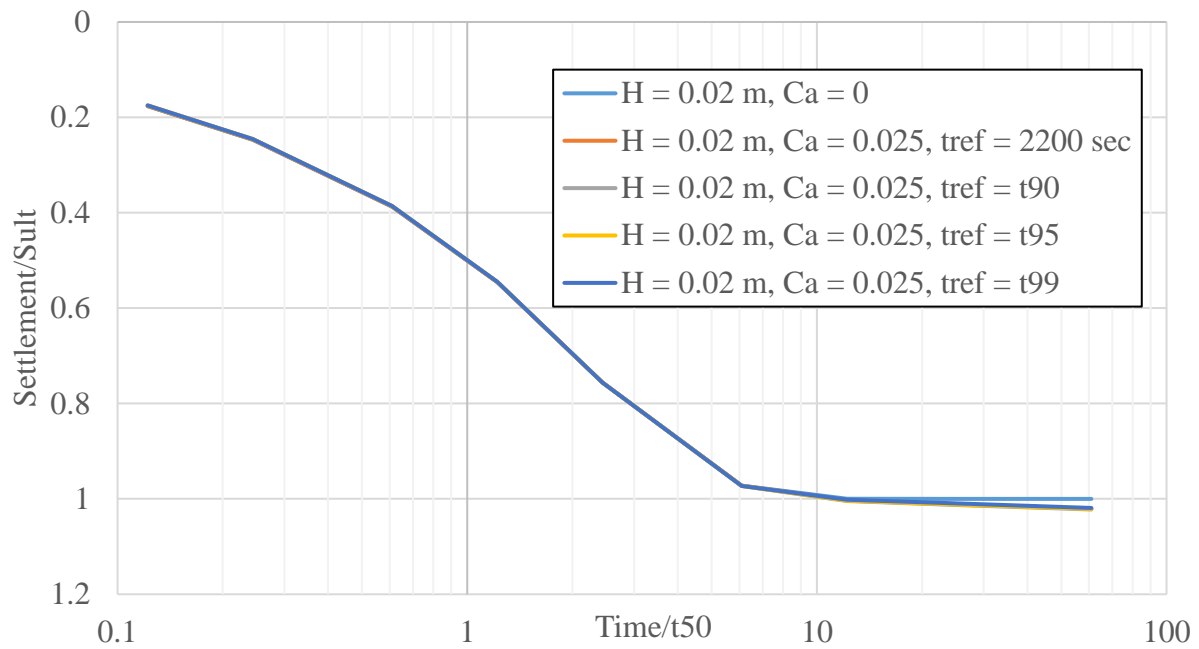
92

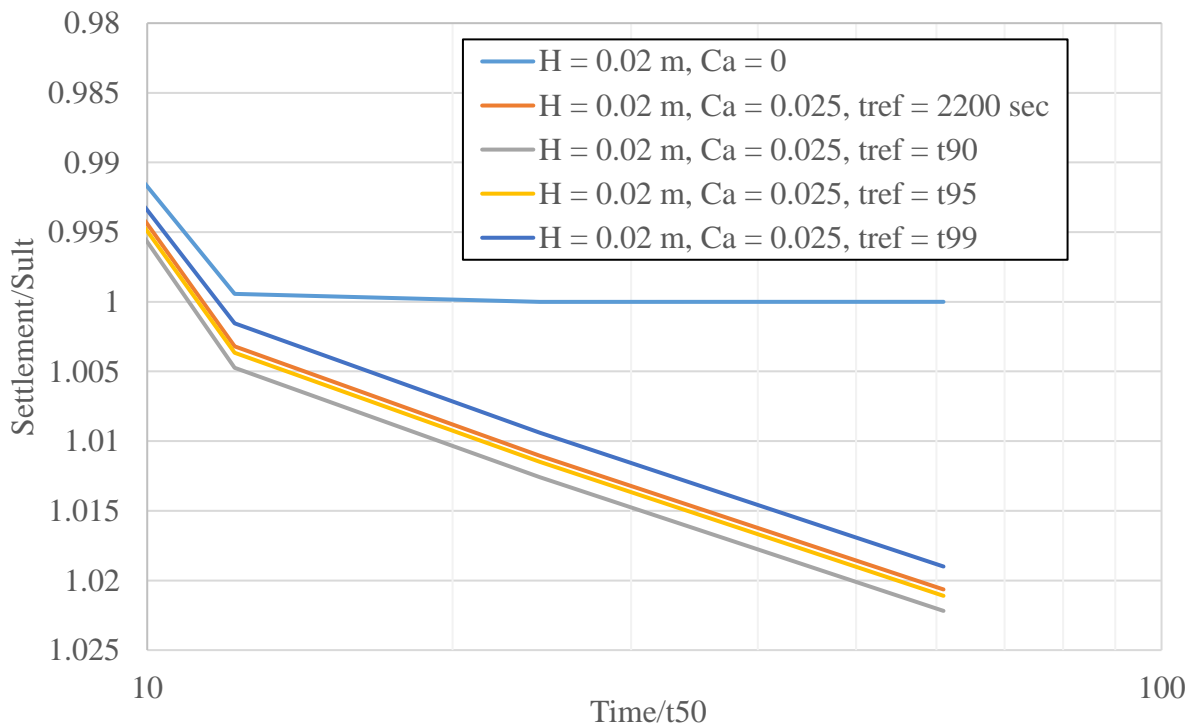Figure 6.4.2i Normalized settlement for Benchmark 1 w/creep, H=0.02 m, updated t_{ref} values

Figure 6.4.2j Magnified normalized settlement for Benchmark 1 w/creep, H=0.02 m, updated t_{ref} values

93

6.4.3 Benchmark 1 Case w/ Creep Final Remarks

Numerical solutions developed for Benchmark 1 problem with creep indicate the importance of selecting consistent normalization parameters, as well as selecting the appropriate reference time.   The reference time should correspond to the end of primary (EOP) consolidation defined by the magnitude of excess pore pressures or the estimated percent settlement. If the reference time selection corresponds to the realized percentage of settlement, the time corresponding to the degree of settlement of more than 90 percent is recommended for the secondary compression analyses. In practice, the reference time corresponding to 95 or 99 percent settlement is often used. Ideally, the reference time and the secondary compression index would be selected by calibrating results from the numerical model to the available field data.

7. CONCLUSIONS

This thesis presents results of numerical investigations of linear and nonlinear consolidation and creep. Calculations were conducted by using several model codes available in today's engineering practice.

Models based on Gibson's (1967) theory are well suited to deal with large strain consolidation problems. The mesh updating approach can be used to analyze large strain consolidation problems, however, a numerical implementation of this approach is more likely to lead to convergence problems (e.g. PLAXIS model). Numerical approach based on the use of material coordinates (CONDES model) is likely to be more stable although the equivalent one-dimensional approach based on updating Eulerian coordinates while using the piece-wise linear finite difference scheme (CS2 model) was successfully used in the past (e.g., Fox and Pu, 2015).

Available numerical models that account for secondary compression are limited. This thesis considered two secondary compression models that are available to practicing engineers: iConsol.js and PLAXIS. In addition, a simplified version of the creep model was developed in Mathematica. While both iConsol.js and PLAXIS use a single parameter, Ca, to define slope of the secondary compression curve, results from these two models may exhibit significant differences. Results in this thesis demonstrate that the model differences are due to implementation of the constitutive models and the definition of time that defines start of the secondary consolidation.

Leroueil et al (1985) developed the model accounting for variability of the secondary compression index, Ca, with the strain rate. However, this model is rarely used in practice due to relative complexity of implementation and testing requirements to determine model parameters.

95

This study indicates the need to validate model results by using laboratory data collected during geotechnical investigations and field monitoring. The need to validate model results is exacerbated by potential errors identified in iConsol.js numerical scheme and by "artificial" stiffness of the Soft Soil Creep model in PLAXIS observed for low values of the secondary compression index.

A comparison between linear and nonlinear consolidation models was based on the degree of consolidation defined in terms of settlements and in terms of excess pore pressure. For large strain consolidation problems, the degrees of consolidation based on settlement and excess pore pressure have different values whereas they are the same when considering the Terzaghi's consolidation theory. The use of graphical methods by Cassagrande and Taylor provided favorable agreement with the corresponding non-linear model when estimating times of consolidation. However, the estimated coefficient of consolidation (predicted by graphical methods when analyzing time-settlement curve from a non-linear model) may be significantly larger than the average c_v value based on the actual (non-linear) compressibility and permeability parameters. The use of Terzaghi's consolidation theory should be restricted to small strain applications characterized by relatively small changes in material properties during the consolidation process. Linear consolidation models based on the classical (Terzaghi's) consolidation theory are suitable for small-strain consolidation problems dealing with relatively stiff soil deposits.

BIBLIOGRAPHY

Bartholomeeusen, G. (2003). Compound shock waves and creep behavior in sediment beds, Ph.D. thesis, University of Oxford, Oxford, United Kingdom.

Biot, M. A. (1940). General theory of three-dimensional consolidation. *Journal of Applied Physics*, **12**, 155-164.

Bjerrum, L. (1967). Engineering geology of Norwegian normally consolidated marine clays as related to settlements of buildings. *Geotechnique*, **17**(2), 83 – 118.

Brandenberg, S. J. (2017). iConsol.js: A javascript implicit finite difference code for nonliear consolidation and secondary compression. *International Journal of Geomechanics*, 17(6)

Brink, N. R. (2012). Numerical modeling of consolidation process in hydraulically deposited soils, M.S. thesis, University of Colorado, Boulder, Colorado.

Buisman, A. S. K. (1936). Results of long duration settlement tests. *Proceedings 1st international conference on soil mechanics and foundation engineering*, **1**, 103 – 106.

Choi, Y. K. (1982). Consolidation behavior of natural clays, Ph.D. thesis, University of Illinois, Urbana, Illinois.

Coduto, D. P., Yeung, M. –C., & Kitch, W. A. (2010). *Geotechnical engineering : Principles and practices*. Ipper Saddle River, Pearson.

Courant, R., Friedrichs, K., & Lewy, H. On the partial difference equations of mathematical physics. *IBM Journal*, **11**, 215 – 234.

Craig, R. F. (1997). *Soil Mechanics*. London, Spon Press.

Crank, J., & Nicolson, P. (1947). A practical method for numerical evaluation of solutions of partial differential equations of the heat conduction type. *Proc. Cambridge Philos. Soc.*, **43**(1), 50 – 67.

Darcy, H. P. G. (1856). Les fontaines publiques de la ville de Dijon. Dalmont, Paris.

Fox, P. J., & Berles, J. D. (1997). CS2 : A piecewise-linear model for large strain consolidation. *Int. J. Numer. Anal. Methods Geomech.*, **21**(7), 453 – 475.

Fox, P. J., & Pu, H. (2015). Benchmark problems for large strain consolidation. *J. Geotech. Geoenviron. Eng.*, 10.1061/(ASCE)GT.1943-5606.0001357, 06015008.

Gersevanov, N. M. (1934). Dinamika Mekhaniki Gruntov. Grosstroiisdat, **2**.

Gibson, R. E., England, G. L., & Hussey, M. J. L. (1967). The theory of one – dimensional consolidation of saturated clays. 1. Finite non – linear consolidation of thin homogeneous layers. *Geotechnique*, **17**, 166 – 176.

Hansen, B. (1969). A mathematical model for creep phenomena in clay. *Proceedings seventh international conference on soil mechanics and foundation engineering, Specialty session 12*, 12 – 18.

Houkes, C. B. (2016). Review and validation of settlement prediction methods for organic soft soils, on the basis of three case studies from the Netherlands, Ph.D. thesis, Delft University of Technology, Delft, Netherland.

Jamiolkowski, M., Ladd, C. C., Germaine, J. T., & Lancellotta, R. (1985). New developments in field and laboratory testing of soils. *Proceedings eleventh international conference on soil mechanics and foundation engineering*, AA Balkema, 57 – 153.

Koppejan, A. W. (1948). A formula combining the Terzaghi load – compression relationshiop and the Buisman secular time effect. *Proceedings of the second international conference on soil mechanics and foundation engineering*, 32 – 37.

Kurz, D., Sharma, J., Alfaro, M., & Graham, J. (2016). Semi – empirical elastic – thermoviscoplastic model for clay. *Canadian Geotechnical Journal.*, **53**(10), 1583 – 1599.

Leonards, G. A. (1977). Panel discussion, *Proceedings ninth international conference on soil mechanics and foundation engineering,* Tokyo, **3**, 384 – 386.

Leroueil, S. (2006). The isotache approach. Where are we 50 years after its development by professor Suklje? (2006 Prof. Suklje's Memorial Lecture), *Proceedings of the 13th Danube – European Conference on Geotechnical Engineering*, Ljubljana, 55 – 88.

Leroueil, S., Kabbaj, M., Tavenas, F., & Bouchard, R. (1985). Stress – strain – strain rate relation for the compressibility of sensitive natural clays. *Geotechnique*, **35**(2), 159 – 180.

Lo, K. Y. (1961). Secondary compression of clays, *Journal of the soil mechanics and foundation division*, **87**(SM4), 61 – 88.

Mesri, G., & Castro, A. (1987). C_α/C_c concept and K_0 during secondary compression. *Journal of geotechnical engineering*, **113**(3), 230 – 247.

Mesri, G., & Choi, Y. K. (1985). The uniqueness of the end-of-primary (EOP) void ratio – effective stress relationship. *Proceedings 11th international conference on soil mechanics and foundation engineering,* San Francisco, **2**, 587 – 590.

Mesri, G., & Godlewski, P. M. (1977). Time – and stress – compressibility interrelationship. *Journal of geotechnical engineering*, **103**(GT5), 417 – 430.

Suklje, L. (1957). The analysis of the consolidation process by the isotache method. *Proceedings of the fourth international conference on soil mechanics and foundation engineering*, London, **1**, 200 – 206.

Szavits – Nossan, V. (1988). Intrinsic time behavior of cohesive soils during consolidation, Ph.D. thesis, University of Colorado, Boulder, Colorado.

Watabe, Y., Udaka, K., Nakatani., & Leroueil, S. (2012). Long – term consolidation behavior interpreted with isotache concept for worldwide clays. *The Japanese geotechnical society*, **52**(3), 449 – 464.

Yao, D. T. C., & Znidarcic, D. (1997). Crust formation and desiccation characteristics for phosphatic clays (User's manual for computer program CONDES0). *The Florida institute of Phosphate research*, **4**, 55-134.

APPENDIX A

(1) Cassagrande Method
For case H = 0.02 m, external stress 40 kPa, with no creep
t_{100} = 7.664E-05 year, t_{50} = 1.278E-05 year, S_{100} = 1.625E-03 m, S_{50} = 8.147E-04 m
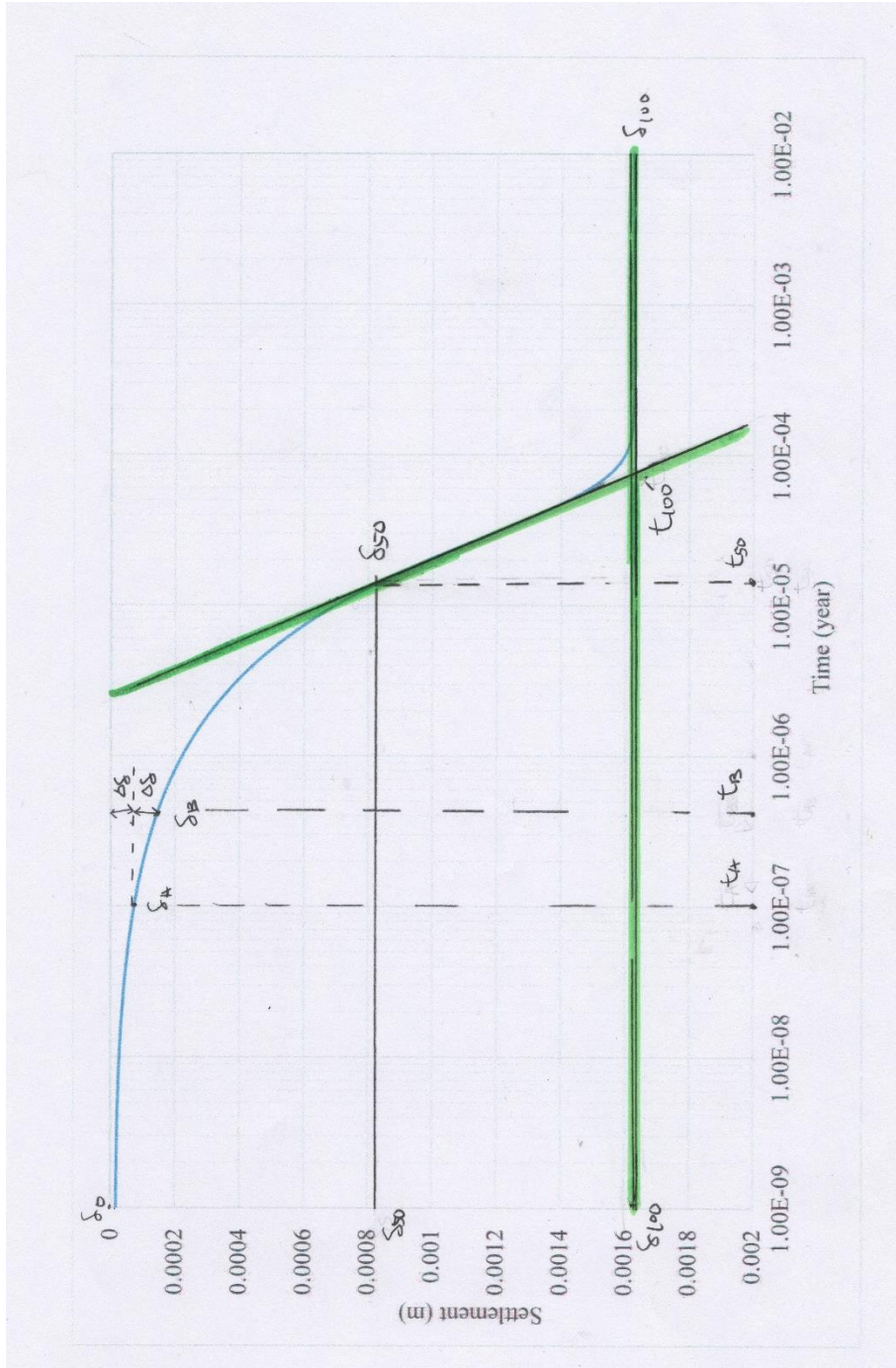
(2) Taylor Method
For case H = 0.02 m, external stress 40 kPa, with no creep
t_{90} = 5.625E-05 year, t_{50} = 1.278E-05 year, S_{90} = 1.463E-03 m, S_{50} = 8.533E-04 m

101